SPECIAL ISSUE ON QUANTUM INTEGRABILITY IN OUT OF EQUILIBRIUM SYSTEMS

Quench dynamics and relaxation in isolated integrable quantum spin chains

Journal of Statistical Mechanics: Theory and Experiment
An IOP and SISSA journal

Special Issue on Quantum Integrability in Out of Equilibrium Systems

Quench dynamics and relaxation in isolated integrable quantum spin chains

Fabian H L Essler[1] **and Maurizio Fagotti**[2]

[1] The Rudolf Peierls Centre for Theoretical Physics, Oxford University, Oxford OX1 3NP, UK
[2] Département de Physique, École Normale Supérieure/PSL Research University, CNRS, 24 rue Lhomond, 75005 Paris, France
E-mail: Fabian.Essler@physics.ox.ac.uk

Received 22 March 2016
Accepted for publication 8 May 2016
Published 24 June 2016

Online at stacks.iop.org/JSTAT/2016/064002
doi:10.1088/1742-5468/2016/06/064002

Abstract. We review the dynamics after quantum quenches in integrable quantum spin chains. We give a pedagogical introduction to relaxation in isolated quantum systems, and discuss the description of the steady state by (generalized) Gibbs ensembles. We then turn to general features in the time evolution of local observables after the quench, using a simple model of free fermions as an example. In the second part we present an overview of recent progress in describing quench dynamics in two key paradigms for quantum integrable models, the transverse field Ising chain and the anisotropic spin-1/2 Heisenberg chain.

Keywords: generalized Gibbs ensemble, integrable spin chains and vertex models

J. Stat. Mech. (2016) 064002

1742-5468/16/064002+69$33.00

Contents

1. Introduction

An *isolated* many-particle quantum system is characterized by the absence of any coupling to its environment. According to the laws of quantum mechanics its time evolution is unitary and governed by the time dependent Schrödinger equation. In order to specify the state $|\Psi(t)\rangle$ of the system at a given time t, it is then sufficient to know its Hamiltonian H and its state at an earlier time

$$|\Psi(t)\rangle = \mathrm{e}^{-\mathrm{i}Ht}|\Psi(0)\rangle. \tag{1}$$

In spite of this purely unitary evolution, macroscopic systems are expected to eventually 'relax' in some way and be amenable to a description by quantum Statistical Mechanics [1]. For many-particle systems it is convenient to focus on the time evolution of the expectation values of particular observables of interest rather than the state itself, i.e. one considers

J. Stat. Mech. (2016) 064002

$$\langle\Psi(t)|\mathcal{O}|\Psi(t)\rangle. \tag{2}$$

Historically, studies of many-particle quantum systems such as electronic degrees of freedom in solids mainly focussed on equilibrium properties at zero and finite temperature. This is because in the context of solids, the many-body system of interest is typically coupled to an 'environment', i.e. other degrees of freedom, the presence of which is felt after very short time scales. The situation changed dramatically about a decade ago, when it became possible to experimentally investigate the non-equilibrium dynamics of clouds of ultra-cold, trapped atoms [2–17] (see also the review by Langen, Gasenzer and Schmiedmayer in this volume [18]). These are by design almost isolated. Moreover the natural energy scale underlying the dynamics is incredibly small, so that there is a long time window (on the order of seconds) for conducting experiments. The main effect of the coupling to the environment is particle loss through heating. This eventually becomes significant, but over an intermediate time window the dynamics is to a good approximation unitary. It is important to note in view of the following discussion that finite size effects are often important in cold atom systems, and as a result of the trapping potential these systems are not translationally invariant. They are however highly tuneable both with regards to Hamiltonian parameters and their effective dimensionality. This was exploited in the seminal *Quantum Newton's Cradle* experiments by Kinoshita, Wenger and Weiss [3]. These investigated the non-equilibrium evolution of one, two and three dimensional Bose gases that were initially driven out of equilibrium. While the two and three dimensional systems were seen to relax very quickly towards an equilibrium state, the behaviour in the one dimensional case was very different. In [3] this was attributed to the presence of approximate conservation laws. Neglecting the trap, the Hamiltonian is well approximated by the Lieb–Liniger model [19]

$$H_{\mathrm{LL}} = -\frac{\hbar^2}{2m}\sum_{j=1}^{N}\frac{\partial^2}{\partial x_j^2} + c\sum_{j<k}\delta(x_j - x_k). \tag{3}$$

The Hamiltonian (3) is integrable and as a result has an infinite number of conservation laws I_n [20, 21] such that

$$[H, I_n] = [I_n, I_m] = 0. \tag{4}$$

It is intuitively clear that conservation laws will affect the quantum dynamics, because they impose constraints of the form

$$\langle\Psi(t)|I_n|\Psi(t)\rangle = \text{const.} \tag{5}$$

The difference in behaviours between the one and three dimensional Quantum Newton's Cradle experiments suggested that the non-equilbirium dynamics of integrable models is unusual. This was one of the motivations for the recent intense theoretical efforts aimed at understanding the non-equilibrium dynamics of integrable quantum many-particle systems. Integrable models come in a variety of guises, the two main classes being

J. Stat. Mech. (2016) 064002

- Lattice models:
  These include non-interacting fermion and boson theories [22–24], models that can be mapped to free fermions like the transverse-field Ising [25–43] and XY chains [44–52], spin models like the Heisenberg chain [53–72] and electronic theories like the Hubbard model [73–77].
- Continuum models:
  These include free field theories like the Klein–Gordon [78–80] and Luttinger models [53, 81–86] (see the review by Cazalilla and Chung [87] in this volume), conformal field theories [80, 89–93] (see the review by Calabrese and Cardy [88] in this volume), massive relativistic field theories like the sine-Gordon [94–96], sinh-Gordon [97–100] and nonlinear sigma models [101], and non-relativistic field theories like the Lieb–Liniger model [102–114]. In continuum models the spectrum of elementary excitations is unbounded, which leads to certain differences as compared to lattice models.

In this review we focus on the equilibrium dynamics in integrable lattice models. We moreover restrict our discussion to a particular protocol for inducing out of equilibrium dynamics, the so-called *quantum quench*. We note that other protocols have been studied in the literature. One example are *ramps* [115, 116], which are of interest in relation to the Kibble–Zurek mechanism [117].

The outline of this review is as follows. In section 2 we define what we mean by a quantum quench. This is followed by a discussion in section 3, of how isolated many-particle quantum systems relax, and of how to describe their late time behaviour. In section 4 we provide a simple example that shows these ideas at work. Having established a framework for the late time behaviour after a quantum quench, section 5 turns to the discussion of general features of the evolution of observables at finite times, such as how correlations spread through the system. Section 6 is concerned with one of the key paradigms of quantum quenches, the transverse field Ising chain (TFIC). This constitutes a non-trivial example, for which it is nevertheless possible to obtain exact results in closed form. From the point of view of quantum integrability the TFIC is quite special, because it can be mapped onto a non-interacting fermionic theory by means of a (nonlocal) Jordan–Wigner transformation. The case of fully *interacting* integrable models (defined as having scattering matrices that are different from ± 1) is discussed in section 7. We conclude with an outlook on some open problems of current interest in section 8.

Apart from the other contributions to this Special Issue, there have been several previous reviews [116, 118–121] on closely related topics. They differ considerably in perspective, focus, scope and style, and are therefore largely complementary to ours.

2. The essence of a global quantum quench

Our starting point is an isolated many-particle quantum system characterized by a time-independent, translationally invariant Hamiltonian $H(h)$ with only short-range interactions. Here h is a system parameter such as a magnetic field, or an interaction

J. Stat. Mech. (2016) 064002

strength. An example we will return to frequently throughout this review is the transverse field Ising chain (TFIC)

$$H(h) = -J\sum_{j=1}^{L}\sigma_j^x\sigma_{j+1}^x + h\sigma_j^z, \tag{6}$$

where σ_j^α are Pauli matrices acting on a spin-1/2 on site j of a one dimensional ring, and $\sigma_{L+1}^\alpha \equiv \sigma_1^\alpha$ ($\alpha = x, y, z$). The short-ranged nature of $H(h)$ is an essential condition, and it is known that models with infinite range interactions such as the BCS problem [122] exhibit very different behaviours when driven out of equilibrium. Let us imagine that we somehow prepare our system in the ground state $|\Psi(0)\rangle$ of $H(h_0)$. This state is highly non-generic in the sense that it has low entanglement [123–125]. At time $t = 0$ we then suddenly 'quench' the system parameter to a new value h, and then consider subsequent unitary time evolution with our new Hamiltonian $H(h)$. As the change of Hamiltonian is assumed to be instantaneous, the system remains in state $|\Psi(0)\rangle$ ('sudden approximation'). At times $t > 0$ the state of the system is found by solving the time-dependent Schrödinger equation

$$|\Psi(t)\rangle = \mathrm{e}^{-\mathrm{i}H(h)t}|\Psi(0)\rangle. \tag{7}$$

We are interested in the cases where in a large, finite volume the initial state $|\Psi(0)\rangle$ has non-zero overlaps with an exponentially large number of the eigenstates of $H(h)$. The case where $|\Psi(0)\rangle$ has non-zero overlaps with only a finite, system-size independent number of eigenstates is equivalent to the one discussed in undergraduate Quantum Mechanics courses. In terms of energy eigenstates

$$H(h)|n\rangle = E_n|n\rangle, \quad E_n \geqslant E_0, \tag{8}$$

we can express the state of the system at time t as

$$|\Psi(t)\rangle = \sum_n \langle n|\Psi(0)\rangle\, \mathrm{e}^{-\mathrm{i}E_n t}|n\rangle. \tag{9}$$

Our objective is the description of *expectation values* of a certain class of operators $\mathcal{O}$, that will be defined in detail later, in the state $|\Psi(t)\rangle$

$$\langle\Psi(t)|\mathcal{O}|\Psi(t)\rangle = \sum_{n,m}\langle\Psi(0)|n\rangle\,\langle m|\Psi(0)\rangle\,\langle n|\mathcal{O}|m\rangle \mathrm{e}^{-\mathrm{i}(E_m - E_n)t}. \tag{10}$$

All the interesting phenomena after a quantum quench arise from the presence of the oscillatory factors $\mathrm{e}^{-\mathrm{i}(E_m-E_n)t}$, which induce quantum mechanical interference effects [126], in the double sum over exponentially (in system size) many terms. We note that focussing on expectation values is not as restrictive as it may first appear, as it still allows us to consider the full probability distributions of the observables we are interested in.

A crucial property of a global quantum quench is that energy is conserved at all $t > 0$, and that the post-quench energy density is larger than the ground state energy per site

$$e = \lim_{L\to\infty}\frac{1}{L}\langle\Psi(t)|H(h)|\Psi(t)\rangle > \lim_{L\to\infty}\frac{E_0}{L}. \tag{11}$$

J. Stat. Mech. (2016) 064002

This means that through the quantum quench we explore a region of Hilbert space that is *macroscopically* different from the sector containing the ground state and low-lying excitations.

In practice one often considers more general 'quench protocols', where for example $H(h)$ and/or $|\Psi(0)\rangle$ are invariant only under translations by 2, 3, ... sites [51, 63, 127], and initial states that are not necessarily pure [78], but are described by a density matrix $\rho(0)$. Considering $\rho(0)$ to be a thermal density matrix provides a simple way of varying the energy density e 'injected' into the system. It is essential for our purposes that the initial density matrix $\rho(0)$ has a cluster decomposition property [128]

$$\lim_{|x-y|\to\infty} \mathrm{Tr}\,[\rho(0)\mathcal{O}(x)\mathcal{O}(y)] = \mathrm{Tr}\,[\rho(0)\mathcal{O}(x)]\,\mathrm{Tr}\,[\rho(0)\mathcal{O}(y)]\,, \tag{12}$$

and we elaborate on this point in appendix A. Invariance of the initial density matrix under translations is another key requirement. Inhomogeneous initial conditions have been considered by many authors in the literature, see e.g. [44, 54, 55, 106, 129–139, 140–152], and the reviews by Bernard and Doyon [153] and by Vasseur and Moore [154] in this volume, but we will not consider them here.

3. Relaxation in isolated quantum systems

Given that we are considering an isolated quantum system, an obvious question is in what sense it may relax to a stationary state at late times after we have driven it out of equilibrium. In order to sharpen the following argument, let us revisit the case discussed in section 2, namely an isolated system initially prepared in a pure state $|\Psi(0)\rangle$, that is not an eigenstate of the (time independent) Hamiltonian $H(h)$ describing the time evolution after our quantum quench. Let us now consider the following class of hermitian operators

$$\mathcal{O}_{jk} = |j\rangle\langle k| + |k\rangle\langle j|. \tag{13}$$

Their expectation values in the state $|\Psi(t)\rangle$ can be expressed using (9) as

$$\langle\Psi(t)|\mathcal{O}_{jk}|\Psi(t)\rangle = \mathrm{e}^{\mathrm{i}(E_j-E_k)t}\langle\Psi(0)|j\rangle\langle k|\Psi(0)\rangle + \text{c.c.} \tag{14}$$

We see that generically the right hand side exhibits periodic oscillatory behaviour in time. Hence the observables $\mathcal{O}_{jk}$ typically do not relax at late times. A crucial point is that $\mathcal{O}_{jk}$ are generally very nonlocal in space. As locality is an important concept in quantum quenches it is useful to define what we mean by a local operator.

Definition 1. Local Operators.

In lattice models an operator $\mathcal{O}$ is called *local* if in the thermodynamic limit $\mathcal{O}$ acts non-trivially only on a finite number of sites separated by a finite distance. For a quantum spin-1/2 chain with L sites examples of local operators are

$$\sigma_j^\alpha, \quad \sigma_j^\alpha\sigma_{j+k}^\beta, \quad \prod_{j=1}^{k}\sigma_j^{\alpha_j}, \qquad k \text{ fixed}, \tag{15}$$

where σ_j^α ($\alpha = x, y, z$) are Pauli matrices acting on site j. On the other hand operators such as

$$\sigma_1^x \sigma_{L/2}^x, \qquad \prod_{j=1}^{L/2} \sigma_j^{\alpha_j} \tag{16}$$

are nonlocal. Acting with a local operator on a state $|\psi\rangle$ does not change its macroscopic properties (e.g. its energy per volume in the thermodynamic limit).

Definition 2. Range of a local operator.

The range of a local operator $\mathcal{O}$ is the size of the largest interval on which it acts non-trivially. For the examples above we have

$$\mathrm{range}(\sigma_j^\alpha) = 1, \quad \mathrm{range}(\sigma_j^\alpha \sigma_{j+k}^\beta) = k+1, \quad \mathrm{range}\left(\prod_{j=1}^{k} \sigma_j^{\alpha_j}\right) = k. \tag{17}$$

3.1. Local relaxation

The previous argument shows that an isolated quantum system prepared in a pure state cannot relax in its entirety. However, it can and does relax *locally in space* [26, 28, 126, 155–157]. To explain this concept let us consider the example of a one-dimensional spin system with Hamiltonian H with only short-range interactions. An example would be the TFIC (6). We partition the entire system into an arbitrary but finite subsystem B and its complement A. Eventually we will take the thermodynamic limit while keeping B fixed. Let us prepare our spin system at time $t = 0$ in some initial density matrix $\rho(0)$ that is not an eigenstate of H. At later times the entire system is characterized by the density matrix

$$\rho(t) = \mathrm{e}^{-\mathrm{i}Ht} \rho(0) \mathrm{e}^{\mathrm{i}Ht}. \tag{18}$$

The *reduced density matrix* of the subsystem B is obtained by tracing out the degrees of freedom in A

$$\rho_B(t) = \mathrm{Tr}_A \rho(t). \tag{19}$$

It is instructive to give an explicit representation of the reduced density matrix for our spin chain example. An orthonormal basis of states is given by

$$|\sigma_1, \sigma_2, \ldots, \sigma_L\rangle = \bigotimes_{j=1}^{L} |\sigma_j\rangle_j, \quad \sigma_j = \pm 1, \tag{20}$$

where $|\sigma_j\rangle_j$ denote the two eigenstates of S_j^z. Let us take our subsystem B to consist of sites $1, 2, \ldots \ell$ for simplicity. The reduced density matrix is then

$$\begin{aligned} \rho_B(t) &= \sum_{\sigma_{\ell+1}, \ldots, \sigma_L} \left(\bigotimes_{k=\ell+1}^{L} {}_k\langle\sigma_k| \right) \rho(t) \left(\bigotimes_{n=\ell+1}^{L} |\sigma_n\rangle_n \right) \\ &= 2^{-\ell} \sum_{\alpha_1, \ldots, \alpha_\ell = 0, x, y, z} \mathrm{Tr}\left[\rho(t) \sigma_1^{\alpha_1} \sigma_2^{\alpha_2} \ldots \sigma_\ell^{\alpha_\ell}\right] \sigma_1^{\alpha_1} \sigma_2^{\alpha_2} \ldots \sigma_\ell^{\alpha_\ell}, \end{aligned} \tag{21}$$

J. Stat. Mech. (2016) 064002

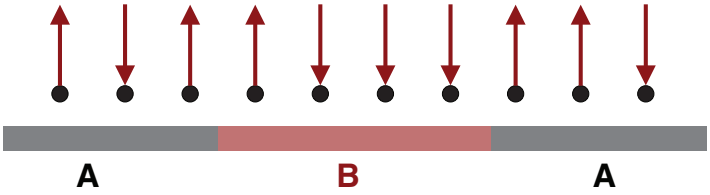

Figure 1. Local relaxation in an isolated many-particle quantum system: we partition the entire system into an arbitrary *finite* subsystem B and its complement A. We then take the thermodynamic limit while keeping B fixed. Expectation values of all operators that act non-trivially only in B will relax to stationary values at late times.

where we have defined $\sigma_j^0 = \mathbb{1}_j$. Equation (21) shows that the matrix elements of $\rho_B(t)$ are equal to particular correlation functions of local operators acting non-trivially only on B, and that $\rho_B(t)$ in fact encodes all such correlators.

Definition 3. Local Relaxation.

We say that our system relaxes locally if the limit

$$\lim_{t\to\infty}\lim_{L\to\infty}\rho_B(t) = \rho_B(\infty) \tag{22}$$

exists for any finite subsystem B (see figure 1).

Definition 4. Stationary State.

Consider a system that relaxes locally in the sense just defined. Then its stationary state is defined as a time-independent density matrix ρ^{SS} for the full system such that for any finite subsystem B

$$\lim_{L\to\infty}\mathrm{Tr}_A(\rho^{\mathrm{SS}}) = \rho_B(\infty), \tag{23}$$

where A is the complement of B. We stress that this equivalence applies only at the level of finite subsystems in the thermodynamic limit and not for the density matrices of the full system.

Definition 5. Local equivalence of ensembles.

Let ρ_1 and ρ_2 be two density matrices. We call the corresponding two ensembles locally equivalent, if in the thermodynamic limit the reduced density matrices for any finite subsystem B coincide, i.e.

$$\lim_{|A|\to\infty}\mathrm{Tr}_A(\rho_1) = \lim_{|A|\to\infty}\mathrm{Tr}_A(\rho_2). \tag{24}$$

Here A is the complement of B and $|A|$ denotes its volume. We denote local equivalence by

$$\rho_1 =_{\mathrm{loc}} \rho_2. \tag{25}$$

A key problem in the field of non-equilibrium dynamics is the determination of the stationary state density matrix. A crucial role is played by symmetries of the

J. Stat. Mech. (2016) 064002

Hamiltonian. In translationally invariant systems there are essentially two paradigms for local relaxation, and we turn to their respective descriptions next. Before doing so an important comment is in order. By design our focus is on local operators, which in turn leads us to define local relaxation in the sense formulated above. In practice one might be interested in observables that are formally not captured by our framework, and yet might relax to stationary values. An example would be expectation values of the momentum distribution function, which is the Fourier transform of the single particle Green's function [24, 158]. The relaxational properties of such quantities are at present not understood in general, and further investigation is called for.

3.2. Thermalization

As we are dealing with an isolated system, energy is always a conserved quantity

$$E = \mathrm{Tr}(\rho(t)H) = \mathrm{Tr}(\mathrm{e}^{-\mathrm{i}Ht}\rho(0)\mathrm{e}^{\mathrm{i}Ht}H) = \mathrm{Tr}(\rho(0)H). \tag{26}$$

In absence of other conserved quantities isolated systems are believed to locally relax to thermal equilibrium. This is known as *thermalization* [1, 159, 160]. In the framework we have set up, this means that our stationary state is described by a Gibbs ensemble

$$\rho^{\mathrm{SS}} =_{\mathrm{loc}} \rho^{\mathrm{Gibbs}} = \frac{\mathrm{e}^{-\beta_{\mathrm{eff}}H}}{\mathrm{Tr}(\mathrm{e}^{-\beta_{\mathrm{eff}}H})}. \tag{27}$$

Here the inverse effective temperature β_{eff} is fixed by the initial value of the energy density

$$e \equiv \lim_{L\to\infty}\frac{1}{L}\mathrm{Tr}(\rho(0)H) = \lim_{L\to\infty}\frac{1}{L}\mathrm{Tr}(\rho^{\mathrm{Gibbs}}H). \tag{28}$$

We once again stress that (27) implies only that in the thermodynamic limit the stationary state is *locally* indistinguishable from a Gibbs ensemble in the sense that expectation values of all operators that act non-trivially only in a finite subsystem are identical to the corresponding thermal expectation values. The physical picture underlying thermalization is that the infinitely large complement of our subsystem acts like a heat bath with an effective inverse temperature β_{eff}.

We note that β_{eff} defined in this way can be either positive or negative. The meaning of a negative temperature in this context is as follows. Let us consider a Hamiltonian with bounded spectrum (e.g. a quantum spin model). Then the average energy associated with H is

$$\bar{e} = \lim_{L\to\infty}\frac{1}{L}\mathrm{Tr}(H). \tag{29}$$

Depending on our initial density matrix we now have two possibilities

$$\begin{aligned} e < \bar{e} &\Rightarrow \beta_{\mathrm{eff}} > 0, \\ e > \bar{e} &\Rightarrow \beta_{\mathrm{eff}} < 0. \end{aligned} \tag{30}$$

We note that negative temperature ensembles have been observed experimentally in [161].

J. Stat. Mech. (2016) 064002

3.3. Generalized Gibbs ensembles (GGE)

We now turn to the case of systems with additional *local conservation laws* $I^{(n)}$. These are operators that commute with the Hamiltonian

$$[H, I^{(n)}] = 0, \tag{31}$$

and have the property that their densities are local operators. In most of the cases of interest these conservation laws also commute with one another

$$[I^{(n)}, I^{(m)}] = 0, \tag{32}$$

and we will assume this to be the case in the following. We note that exceptions to (32) are known [51, 92, 93] (see also section 3.3.1). What we mean by local conservation laws is best explained by an example. The TFIC (6) has infinitely many local conservation laws in the thermodynamic limit [162]

$$\begin{aligned} I^{(1,+)} &= H(h), \\ I^{(n,+)} &= -J\sum_j (S^{xx}_{j,j+n} + S^{yy}_{j,j+n-2}) + h(S^{xx}_{j,j+n-1} + S^{yy}_{j,j+n-1}) \equiv \sum_j \mathcal{I}^{(n,+)}_j, \\ I^{(n,-)} &= -J\sum_j (S^{xy}_{j,j+n} - S^{yx}_{j,j+n}) \equiv \sum_j \mathcal{I}^{(n,-)}_j, \end{aligned} \tag{33}$$

where $n \geqslant 1$ and we have defined

$$S^{\alpha\beta}_{j,j+\ell} = \sigma^\alpha_j \left[\prod_{k=1}^{\ell-1} \sigma^z_{j+k}\right] \sigma^\beta_{j+\ell}, \quad S^{yy}_{j,j} = -\sigma^z_j. \tag{34}$$

The conservation laws themselves are *extensive*, but their densities $\mathcal{I}^{(n,\pm)}_j$ involve only finite numbers of neighbouring sites ($n+1$ sites for $I^{(n,\pm)}$). As a consequence of (31), expectation values of the conservation laws as well as their densities are time independent

$$\frac{1}{L}\mathrm{Tr}(\rho(t) I^{(n,\pm)}) = \mathrm{Tr}(\rho(t)\mathcal{I}^{(n,\pm)}_j) = \frac{1}{L}\mathrm{Tr}(\rho(0) I^{(n,\pm)}) \equiv \frac{E^{(n,\pm)}}{L}, \tag{35}$$

where in the first step we used translational invariance. An obvious question at this point is why we insist on conservation laws to be local. The answer lies in the simple fact that *any* Hamiltonian has at least as many nonlocal conservation laws as there are basis states in the Hilbert space. Let us consider one-dimensional projectors on energy eigenstates

$$H|n\rangle = E_n|n\rangle, \quad P_n = |n\rangle\langle n|. \tag{36}$$

Then we clearly have

$$[P_n, P_m] = 0 = [P_n, H], \tag{37}$$

which imply that the expectation values of all P_n are time independent. Importantly, these conservation laws are not local, and as they exist for any Hamiltonian they are not expected to have any profound effect. In contrast, local conservation laws are

rather special and, as is clear from (35), have important consequences for local relaxation after quantum quenches.

An immediate consequence of (35) is that systems with local conservation laws cannot thermalize after a quantum quench, because the system retains memory of the initial expectation values of all conserved quantities at all times. The maximum entropy principle [163] then suggests that the stationary state density matrix should be given by a GGE [164]

$$\rho^{\mathrm{GGE}} = \frac{\mathrm{e}^{-\sum_n \lambda_n I^{(n)}}}{\mathrm{Tr}\left(\mathrm{e}^{-\sum_n \lambda_n I^{(n)}}\right)}. \tag{38}$$

Here λ_n are Lagrange multipliers that are fixed by the initial conditions (35), as we require that

$$\lim_{L\to\infty} \frac{E^{(n,\pm)}}{L} = \lim_{L\to\infty} \frac{1}{L} \mathrm{Tr}(\rho^{\mathrm{GGE}} I^{(n)}). \tag{39}$$

3.3.1. Local conservation laws versus mode occupation numbers In free theories GGEs are often formulated using conserved mode occupation numbers [164]. This is usually equivalent to our formulation in terms of local conservation laws in these cases [28] as we now demonstrate for a simple example. Let us consider a fermionic tight binding model

$$H = -J\sum_j c_j^\dagger c_{j+1} + c_{j+1}^\dagger c_j - \mu \sum_j c_j^\dagger c_j, \quad \{c_j, c_n^\dagger\} = \delta_{j,n}. \tag{40}$$

The Hamiltonian is easily diagonalized by going to momentum space

$$H = \sum_k \left[-2J\cos(k) - \mu\right] c^\dagger(k) c(k). \tag{41}$$

The mode occupation operators $n(k) = c^\dagger(k)c(k)$ commute with the Hamiltonian and with one another. However, the $n(k)$ are neither local nor extensive. An equivalent set of local, extensive conserved quantities is easily found

$$\begin{aligned} I^{(n,+)} &= 2J\sum_k \cos(nk)\; c^\dagger(k)c(k) = J\sum_j c_j^\dagger c_{j+n} + c_{j+n}^\dagger c_j, \\ I^{(n,-)} &= 2J\sum_k \sin(nk)\; c^\dagger(k)c(k) = \mathrm{i}J\sum_j c_j^\dagger c_{j+n} - c_{j+n}^\dagger c_j. \end{aligned} \tag{42}$$

The crucial point is that these conservation laws are *linearly* related to the mode occupation numbers. This implies that the GGE describing the stationary state after a quantum quench to the Hamiltonian H can be constructed either from the local conservation laws, or from the mode occupation numbers

$$\rho^{\mathrm{GGE}} = \frac{\mathrm{e}^{-\sum_n \lambda_{n,+} I^{(n,+)} + \lambda_{n,-} I^{(n,-)}}}{\mathrm{Tr}\left(\mathrm{e}^{-\sum_n \lambda_{n,+} I^{(n,+)} + \lambda_{n,-} I^{(n,-)}}\right)} = \frac{\mathrm{e}^{-\sum_k \mu_k\, n(k)}}{\mathrm{Tr}(\mathrm{e}^{-\sum_k \mu_k\, n(k)})}. \tag{43}$$

J. Stat. Mech. (2016) 064002

At this point a word of caution is in order. There are cases in which local conservation laws exist that cannot be expressed in terms of mode occupation operators. In non-interacting theories this occurs if the dispersion relation in the finite volume has additional symmetries. An example is provided by setting $\mu = 0$ in our tight-binding model (40), in which case the dispersion has the symmetry $\epsilon(p) = -\epsilon(\pi - p)$. In this case the following operator commutes with the Hamiltonian

$$\sum_j (-1)^j [c_j c_{j+1} - c_j^\dagger c_{j+1}^\dagger] = \sum_k \mathrm{e}^{-\mathrm{i}k} c(\pi - k) c(k) + \mathrm{h.c.} \qquad (\mu = 0), \tag{44}$$

but is clearly neither expressible in terms of mode occupation operators, nor does it commute with the latter. In cases like this the stationary state is not always locally equivalent to a GGE of the form (43) since the constraints arising from the additional local charges must be imposed as well [51, 93, 165].

3.4. Generalized microcanonical ensemble (GMC)

In equilibrium Statistical Physics it is well known that in the thermodynamic limit the Gibbs ensemble becomes equivalent to the microcanonical ensemble. In the quench context analogous equivalences of ensembles hold, and we now turn to their discussion.

3.4.1. Generic systems We have stated above that generic systems thermalize when their stationary state density matrix is equal to a Gibbs ensemble in the sense of (23) and (27), where the effective temperature is fixed by the energy density e given by (28). There is strong numerical evidence [160, 166–175] that an equivalent microcanonical ensemble can be constructed in the form

$$\rho^{\mathrm{MC}} = |n\rangle\langle n|, \tag{45}$$

where $|n\rangle$ is *any* energy eigenstate (of the post-quench Hamiltonian) with energy density e. Importantly, no averaging over a microcanonical energy shell is required. This implies that in generic systems all energy eigenstates at a given energy density are locally indistinguishable and thermal. The microcanonical description for the stationary state of a thermalizing system is then

$$\rho^{\mathrm{SS}} =_{\mathrm{loc}} \rho^{\mathrm{MC}}. \tag{46}$$

3.4.2. Systems with local conservation laws If a system has local conservation laws other than energy the above construction needs to be modified. This was first discussed in the non-interacting case by Cassidy *et al* [22] and subsequently generalized to interacting integrable models by Caux and Essler [176]. Let us recall that the 'initial data' for a (post quench) system with local conservation laws $I^{(n)}$ and Hamiltonian $H = I^{(1)}$ is

$$\mathrm{e}^{(n)} = \lim_{L\to\infty} \frac{1}{L} \mathrm{Tr}(\rho(0) I^{(n)}). \tag{47}$$

The stationary state is then locally equivalent to the density matrix

$$\rho^{\mathrm{SS}} =_{\mathrm{loc}} \rho^{\mathrm{GMC}} = |\Phi\rangle\langle\Phi|, \tag{48}$$

where $|\Phi\rangle$ is a simultaneous eigenstate of all local conservation laws such that

$$\lim_{L\to\infty}\left[\frac{1}{L}I^{(n)}-\mathrm{e}^{(n)}\right]|\Phi\rangle=0. \tag{49}$$

Conditions (49) ensure that all $I^{(n)}$ have the correct expectation values (47) in the stationary state. An obvious question is how to construct $|\Phi\rangle$ in practice. For non-interacting lattice models this is often straightforward as we now discuss. In free theories the Hamiltonian is diagonalized in terms of mode occupation operators $n(k)=c^\dagger(k)c(k)$

$$H=\sum_k \epsilon(k)n(k),\quad [n(k),n(q)]=0=[n(k),H]. \tag{50}$$

As discussed above the $n(k)$ are in one-to-one correspondence with local conservation laws and can therefore be used to construct GGEs. The initial conditions (47) therefore fix the densities $\rho(k)$ of particles with momentum k

$$\mathrm{Tr}(\rho(0)n(k))=\rho(k). \tag{51}$$

In a large, finite volume L, the state $|\Phi\rangle$ can then be taken as a Fock state

$$|\Phi\rangle=\prod_{j=1}^{N}c^\dagger(k_j)|0\rangle,\quad c(q)|0\rangle=0. \tag{52}$$

The k_j need to be chosen to reproduce the correct particle density $\rho(k)$ in the thermodynamic limit $N,L\to\infty$, $n=N/L$ fixed. Noting that $\Delta n=\rho(k)\Delta k$ we see that a possible choice is

$$k_{j+1}=k_j+\frac{1}{L\rho(k_j)}. \tag{53}$$

In practice we can determine $\rho(k)$ from (51), construct the state $|\Phi\rangle$ from (52) and (53), and then use it to form ρ^{GMC}. In interacting theories the construction is analogous but considerably more involved and will be discussed in section 7.

In contrast to the non-integrable case, energy eigenstates at a given energy density e are *not* all locally indistinguishable and thermal. While the *typical* state at a given e is thermal in this case as well, there exist other, non-thermal, macro-states at a given e. However, their entropies are smaller than the one of the thermal equilibrium state. A more detailed discussion is given in appendix B.

3.5. Time averaged relaxation and diagonal ensemble

In the literature a different definition of relaxation after quantum quenches in finite systems is widely used [118, 121]. Let us for simplicity consider a one-dimensional system on a ring of length L, which is initially prepared in a state with density matrix $\rho(0)$. The *time average* of an operator $\mathcal{O}$ is then defined as

$$\bar{\mathcal{O}}_L=\lim_{T\to\infty}\frac{1}{T}\int_0^T \mathrm{d}t\ \mathrm{Tr}(\rho(t)\,\mathcal{O}), \tag{54}$$

J. Stat. Mech. (2016) 064002

where we have introduced the subscript L to indicate that the system size is kept fixed at L, and where we assumed the limit $T\to\infty$ to exist. The operator $\mathcal{O}$ is then said to relax if its expectation value is very close to its time average most of the time, i.e. if

$$\frac{1}{T}\int_0^T \mathrm{d}t[\mathrm{Tr}(\rho(t)\,\mathcal{O})-\bar{\mathcal{O}}_L]^2 \ll \bar{\mathcal{O}}_L^2. \tag{55}$$

Physically this way of thinking about relaxation is very different from ours. This is most easily understood for a non-interacting system, which by construction features stable particle and hole excitations. Let us denote their maximal group velocity by v_{max}. In time averaged relaxation one considers times t such that $v_{\mathrm{max}}t\gg L$, i.e. the stable excitations traverse the entire system many times. In contrast, our way of defining relaxation is based on taking the thermodynamic limit first, and then considering late times.

A natural question to ask is what statistical ensemble describes the averages $\bar{\mathcal{O}}$. To see this let us consider time evolution with a Hamiltonian H that has non-degenerate eigenvalues E_n. Expanding the density matrix in the basis of energy eigenstates gives

$$\rho(t)=\sum_{n,m}\langle n|\rho(0)|m\rangle\,\mathrm{e}^{-\mathrm{i}(E_n-E_m)t}|n\rangle\langle m|. \tag{56}$$

Substituting this back into (54) and using that the energy eigenvalues are non-degenerate we arrive at

$$\bar{\mathcal{O}}_L=\sum_n\langle n|\rho(0)|n\rangle\,\langle n|\mathcal{O}|n\rangle. \tag{57}$$

This shows that time averages involve only the diagonal elements (in the energy eigenbasis) of the density matrix. The description (57) is known as *diagonal ensemble*. Is there a relation between the subsystem view of relaxation and the time-averaged one? It is believed that for local operators $\mathcal{O}$ the two viewpoints are in fact equivalent in the sense that

$$\lim_{L\to\infty}\bar{\mathcal{O}}_L=\mathrm{Tr}\,[\rho^{SS}\mathcal{O}]. \tag{58}$$

In the case of the TFIC this has been shown in appendix E of [26] and elaborated on in [30].

3.6. Symmetry restoration

An interesting question in the quantum quench context concerns problems where the Hamiltonian is invariant under a symmetry operation, but the initial state after the quench is not. If we denote the symmetry operation by U, then we have

$$[H,U]=0,\qquad U|\Psi(0)\rangle\neq|\Psi(0)\rangle. \tag{59}$$

The question is then, whether or not the symmetry associated with U is restored in the stationary state

$$[\rho^{\mathrm{SS}},U]\stackrel{?}{=}0. \tag{60}$$

The answer to this is quite straightforward for the stationary states we have considered here, which are described by (generalized) Gibbs ensembles

$$\rho^{\mathrm{SS}} =_{\mathrm{loc}} \rho_{\mathrm{GGE}} = \frac{1}{Z_{\mathrm{GGE}}} \mathrm{e}^{-\sum_n \lambda_n I^{(n)}}. \tag{61}$$

Clearly, if U is a symmetry of all local conservation laws

$$[I^{(n)}, U] = 0, \quad \forall n, \tag{62}$$

the symmetry associated with U will be restored in the stationary state. Conversely, if there is at least one conservation law for which $[I^{(s)}, U] \neq 0$, then the symmetry will remain broken in the stationary state. It is useful to consider some explicit examples.

3.6.1. Spin-flip symmetry The TFIC Hamiltonian (6) is invariant under rotations in spin space around the z-axis by 180 degrees

$$U\sigma_\ell^\alpha U^\dagger = -\sigma_\ell^\alpha, \quad \alpha = x, y, \qquad U\sigma_\ell^z U^\dagger = \sigma_\ell^z. \tag{63}$$

A quantum quench of the transverse field starting in the ordered phase $h < 1$ leads to an initial state that breaks this symmetry. However, the local conservation laws (33) that characterize the stationary state are invariant with respect to spin reflection. As a result the spin flip symmetry is restored in the stationary state [28], as will be shown in section 6.

3.6.2. Parity symmetry The Hamiltonian of the tight-binding model (40) is invariant under the parity transformation (reflection across a link)

$$Uc_\ell^\dagger U^\dagger = c_{1-\ell}^\dagger. \tag{64}$$

On the other hand, the set of charges $I^{(n,-)}$ in (42) is odd under U, and hence a quantum quench from a state that is not parity even does not generally result in a parity-symmetric stationary state. As an example we may consider the time evolution of the ground state $|\Psi(0)\rangle$ of the following Hamiltonian

$$H_0 = \sum_\ell \frac{\mathrm{i}}{4}(3c_\ell^\dagger c_{\ell+1} - 3c_{\ell+1}^\dagger c_\ell - c_\ell^\dagger c_{\ell+1}^\dagger + c_{\ell+1}c_\ell) + \mu_0 c_\ell^\dagger c_\ell. \tag{65}$$

For $|\mu_0| < \sqrt{2}$, $|\Psi(0)\rangle$ is not parity-symmetric and the expectation value of $I^{(n,-)}$ is nonzero

$$\langle\Psi(0)|I^{(n,-)}|\Psi(0)\rangle = J\frac{1-(-1)^n}{2}\frac{\cos\left(n\arcsin\left(\frac{|\mu_0|}{\sqrt{2}}\right)\right)}{\pi n} \neq 0. \tag{66}$$

As $I^{(n,-)}$ are conserved we must have

$$\lim_{L\to\infty}\frac{1}{L}\mathrm{Tr}(\rho^{\mathrm{SS}}\, I^{(n,-)}) = \lim_{L\to\infty}\frac{1}{L}\langle\Psi(0)|I^{(n,-)}|\Psi(0)\rangle, \tag{67}$$

and consequently the stationary state cannot be not symmetric under (64). We note that the above symmetry argument does not guarantee a non-zero value for the expectation value in (66), as there could be other symmetries that force it to vanish.

J. Stat. Mech. (2016) 064002

3.6.3. Translational symmetry If we allow the initial state to partially break translational symmetry the situation can become significantly more complicated. An interesting example is provided by the quantum XY model [177]

$$H_{\mathrm{XY}} = J\sum_{\ell=1}^{L} \frac{1+\gamma}{4}\sigma_\ell^x\sigma_{\ell+1}^x + \frac{1-\gamma}{4}\sigma_\ell^y\sigma_{\ell+1}^y, \tag{68}$$

where we take L to be even. As long as we consider quenches from translationally invariant initial states, the stationary behaviour is described by a GGE constructed from local conservation laws $Q^{(n,\pm)}$ along the lines described above. The situation changes for initial states $|\Psi_2(0)\rangle$ that are invariant only under translations by two sites. One might naively expect that translational symmetry gets restored in the stationary state, but this is in fact not the case [51]. This can be understood by noting that H has local conservation laws that are not translationally invariant, an example being

$$J_1^+ = \sum_{\ell=1}^{L}(-1)^\ell\left[\frac{1+\gamma}{4}\sigma_\ell^x\sigma_{\ell+1}^x - \frac{1-\gamma}{4}\sigma_\ell^y\sigma_{\ell+1}^y\right], \quad [J_1^+, H_{\mathrm{XY}}] = 0. \tag{69}$$

Generically one will have $\langle\Psi_2(0)|J_1^+|\Psi_2(0)\rangle \neq 0$, and as J_1^+ is conserved, translational invariance must remain broken at all times. The construction of a GGE in this case is complicated by the fact that J_1^+ does not commute with all $Q^{(n,\pm)}$, and involves an initial state dependent selection of mutually commuting local conservation laws.

3.7. Truncating generalized Gibbs ensembles

As we have seen above, GGEs in integrable models involve infinite numbers of conservation laws in the thermodynamic limit. A natural question to ask is whether all of these are equally important for the description of the stationary state, or whether certain classes are more important than others. A general framework for investigating this question was developed in [28] and then applied to the specific example of quenches in the TFIC. The main findings are conjectured to apply much more generally to quenches in integrable models. A key measure of importance of a given conservation law is its *degree of locality* [28] D_{loc}. This is straightforward to quantify for conservation laws like (33), which have densities that act non-trivially only on a fixed number of $n+1$ neighbouring sites,

$$I^{(n)} = \sum_j \mathcal{I}_j^{(n)}, \quad \mathrm{range}(\mathcal{I}_j^{(n)}) = n+1 \qquad \Rightarrow D_{\mathrm{loc}}(I^{(n)}) = n+1. \tag{70}$$

The idea of [28] was to select various finite subsets $\{J_m|m=1,\ldots,y\} \subset \{I^{(n)}\}$, and ask how well the density matrices

$$\rho^{\mathrm{pGGE},y} = \frac{\mathrm{e}^{-\sum_{n=1}^{y}\lambda_n^{(y)}J_n}}{\mathrm{Tr}\left(\mathrm{e}^{-\sum_{n=1}^{y}\lambda_n^{(y)}J_n}\right)} \tag{71}$$

approximate the full GGE density matrix. Here the Lagrange multipliers $\lambda_n^{(y)}$ are fixed by imposing the appropriate initial conditions

$$\lim_{L\to\infty}\frac{\langle\Psi(0)|J_n|\Psi(0)\rangle}{L}=\lim_{L\to\infty}\frac{1}{L}\mathrm{Tr}(\rho^{\mathrm{pGGE},y}J_n),\quad n=1,\ldots,y. \tag{72}$$

A useful way of comparing the full ρ^{GGE} and partial $\rho^{\mathrm{pGGE},y}$ GGEs is through a distance $\mathcal{D}(\rho_\ell,\rho'_\ell)$ on the space of reduced density matrices on an interval of length ℓ. In order for $\rho^{\mathrm{pGGE},y}$ to be a good approximation to ρ^{GGE} it should be possible to make the distance between their respective reduced density matrices arbitrarily small

$$\mathcal{D}(\rho_\ell^{\mathrm{GGE}},\rho_\ell^{\mathrm{pGGE},y})\overset{!}{<}\epsilon,\quad\forall\,\ell. \tag{73}$$

The findings of [28] show that if even a single conservation law with small degree of locality is excluded, the approximation (71) immediately becomes very poor, and the only way to achieve (73) is by retaining all conservation laws with the smallest degrees of locality (70), i.e. by considering 'truncated GGEs' of the form

$$\rho^{\mathrm{tGGE,y}}=\frac{\mathrm{e}^{-\sum_{n=1}^{y}\lambda_n^{(y)}I^{(n)}}}{\mathrm{Tr}\left(\mathrm{e}^{-\sum_{n=1}^{y}\lambda_n^{(y)}I^{(n)}}\right)}. \tag{74}$$

The value of y is then determined by the required degree of accuracy ϵ in (73). A consequence of these findings is that the full GGE can in fact be *defined* as the limit of truncated GGEs

$$\rho^{\mathrm{GGE}}\equiv\lim_{y\to\infty}\rho^{\mathrm{tGGE,y}}. \tag{75}$$

The limiting procedure (75) was originally introduced in a non-interacting model (the transverse-field Ising) [28], and has since proved very useful for the construction of GGEs and the calculation of the stationary state values of local observables in interacting integrable models [17, 58, 59, 64, 178].

To exhibit the above ideas more explicitly it is useful to consider the example of a transverse field quench in the disordered phase of the TFIC [28]. Figure 2 shows results for an appropriately defined distance between the reduced density matrices of the full and truncated GGEs as a function of the number y of conservation laws retained in (74). Ten different subsystem sized $\ell=5,10,\ldots,50$ are shown.

We see that for a given subsystem size ℓ the distance $\mathcal{D}(\rho_\ell^{\mathrm{GGE}},\rho_\ell^{\mathrm{pGGE,y}})$ starts decaying exponentially in y above an ℓ-dependent value. This means that conservation laws $I^{(n)}$ with $n\gg\ell$ play a negligible role in describing stationary state properties in a subsystem of size ℓ. The main message is then as follows:

The smaller the degree of locality of a conservation law is, the more important it is for describing the stationary properties of local observables.

3.8. Dynamical properties in the stationary state

It is clearly of interest to go beyond the equal time correlators we have discussed so far and consider dynamical (non equal time) correlations. In particular one can envisage using them to characterize the stationary state in the same way they are used in thermal equilibrium. An example would be the measurement of dynamical response

J. Stat. Mech. (2016) 064002

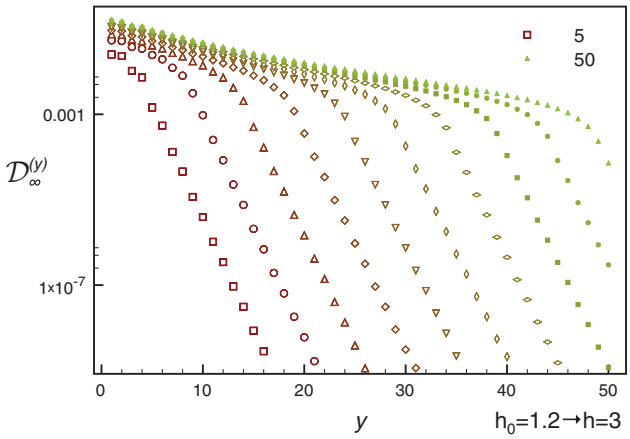

Figure 2. Distance $\mathcal{D}_\infty^{(y)} = \mathcal{D}(\rho_\ell^{\mathrm{GGE}}, \rho_\ell^{\mathrm{tGGE,y}})$, as defined in (156), between the GGE and the truncated GGEs obtained by taking into account local conservation laws with densities involving at most $y+1$ consecutive sites. The quench is from $h_0 = 1.2$ to $h = 3$ and the subsystem size ranges from $\ell = 5$ to $\ell = 50$. Colors and sizes change gradually as a function of the size ℓ. For $y > \ell$, the distance starts decaying exponentially in y, with an ℓ-independent decay rate *(Figure taken from* [28]*.)*.

functions in the stationary state by e.g. photoemission spectroscopy [179]. For such purposes the objects of interest are of the form

$$\lim_{t\to\infty} \langle \Psi(t) | \mathcal{O}_1(t_1) \cdots \mathcal{O}_n(t_n) | \Psi(t) \rangle, \qquad \mathcal{O}_j(t) = \mathrm{e}^{\mathrm{i}Ht} \mathcal{O}_j \mathrm{e}^{-\mathrm{i}Ht}, \tag{76}$$

where $\mathcal{O}_j$ are local observables. The problem one is faced with is that the descriptions of the stationary state by statistical ensembles (GGE, GMC) *a priori* hold only at the level of finite subsystems in the thermodynamic limit. On the other hand, time dependent operators act by construction non-trivially on the entire system, which moves them beyond the remit of applicability of the framework set out above. This issue was addressed in [29], which established that the stationary state density matrix ρ^{SS} that describes the local relaxation in fact provides a correct description of dynamical correlations as well, i.e.

$$\lim_{t\to\infty} \langle \Psi(t) | \mathcal{O}_1(t_1) \cdots \mathcal{O}_n(t_n) | \Psi(t) \rangle = \mathrm{Tr}[\rho^{\mathrm{SS}} \mathcal{O}_1(t_1) \cdots \mathcal{O}_n(t_n)]. \tag{77}$$

The proof of this statement is based on the Lieb–Robinson bound (see section 5.1) and more specifically on a theorem by Bravyi, Hastings, and Verstraete [180], who showed that time-evolving operators (in the Heisenberg picture) are well approximated by local operators with a range that increases linearly in time. We stress that (77) does not depend on which statistical ensemble describes the local relaxation in the stationary state, i.e. for generic systems ρ^{SS} would be a Gibbs or a microcanonical density matrix, while for integrable systems it would be that of a GGE or GMC.

The issue of whether or not a fluctuation dissipation relation (FDR) holds in the stationary state was investigated in [29, 38, 41, 181]. In thermal equilibrium, the FDR

J. Stat. Mech. (2016) 064002

connects the imaginary part of the linear response function $\chi_{AB}(\omega, \vec{q}|\rho)$ of two observables A, B to the corresponding spectral function $S_{AB}(\omega, \vec{q}|\rho)$

$$-\frac{1}{\pi}\mathrm{Im}\ \chi_{AB}(\omega, \vec{q}\ |\rho^{\mathrm{Gibbs}}(\beta)) = (1-\mathrm{e}^{-\beta\omega})S_{AB}(\omega, \vec{q}\ |\rho^{\mathrm{Gibbs}}(\beta)). \tag{78}$$

Here we have defined

$$\begin{aligned}\chi_{AB}(\omega, \vec{q}\ |\rho) &= -\frac{\mathrm{i}}{L}\sum_{j,\ell}\int_0^\infty \mathrm{d}t\ \mathrm{e}^{\mathrm{i}\omega t-\mathrm{i}\vec{q}\cdot(\vec{r}_j-\vec{r}_\ell)}\ \ \mathrm{Tr}(\rho\ [A_j(t), B_\ell]),\\ S_{AB}(\omega, \vec{q}\ |\rho) &= \frac{1}{L}\sum_{j,\ell}\int_{-\infty}^\infty \frac{\mathrm{d}t}{2\pi}\ \mathrm{e}^{\mathrm{i}\omega t-\mathrm{i}\vec{q}\cdot(\vec{r}_j-\vec{r}_\ell)}\ \ \mathrm{Tr}(\rho\ A_j(t)B_\ell).\end{aligned} \tag{79}$$

In the derivation of (78) one uses that in thermal equilibrium the spectral function for negative and positive frequencies are related in a simple way

$$S_{BA}(-\omega, -\vec{q}\ |\rho^{\mathrm{Gibbs}}(\beta)) = \mathrm{e}^{-\beta\omega}S_{AB}(\omega, \vec{q}\ |\rho^{\mathrm{Gibbs}}(\beta)). \tag{80}$$

Let us now turn to FDRs in the steady state after quantum quenches. Clearly, if the system thermalizes (27), the equilibrium FDR (78) with inverse temperature β_{eff} applies. If on the other hand the system locally relaxes to a GGE, the imaginary part of the linear response function ceases to be proportional to the spectral function [29, 38, 41]. This can be traced back to the absence of a simple relationship between the spectral functions at positive and negative frequencies. However, the basic form of the FDR still holds [29]

$$-\frac{1}{\pi}\mathrm{Im}\ \chi_{AB}(\omega, \vec{q}\ |\rho^{\mathrm{GGE}}) = S_{AB}(\omega, \vec{q}\ |\rho^{\mathrm{GGE}}) - S_{BA}(-\omega, -\vec{q}\ |\rho^{\mathrm{GGE}}). \tag{81}$$

4. A simple example

In order to see the ideas presented above at work, we now consider the specific example of a one dimensional fermionic pairing model

$$H(\Delta, \mu) = -J\sum_{j=1}^{L} c_j^\dagger c_{j+1} + c_{j+1}^\dagger c_j - \mu\sum_{j=1}^{L} c_j^\dagger c_j + \Delta\sum_{j=1}^{L} c_j^\dagger c_{j+1}^\dagger + c_{j+1}c_j. \tag{82}$$

Here $c_j^\dagger$, c_j are canonical fermion creation and annihilation operators at site j and $\{c_j, c_n^\dagger\} = \delta_{j,n}$. In momentum space we have

$$H(\Delta, \mu) = \sum_k \epsilon_0(k)\ c^\dagger(k)c(k) - \mathrm{i}\Delta\sin(k)(c^\dagger(k)c^\dagger(-k) - c(-k)c(k)), \tag{83}$$

where we have defined $\epsilon_0(k) = -2J\cos(k) - \mu$ and

$$c_j = \frac{1}{\sqrt{L}}\sum_k \mathrm{e}^{-\mathrm{i}kj}c(k). \tag{84}$$

J. Stat. Mech. (2016) 064002

The Hamiltonian (83) is diagonalized by a Bogoliubov transformation

$$\begin{pmatrix} \alpha(k) \\ \alpha^\dagger(-k) \end{pmatrix} = \begin{pmatrix} \cos(\Theta_k/2) & -\mathrm{i}\sin(\Theta_k/2) \\ -\mathrm{i}\sin(\Theta_k/2) & \cos(\Theta_k/2) \end{pmatrix} \begin{pmatrix} c(k) \\ c^\dagger(-k) \end{pmatrix}, \quad k \neq 0, \tag{85}$$

where

$$\epsilon(k) = \sqrt{(2J\cos(k)+\mu)^2 + 4\Delta^2\sin^2(k)}, \quad \mathrm{e}^{\mathrm{i}\Theta_k} = \frac{-2J\cos(k) - \mu + 2\mathrm{i}\Delta\sin(k)}{\epsilon(k)}. \tag{86}$$

Defining $\alpha(0) = c^\dagger(0)$ we find

$$H(\Delta,\mu) = \sum_k \epsilon(k)\, \alpha^\dagger(k)\alpha(k) + \text{const.} \tag{87}$$

Let us now implement a quantum quench by initially preparing our system in the ground state of $H(\Delta,\mu)$, and at $t=0$ quenching the pairing amplitude from Δ to zero. The initial state is the Bogoliubov fermion vacuum

$$|\Psi(0)\rangle = |0\rangle, \quad \alpha(k)|0\rangle = 0 \ \forall k. \tag{88}$$

The time evolution of the fermion annihilation operators is obtained by solving the Heisenberg equations of motion $\frac{\mathrm{d}}{\mathrm{d}t}c(k,t) = \mathrm{i}[H(0,\mu), c(k,t)] = -\mathrm{i}\epsilon_0(k)c(k,t)$, which gives

$$c(k,t) = \mathrm{e}^{-\mathrm{i}\epsilon_0(k)t}c(k) = \mathrm{e}^{-\mathrm{i}\epsilon_0(k)t}\left[\cos(\Theta_k/2)\,\alpha(k) - \mathrm{i}\sin(\Theta_k/2)\,\alpha^\dagger(-k)\right]. \tag{89}$$

The fermion two-point functions at $t>0$ are thus equal to

$$\begin{aligned} \langle\Psi(t)|\, c^\dagger(k)c(q)|\Psi(t)\rangle &= \langle 0|\, c^\dagger(k,t)c(q,t)|0\rangle = \delta_{k,q}\sin^2(\Theta_k/2), \\ \langle\Psi(t)|\, c(k)c(q)|\Psi(t)\rangle &= \delta_{k,-q}\frac{\mathrm{i}}{2}\sin\Theta_k\ \mathrm{e}^{-2\mathrm{i}\epsilon_0(k)t}. \end{aligned} \tag{90}$$

In position space we obtain

$$\begin{aligned} \langle\Psi(t)|\, c^\dagger_{j+\ell}c_j|\Psi(t)\rangle &= \frac{1}{L}\sum_k \mathrm{e}^{\mathrm{i}k\ell}\sin^2(\Theta_k/2) = f_L(\ell), \\ \langle\Psi(t)|\, c_{j+\ell}c_j|\Psi(t)\rangle &= \frac{1}{L}\sum_k \mathrm{e}^{-\mathrm{i}k\ell}\frac{\mathrm{i}}{2}\sin\Theta_k\ \mathrm{e}^{-2\mathrm{i}\epsilon_0(k)t} = g_L(\ell,t). \end{aligned} \tag{91}$$

Importantly, multi-point correlation functions can be calculated by Wick's theorem, e.g.

$$\langle\Psi(t)|\, c^\dagger_j c^\dagger_k c_n c_m|\Psi(t)\rangle = g^*_L(k-j,t)g_L(n-m,t) - f_L(j-n)f_L(k-m) + f_L(k-n)f_L(j-m). \tag{92}$$

In the limit $L\to\infty$ we can turn the sums in (91) into integrals, which at late times can be evaluated by a stationary phase approximation. At infinite times we obtain

$$\begin{aligned} \lim_{L\to\infty} f_L(\ell) &= \int_0^{2\pi}\frac{\mathrm{d}k}{2\pi}\,\mathrm{e}^{\mathrm{i}k\ell}\ \sin^2(\Theta_k/2), \\ \lim_{t\to\infty}\lim_{L\to\infty} g_L(\ell,t) &= 0. \end{aligned} \tag{93}$$

Importantly the 'anomalous' average $\langle\Psi(t)|\, c_{j+\ell}c_j|\Psi(t)\rangle$ vanishes in this limit. We can now immediately conclude that our system relaxes locally to some steady state: any operator $\mathcal{O}$ acting non-trivially only on a given, finite subsystem B can be expressed in terms of fermionic creation and annihilation operators acting only on sites in B. We then can use Wick's theorem to express the expectation value of $\langle\Psi(t)|\mathcal{O}|\Psi(t)\rangle$ in terms of the functions $f_L(\ell)$ and $g_L(\ell, t)$. After taking the infinite volume limit $L\to\infty$, the limit $t\to\infty$ of the resulting expression exists. This argument shows that the steady state is completely characterized by the two-point functions (93) and the fact that Wick's theorem holds.

4.1. Generalized Gibbs ensemble

According to our previous discussion the steady state should be described by the GGE (43), where the Lagrange multipliers are fixed by

$$\mathrm{Tr}[\rho^{\mathrm{GGE}}c^\dagger(k)c(k)] = \frac{1}{1+\mathrm{e}^{\mu_k}} = \langle\Psi(0)|\, c^\dagger(k)c(k)|\Psi(0)\rangle = \sin^2(\Theta_k/2). \tag{94}$$

As the GGE density matrix is Gaussian a Wick's theorem holds, and as a consequence of (94) the two-point functions in the GGE coincide with those of our steady state. As we have a Wick's theorem in the steady state as well, the GGE correctly reproduces *all* multi-point correlation functions. This proves that the steady state in our example is locally equivalent to the GGE (43) and (94).

5. Spreading of correlations after a quantum quench

Let us now turn to the time dependence of the expectation values of local operators after a quantum quench. As an example we consider the connected correlation function of the fermionic density $n_j = c_j^\dagger c_j$ in our example of section 4

$$S_L(\ell, t) = \langle\Psi(t)|\, n_{j+\ell}n_j|\Psi(t)\rangle - \langle\Psi(t)|\, n_{j+\ell}|\Psi(t)\rangle\langle\Psi(t)|\, n_j|\Psi(t)\rangle. \tag{95}$$

Application of Wick's theorem gives

$$S_L(\ell, t) = |\, g_L(-\ell, t)|^2 - |\, f_L(\ell)|^2. \tag{96}$$

It is convenient to isolate the time dependent part $|\, g_L(-\ell, t)|^2$, which is shown in figure 3 for a quantum quench, where we start in the ground state of $H(\Delta = 2J, \mu = -J)$ and time evolve with $H(0, \mu = -J)$. At a fixed value of ℓ the connected correlator is exponentially small (in ℓ) until a time

$$t_{\mathrm{F}} = \frac{\ell}{2v_{\max}}, \tag{97}$$

where in our example $v_{\max} = 2J$ is the maximal group velocity of elementary particle and hole excitations of our post-quench Hamiltonian $H(0, \mu = -J)$. At $t \approx t_{\mathrm{F}}$ the connected correlator increases substantially, goes through a maximum, and then decays in an oscillating fashion. A physical explanation for the light cone effect was provided

J. Stat. Mech. (2016) 064002

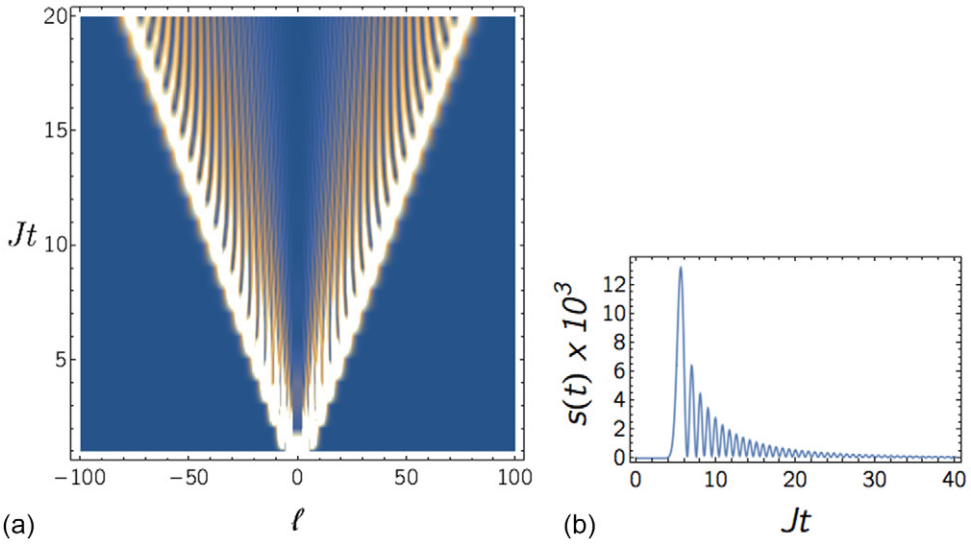

Figure 3. (a) Time dependent part $S_\infty(\ell, t) + |f_\infty(\ell)|^2$ of the connected density-density correlator after a quantum quench where the system is initialized in the ground state of $H(\Delta = 2J, \mu = -J)$, and time evolved with $H(0, \mu = -J)$. A light cone effect is clearly visible. (b) $s(t) = S_\infty(\ell = 20, t) + |f_\infty(20)|^2$ as a function of time.

by Calabrese and Cardy [80, 89]. For a non-interacting, non-relativistic theory like the one in our example it goes as follows. We focus on connected correlation functions of local operators, e.g.

$$G_{\mathcal{O}\mathcal{O}}(r_1, r_2; t) = \langle\Psi(t)|\mathcal{O}(r_1)\mathcal{O}(r_2)|\Psi(t)\rangle - \langle\Psi(t)|\mathcal{O}(r_1)|\Psi(t)\rangle\langle\Psi(t)|\mathcal{O}(r_2)|\Psi(t)\rangle. \tag{98}$$

This is the average of the simultaneous measurement of the observables $\mathcal{O}(r_j)$ minus the product of the averages of separate measurements of $\mathcal{O}_j$ at time t after the quench. The initial state in our case is characterized by a finite correlation length ξ

$$G_{\mathcal{O}\mathcal{O}}(r_1, r_2; t = 0) \propto \mathrm{e}^{-|r_1 - r_2|/\xi}, \tag{99}$$

and is therefore extremely small at large spatial separations. At time $t = 0$ the quantum quench generates a finite density of stable quasiparticle excitations throughout the system. Their dispersion relation is $\epsilon_0(p)$ as our post-quench Hamiltonian is simply $H(0, \mu) = \sum_k \epsilon_0(k) n(k)$. The maximal group velocity of these free fermionic excitations is

$$v_{\max} = \max_p \frac{\mathrm{d}\epsilon_0(p)}{\mathrm{d}p} = 2J. \tag{100}$$

At times $t > 0$ the quasi-particles created by the quench propagate through the system. A measurement at r_j will be influenced by quasi-particles from within the 'backwards light cone' $[r_j - v_{\max}t, r_j + v_{\max}t]$. At all times $t > 0$ this will affect the value of the 1-point functions $\langle\Psi(t)|\mathcal{O}(r_j)|\Psi(t)\rangle$, but the effect cancels in the *connected* two-point function. At time $t^* = \frac{|r_2 - r_1|}{2v_{\max}}$ the backwards light cones emanating from r_1 and r_2 touch,

and the average of measurements at r_1 and r_2 becomes correlated. These connected correlations are induced by quasi-particle pairs created at time $t = 0$ and propagating with group velocities $v_{\max}$ in opposite directions.

Since the work of Calabrese and Cardy light cone effects after quantum quenches have been analyzed in a number of lattice models [25–27, 48, 182–185] and observed in experiments on systems of ultra-cold atomic gases [9, 10] and trapped ions [16, 17]. The experimental work raises the poignant theoretical issue of which velocity underlies the observed light cone effect in non-relativistic systems at finite energy densities. Here there is no unique velocity of light, and quasi-particles in interacting systems will generally have finite life times depending on the details of the initial density matrix. For the case of the spin-1/2 Heisenberg XXZ chain, an integrable model, it was shown in [56] that the light cone propagation velocity in general depends on the energy density of the initial state, and an explanation for this effect in terms of properties of stable excitations at finite energy densities was put forward. More recent theoretical works address the influence of long-range interactions on the spreading of correlations [186–191]. Sufficiently long-range interactions lead to a destruction of light cone effects. Non-relativistic continuum models are also known to exhibit modifications to light cone behaviour [110].

It is useful to contrast the above discussion to the spreading of correlations in equilibrium and after 'local quantum quenches' [192]. In the latter context one is concerned with the spreading of a local perturbation that has been imposed on an equilibrium state. Light cone effects are observed in such situations as well, but the spreading occurs at the maximum group velocity of elementary excitations over the equilibrium state that is being considered. In other words, unlike for global quantum quenches, there is no factor of two.

5.1. Relation to Lieb–Robinson bounds

As shown by Lieb and Robinson [193, 194], the velocity of information transfer in quantum spin chains is effectively bounded. More precisely, there exists a causal structure in commutators of local operators at different times

$$\|[\mathcal{O}_A(t), \mathcal{O}_B(0)]\| \leqslant c \, \min(|A|, |B|) \, \|\mathcal{O}_A\| \, \|\mathcal{O}_B\| \, \mathrm{e}^{-\frac{L-vt}{\xi}}. \tag{101}$$

Here $\mathcal{O}_A$ and $\mathcal{O}_B$ are local operators acting non-trivially only in two subsystems A and B that are spatially separated by a distance L, $\|.\|$ denotes the operator norm and $|A|$ the number of sites in subsystem A. Finally, c, v and ξ are constants. More recently, the Lieb–Robinson bounds have been refined [195, 196] and extended to mixed state dynamics in open quantum systems [196, 197].

The Lieb–Robinson bound has important consequences for quantum quenches starting in initial states with finite correlation lengths, and time evolving under a short-ranged Hamiltonian. It was shown in [180] that (101) implies a bound on the connected two-point correlation functions after such quenches

$$\langle \Psi(t)|\mathcal{O}_A \, \mathcal{O}_B|\Psi(t)\rangle_{\mathrm{conn}} < \bar{c}(|A| + |B|) \, \mathrm{e}^{-\frac{L-2vt}{\chi}}. \tag{102}$$

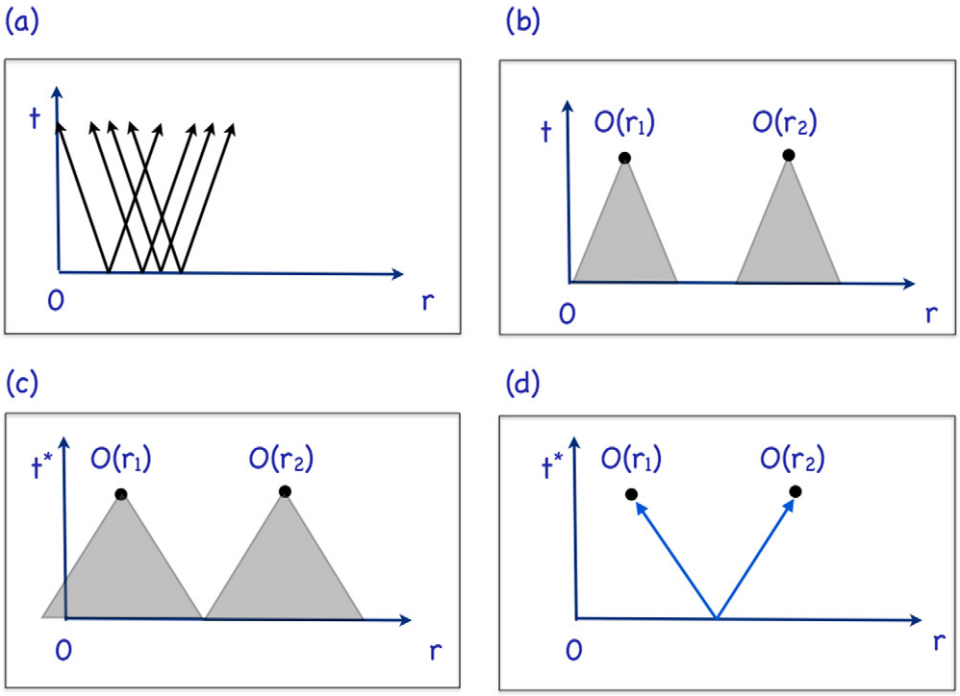

Figure 4. 'Quasi-particle picture' for the light cone effect [89]: (a) At time $t = 0$ the quantum quench creates quasi-particle excitations throughout the system. (b) At time t quasi-particles from within the 'backward light cone' $[r_j - v_{\max}t, r_j + v_{\max}t]$ will affect a measurement at position r_j. This leads to de-phasing of 1-point functions $\langle\Psi(t)|\mathcal{O}(r_j)|\Psi(t)\rangle$. (c) At time $t^* = \frac{|r_2 - r_1|}{2v_{\max}}$ the backwards light cones touch, and measurements at r_1 and r_2 become correlated. (d) Connected correlations are induced by quasi-particle pairs created at time $t = 0$ and propagating with group velocities $v_{\max}$ in opposite directions.

Here $\bar{c}$, v and χ are constants. The bound (102) shows that connected two-point functions of local operators after quantum quenches in spin chains are exponentially small up to times $t = L/2v$ (see figure 4). This tallies very nicely with the light cone effects discussed above. We note that the bound does not provide values for the velocity v or the length χ.

5.2. Finite-size effects

Throughout our discussion we have stressed that we are ultimately interested in taking the thermodynamic limit. In a large but finite system local observables can never truly relax. There always will be *recurrences* [198] such that the return amplitude $\mathcal{F}(t) = |\langle\Psi(0)|\Psi(t)\rangle|$ is arbitrarily close to 1

$$|1 - \mathcal{F}(t)| < \epsilon. \tag{103}$$

However, in many-particle systems these typically occur only at astronomically late times. The exception to this rule are cases in which the spectrum of the post-quench Hamiltonian in a (large) finite volume for some reason has a highly commensurate structure. A very simple example are Hamiltonians with equidistant energy levels $E_n = E_0 + n\delta$, for which we have $\mathcal{F}(2\pi j/\delta) = 1$.

J. Stat. Mech. (2016) 064002

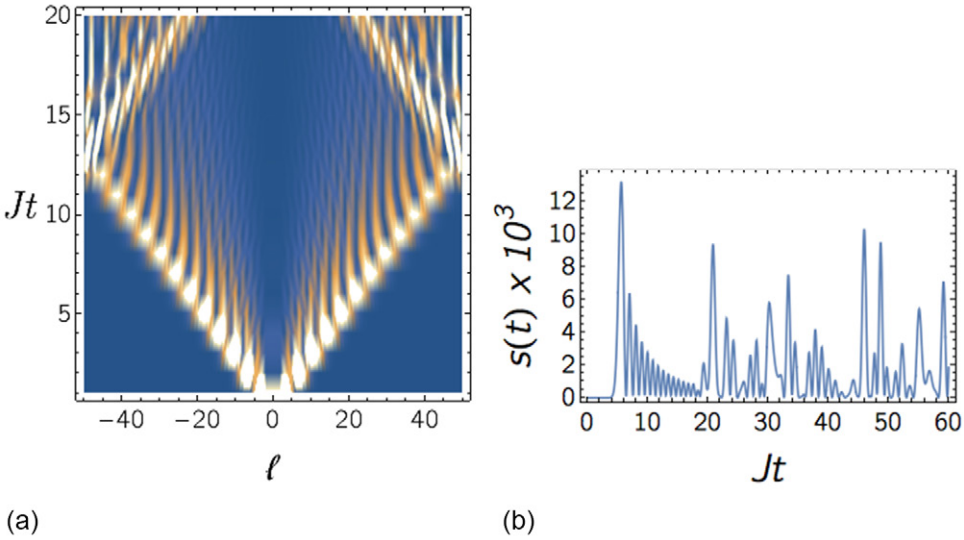

Figure 5. (a) Same as figure 3 but for a finite system with $L = 100$ sites and periodic boundary conditions. At times $Jt > 12.5$ the light cone has traversed the system and eventually causes a revival of the connected correlation function at a given separation ℓ. This is strictly a finite-size effect and has no analog in the thermodynamic limit. (b) $s(t) = S_L(\ell = 20, t) + |f_L(20)|^2$ for $L = 100$ as a function of time.

A more relevant effect in practice are *revivals*, which refers to situations where $\mathcal{F}(t) = \mathcal{O}(1)$. This again requires the finite size energy spectrum to have a certain regularity, as is the case for example in conformal field theories [88, 91].

A different finite-size effect affects all observables and is related to the light cone repeatedly traversing the system [37, 50, 104, 106]. We refer to this effect as a *traversal*. As an example we consider the connected two point function (95) on a finite ring. A density plot is shown for a system of size $L = 100$ in figure 5. We see that the light cone traverses the system and induces a signal in $S_L(\ell, t)$ at a time $(L - |\ell|)/2v_{\max}$ after the light cone first reaches. Clearly at times $t > (L - |\ell|)/2v_{\max}$ correlation functions of the finite system look very different from the ones in the thermodynamic limit. As is shown in figure 6, the traversal in not associated with any revival, because the return amplitude remains exponentially small in the system size.

6. Transverse-field Ising chain (TFIC)

We now turn our attention to a key paradigm for quantum quenches, the transverse-field Ising chain

$$H(h) = -J\sum_{\ell=1}^{L} \sigma_\ell^x \sigma_{\ell+1}^x + h\sigma_\ell^z. \tag{104}$$

Here we impose periodic boundary conditions $\sigma_{L+1}^\alpha \equiv \sigma_1^\alpha$, L even, $h \geqslant 0$ and $J > 0$. We note that the signs of h and J can be reversed by unitary transformations with respectively

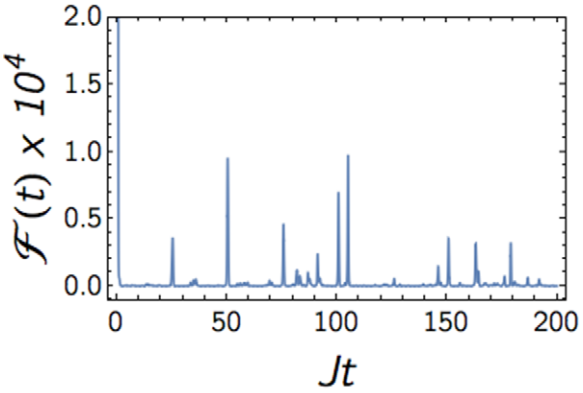

Figure 6. The return probability for the same quench as in figure 3 with $L = 100$ sites and periodic boundary conditions. The overlap with the initial state remains negligible at any time $t > 0$.

$$U_1 = \prod_{\ell=1}^{L} \sigma_\ell^x, \quad U_2 = \prod_{\ell=1}^{L/2} \sigma_{2\ell-1}^x \sigma_{2\ell}^y. \tag{105}$$

The Hamiltonian (104) has a $\mathbb{Z}_2$ symmetry of rotations by π around the z-axis. The ground state phase diagram of the TFIC features a paramagnetic (for $h > 1$) and a ferromagnetic (for $h < 1$) phase, in which the $\mathbb{Z}_2$ symmetry is spontaneously broken. The two phases are separated by a quantum critical point at $h = 1$, which is described by the Ising conformal field theory with central charge $c = 1/2$, see [199].

It is well known that the TFIC admits a representation in terms of non-interacting fermions. However, the Jordan–Wigner transformation between spins and fermions is nonlocal. This renders the TFIC an ideal testing ground for relaxation ideas, in particular in relation to the crucial role played by locality.

The study of non-equilibrium dynamics in the TFIC was initiated in a seminal paper by Barouch, McCoy and Dresden in 1970 [45]. They analyzed the time evolution of the transverse magnetization $\langle\Psi(t)|\sigma_\ell^z|\Psi(t)\rangle$ and observed that it relaxes to a non-thermal value at late times. The focus of research on the TFIC and its two-dimensional classical counterpart then shifted to the determination of equilibrium properties, and it took thirty years before the issue of relaxation after quantum quenches returned to centre stage [34, 35]. A combination of experimental advances in cold atom systems and the theoretical insights gained through the study of quantum quenches in conformal field theories [80, 89, 90] revitalized the quest for obtaining a complete understanding of the quench dynamics in the TFIC. Exact closed form expressions for the time evolution of the entanglement entropy after a global quench were obtained in [48]. By combining free-fermion techniques with numerical methods important insights on thermalization issues were gained [33], and finite-size effects like traversals were analyzed in detail [37]. Exact results for the time evolution of order parameter correlations were finally obtained in [25–27, 40], and it was demonstrated that the stationary state is described by a generalized Gibbs ensemble. The time evolution of reduced density matrices was studied in [28], and the question of which conservation laws are most important for characterizing the stationary state with a given accuracy was resolved.

doi:10.1088/1742-5468/2016/06/064002

J. Stat. Mech. (2016) 064002

References [39, 50] introduced a semi-classical approach to quantum quenches by generalizing a method developed by Sachdev in the context of equilibrium dynamics [199]. Dynamical (non-equal time) correlations were studied in [29, 39, 50] in relation to the question whether the stationary state fulfils a fluctuation-dissipation theorem. Progress on experimental studies of non-equilibrium evolution in TFICs has been more limited. Reference [11] reported results on quantum quenches in a cold atom system described by one dimensional Bose Hubbard chains, which map onto the TFIC in a particular limit. Reference [200] proposed a realization of the TFIC with a time-dependent magnetic field in the framework of circuit QED.

6.1. Fermionic form of the Hamiltonian

Spin chains that can be mapped to free fermions differ in two important aspects from free fermion models like the one we considered in section 4:

- two-point functions of spin operators map onto n-point correlation functions of fermions, where n is related to the distance between the two spins and can be arbitrarily large;
- The ground state of the TFIC in the ordered phase is not a Fock state (as a result of spontaneous symmetry breaking).

The Hamiltonian (104) can be mapped to a fermionic theory by a Jordan–Wigner transformation

$$\sigma^z_\ell = i a_{2\ell} a_{2\ell-1}, \quad \sigma^x_\ell = \left(\prod_{j=1}^{\ell-1} (i a_{2j} a_{2j-1})\right) a_{2\ell-1}, \quad \sigma^y_\ell = \left(\prod_{j=1}^{\ell-1} (i a_{2j} a_{2j-1})\right) a_{2\ell}, \tag{106}$$

Here a_ℓ are Majorana fermions satisfying the anti-commutation relations $\{a_\ell, a_n\} = 2\delta_{\ell n}$. The usual spinless fermions are obtained by taking linear combinations $c^\dagger_\ell = (a_{2\ell-1} + \mathrm{i} a_{2\ell})/2$. It is now straightforward to see that spin–spin correlation functions map onto expectation values of strings of fermions, e.g.

$$\langle \sigma^x_\ell \rangle = (-i)^{\ell-1} \left\langle \prod_{j=1}^{2\ell-1} a_j \right\rangle \qquad \langle \sigma^x_\ell \sigma_{\ell+n} \rangle^x = (-i)^n \left\langle \prod_{j=2\ell}^{2\ell+2n-1} a_j \right\rangle. \tag{107}$$

Application of the Jordan–Wigner transformation to the TFIC Hamiltonian (104) results in a fermion Hamiltonian of the form

$$\begin{aligned} H &= \frac{\mathrm{I} - \mathrm{e}^{\mathrm{i}\pi\mathcal{N}}}{2} H_{\mathrm{R}} + \frac{\mathrm{I} + \mathrm{e}^{\mathrm{i}\pi\mathcal{N}}}{2} H_{\mathrm{NS}}, \\ H_{\mathrm{NS/R}} &= \mathrm{i}J \sum_{j=1}^{L-1} a_{2j} \left[a_{2j+1} - h a_{2j-1} \right] - \mathrm{i}J a_{2L} \left[h a_{2L-1} \mp a_1 \right]. \end{aligned} \tag{108}$$

Here $\mathrm{e}^{\mathrm{i}\pi\mathcal{N}}$ is the fermion parity operator with eigenvalues ± 1

J. Stat. Mech. (2016) 064002

$$e^{i\pi\mathcal{N}} = \prod_{\ell=1}^{L} \sigma_\ell^z = (-i)^L \prod_{j=1}^{2L} a_j, \qquad e^{i\pi\mathcal{N}} a_j = -a_j e^{i\pi\mathcal{N}}. \tag{109}$$

$H_{\mathrm{R,NS}}$ commute with the fermion parity operator, and the full Hamiltonian (108) is therefore block-diagonal: H_{R} (H_{NS}) describes the action on states with an odd (even) number of fermions. We note that the free fermion Hamiltonians $H_{\mathrm{NS/R}}$ are closely related to the pairing model (83) considered earlier

$$H_{\mathrm{R}} = -H(-J, -2hJ) + JhL. \tag{110}$$

6.1.1. Ground states The Hamiltonians $H_{\mathrm{NS/R}}$ can be diagonalized by Bogoliubov transformations to canonical momentum space fermion operators b_p (details can be found in e.g. appendix A of [25])

$$H_{\mathrm{a}}(h) = \sum_{p\in \mathrm{a}} \varepsilon_h(p)\left(b_p^\dagger b_p - \frac{1}{2}\right), \quad \mathrm{a} = \mathrm{R},\ \mathrm{NS}, \tag{111}$$

where the single-particle energy is given by

$$\varepsilon_h(k) = 2J\sqrt{1 + h^2 - 2h\cos k}. \tag{112}$$

The difference between R and NS sectors enters via the allowed values of the momenta, which are $p = \frac{\pi n}{L}$, where n are even/odd integers for R and NS fermions respectively. The ground states of $H_{\mathrm{R,NS}}(h)$ are the fermionic vacua

$$b_p |GS\rangle_{\mathrm{a}} = 0 \ \forall p \in \mathrm{a}, \quad \mathrm{a} = \mathrm{R}, \mathrm{NS}. \tag{113}$$

These vacuum states are also eigenstates of the fermion parity operator

$$e^{i\pi\mathcal{N}} |GS\rangle_{\mathrm{NS}} = |GS\rangle_{\mathrm{NS}}, \qquad e^{i\pi\mathcal{N}} |GS\rangle_{\mathrm{R}} = \mathrm{sgn}(h-1)|GS\rangle_{\mathrm{R}}. \tag{114}$$

From (108) it follows that in the ferromagnetic phase $h < 1$ both fermion vacua are eigenstates of the full Hamiltonian H. Their respective energies are exponentially (in system size) close, and they become degenerate in the thermodynamic limit. Spin-flip symmetry then gets spontaneously broken, and the ground state is either the symmetric or the antisymmetric combination of the two vacuuum states. In the paramagnetic phase $h > 1$ the ground state of H is given by the NS vacuum state. In summary, we have

$$|GS\rangle = \begin{cases} \dfrac{|GS\rangle_{\mathrm{NS}} \pm |GS\rangle_{\mathrm{R}}}{\sqrt{2}} & h < 1 \\ |GS\rangle_{\mathrm{NS}} & h > 1. \end{cases} \tag{115}$$

This shows that for $h < 1$ the ground state of H is not a Fock state.

6.2. Quantum quench of the transverse field

We now consider the following quench protocol. We prepare the system in the ground state of $H(h_0)$, and at time $t = 0$ quench the transverse field to a new value h. At times $t > 0$ we time evolve with the new Hamiltonian $H(h)$. All local operators in spin basis

can be classified according to their fermion parity, and this turns out to be very useful. We have

$$\mathrm{e}^{\mathrm{i}\pi\mathcal{N}}\mathcal{O}_{e/o}\mathrm{e}^{-\mathrm{i}\pi\mathcal{N}} = \pm\mathcal{O}_{e/o}. \tag{116}$$

6.2.1. Quenches originating in the paramagnetic phase For a quench starting in the paramagnetic phase it follows from (115), (108) and (114) that the state of the system at times $t > 0$ is given by

$$|\Psi(t)\rangle = \mathrm{e}^{-\mathrm{i}Ht}|\,GS\rangle \equiv \mathrm{e}^{-\mathrm{i}H_{\mathrm{NS}}t}|\,GS\rangle_{\mathrm{NS}}. \tag{117}$$

This is even under fermion parity. Hence expectation values of odd operators must vanish

$$\langle\Psi(t)|\,O_o|\Psi(t)\rangle = 0. \tag{118}$$

By virtue of the simple form of both the time evolution operator H_{NS} and the initial state $|\mathrm{GS}\rangle_{\mathrm{NS}}$ in (117), expectation values of even operators can be calculated by applying Wick's theorem. This allows the reduction of expectation values of strings of fermion operators to Pfaffians involving only the two-point functions $\langle a_i a_j\rangle$ [46, 47, 177]. For example we have

$$\begin{aligned}\langle\sigma^x_\ell\sigma^x_{\ell+2}\rangle &= -\langle a_{2\ell}a_{2\ell+1}a_{2\ell+2}a_{2\ell+3}\rangle \\ &= -\langle a_{2\ell}a_{2\ell+1}\rangle\langle a_{2\ell+2}a_{2\ell+3}\rangle + \langle a_{2\ell}a_{2\ell+2}\rangle\langle a_{2\ell+1}a_{2\ell+3}\rangle - \langle a_{2\ell}a_{2\ell+3}\rangle\langle a_{2\ell+1}a_{2\ell+2}\rangle.\end{aligned} \tag{119}$$

6.2.2. Quenches originating in the ferromagnetic phase As a result of spontaneous symmetry breaking in the ground state, the situation for quenches originating in the ferromagnetic phase $h_0 < 1$ is more complicated. The time evolved initial state is

$$|\Psi(t)\rangle = \frac{\mathrm{e}^{-\mathrm{i}H_{\mathrm{NS}}t}|\,GS\rangle_{\mathrm{NS}} \pm \mathrm{e}^{-\mathrm{i}H_{\mathrm{R}}t}|\,GS\rangle_{\mathrm{R}}}{\sqrt{2}}. \tag{120}$$

The expectation values of even operators can be expressed in the form

$$\begin{aligned}\langle\Psi(t)|\,\mathcal{O}_e|\Psi(t)\rangle = \quad & \frac{1}{2}\sum_{\mathrm{a}\in\{\mathrm{R},\mathrm{NS}\}}{}_{\mathrm{a}}\langle\,GS|\mathrm{e}^{\mathrm{i}H_{\mathrm{NS}}t}\mathcal{O}_e\mathrm{e}^{-\mathrm{i}H_{\mathrm{NS}}t}|\,GS\rangle_{\mathrm{a}} \\ \underset{L\to\infty}{\longrightarrow}\ & {}_{\mathrm{NS}}\langle\,GS|\mathrm{e}^{\mathrm{i}H_{\mathrm{NS}}t}\mathcal{O}_e\mathrm{e}^{-\mathrm{i}H_{\mathrm{NS}}t}|\,GS\rangle_{\mathrm{NS}}.\end{aligned} \tag{121}$$

In the last line we have used that the expectation values in the R and NS sectors become equal in the thermodynamic limit. The last line in (121) can again be evaluated by application of Wick's theorem.

In contrast, expectation of odd operators cannot be simplified in this way. Instead we have

$$\langle\,GS|\mathrm{e}^{\mathrm{i}Ht}\mathcal{O}_o\mathrm{e}^{-\mathrm{i}Ht}|\,GS\rangle = \pm\mathrm{Re}[{}_{\mathrm{NS}}\langle\,GS|\mathrm{e}^{\mathrm{i}H_{\mathrm{NS}}t}\mathcal{O}_o\mathrm{e}^{-\mathrm{i}H_{\mathrm{R}}t}|\,GS\rangle_{\mathrm{R}}]. \tag{122}$$

Wick's theorem does not apply here, and in order to proceed one commonly resorts to one of the following methods [202]:

J. Stat. Mech. (2016) 064002

1. Using the cluster decomposition property we can obtain (122) from the expectation value of an even operator by considering the limit

$$|\langle GS|\mathrm{e}^{\mathrm{i}Ht}\mathcal{O}_o\mathrm{e}^{-\mathrm{i}Ht}|\,GS\rangle| = \lim_{d\to\infty}\sqrt{{}_{\mathrm{NS}}\langle GS|\mathrm{e}^{\mathrm{i}H_{\mathrm{NS}}t}\mathcal{O}_o(r)\mathcal{O}_o(r+d)\mathrm{e}^{-\mathrm{i}H_{\mathrm{NS}}t}|\,GS\rangle_{\mathrm{NS}}}\,. \quad (123)$$

2. One imposes open boundary conditions on the spins (in that case the Hamiltonian is mapped into a purely quadratic form of fermions) and considers the expectation value of $\mathcal{O}_o$ asymptotically far away from the boundaries.

An alternative method that applies more generally to integrable models was developed in [25–27]. It is based on the observation that the initial state after the quench can be expressed in a squeezed state form, *e.g.*

$$\langle\Psi(0) = \exp\left[\mathrm{i}\sum_{0<p\in\mathrm{NS}} K(p)b_p^\dagger b_{-p}^\dagger\right]GS\rangle_{\mathrm{NS}}. \quad (124)$$

Here $K(p)$ is a function that depends on the quench (see (132)), $b_p^\dagger$ are the aforementioned momentum space Bogoliubov fermion operators. Two point correlation functions can then be written in a Lehmann representation based on energy eigenstates. The matrix elements ('form factors') in the Lehmann representation are known [203], and it is possible to obtain explicit results in the framework of a low-density expansion. We refer the reader to [26, 27] for further details and the explicit calculations. Here we only review and discuss the main results.

6.3. Stationary state properties

Stationary state properties were analyzed in detail in [27]. An important simplification at late times is that expectation values of odd operators go to zero. As discussed above, for quenches originating in the paramagnetic phase they vanish identically because the $\mathbb{Z}_2$ symmetry remains unbroken. On the other hand, for quenches originating in ferromagnetic phase ($h_0 < 1$) their expectation value is generally nonzero (see (122)). However, as shown in [28], expectation values of all odd local operators decay exponentially in time to zero. This leaves us with expectation values for even operators, which can be analyzed by standard free fermion methods. The basic object is the fermion two-point function, which in the thermodynamic limit can be written in the form (see (91))

$$\mathrm{i}\langle a_\ell a_n\rangle\Big|_{\ell\neq n} = \int_{-\pi}^{\pi}\frac{\mathrm{d}k}{2\pi}\left[A_{\ell-n}(k) + B_{\ell-n}(k)\mathrm{e}^{2\mathrm{i}\varepsilon_h(k)t} + B^*_{\ell-n}(k)\mathrm{e}^{-2\mathrm{i}\varepsilon_h(k)t}\right]. \quad (125)$$

Here $A(k)$ and $B(k)$ are smooth functions (we are considering noncritical quenches) that depend on the quench details and $\varepsilon_h(k)$ is the dispersion relation (112). By the Riemann-Lebesgue lemma, in the infinite time limit the fermion two-point functions approach stationary values

$$\lim_{t\to\infty}\mathrm{i}\langle a_\ell a_n\rangle\Big|_{\ell\neq n} = \int_{-\pi}^{\pi}\frac{\mathrm{d}k}{2\pi}A_{\ell-n}(k). \quad (126)$$

J. Stat. Mech. (2016) 064002

Since the expectation value of any even local operator can always be written as a finite sum of finite products of fermion two-point functions (see (119)), the infinite time limit exists and is obtained by replacing (125) with (126). Courtesy of Wick's theorem, the stationary properties of all other even operators can be expressed in terms of (126).

6.3.1. Description of the steady state by a GGE Since expectation values of odd operators vanish at infinite times, the steady state can be constructed in complete analogy to our fermionic example considered in section 4. The appropriate GGE density matrix is of the form

$$\rho_{\mathrm{GGE}} = \frac{\mathrm{e}^{-\sum_{j=1}^{\infty}\lambda_n^+ I^{(n,+)}+\lambda_n^- I^{(n,-)}}}{Z_{\mathrm{GGE}}}, \tag{127}$$

where the conservation laws $I^{(n,\pm)}$ have been reported earlier in (33). The Lagrange multipliers for transverse field quenches were determined in [28]

$$\lambda_j^+ = \left\{\frac{\mathrm{sgn}[(h-1)(h_0-1)]}{\varepsilon_h(0)} + \frac{(-1)^j}{\varepsilon_h(\pi)}\right\}\frac{2}{j}, \qquad \lambda_j^- = 0. \tag{128}$$

The local equivalence of the steady state density matrix to this GGE was demonstrated in [25, 28]

$$\lim_{t\to\infty}|\Psi(t)\rangle\langle\Psi(t)| =_{\mathrm{loc}} \rho_{\mathrm{GGE}}. \tag{129}$$

The GGE can be interpreted as a Gibbs ensemble at inverse temperature $\beta = J^{-1}$ for an effective 'GGE Hamiltonian', defined as

$$H_{\mathrm{GGE}} \equiv J\sum_{j=1}^{\infty}\lambda_j^+ I_j^+. \tag{130}$$

By virtue of (128) this 'Hamiltonian' is long-ranged. It can be diagonalized by combined Jordan–Wigner and Bogoliubov transformations [28], which for a quench from h_0 to h results in

$$H_{\mathrm{GGE}} = \int_{-\pi}^{\pi}\frac{\mathrm{d}p}{2\pi}J\log(K^2(p))\left[b^\dagger(p)b(p) - \frac{1}{2}\right], \tag{131}$$

where

$$K^2(p) = \frac{\sin^2(p)\,(h-h_0)^2}{(\varepsilon_{h_0}(p)\varepsilon_h(p)(2J)^{-2} + 1 + hh_0 - (h+h_0)\cos(p))^2}. \tag{132}$$

The 'dispersion relation' $J\log K^2(p)$ diverges logarithmically at momenta zero and π. This is related to the fact that the mode occupation numbers at these momenta are independent of h, and ultimately produces the algebraic decay (128) of the Lagrange multipliers. These logarithmic singularities do not compromise the cluster decomposition properties of the steady state.

6.3.2. Connected spin–spin correlation functions In the stationary state the connected two-point correlators decay exponentially with distance [26]

J. Stat. Mech. (2016) 064002

$$\rho_c^{\alpha\alpha}(\ell) = \langle \sigma_j^\alpha \sigma_{j+\ell}^\alpha \rangle - \langle \sigma_j^\alpha \rangle \langle \sigma_{j+\ell}^\alpha \rangle \simeq C^\alpha(\ell) \mathrm{e}^{-\ell/\xi_\alpha}. \tag{133}$$

The correlation lengths are given by [26]

$$\xi_z^{-1} = |\ln h_0| + \min(|\ln h_0|, |\ln h|), \tag{134}$$

$$\xi_x^{-1} = \theta_{\mathrm{H}}(h-1)\theta_{\mathrm{H}}(h_0-1) \ln\left[\min(h_0, h_1)\right] - \ln\Big[x_+ + x_- + \theta_{\mathrm{H}}((h-1)(h_0-1))\sqrt{4x_+x_-}\Big], \tag{135}$$

where $\theta_{\mathrm{H}}(x)$ is the Heaviside step function and

$$x_\pm = \frac{[\min(h, h^{-1}) \pm 1][\min(h_0, h_0^{-1}) \pm 1]}{4}, \quad h_1 = \frac{1 + hh_0 + \sqrt{(h^2-1)(h_0^2-1)}}{h + h_0}. \tag{136}$$

The prefactors $C^\alpha(\ell)$ depend on the details of the quench and are listed in appendix C.

6.4. Time dependence

Having established the stationary behaviour of spin correlations, we now turn to their dynamics at late times. The first question of interest is how they relax towards their stationary values.

For even operators we can use Wick's theorem to express spin–spin correlators in terms of the fermion two-point functions (125). At late times the resulting expression can be evaluated by a stationary phase approximation, which gives

$$\langle \mathcal{O}_e \rangle \simeq \langle \mathcal{O}_e \rangle_{\mathrm{GGE}} + O(t^{-n[\mathcal{O}_e]/2}). \tag{137}$$

Here the exponent $n[\mathcal{O}_e]$ is an integer that depends on the particular even operator under consideration.

Expectation values of odd operators were argued in [28] to decay exponentially in time

$$\langle \mathcal{O}_o \rangle \simeq O(\mathrm{e}^{-t/\tau[\mathcal{O}_o]}), \tag{138}$$

where $\tau[\mathcal{O}_o]$ denotes a relaxation time. Having established the gross structure of the late time dynamics, we now turn to a more quantitative description.

6.4.1. One-point functions

Longitudinal spin operator The longitudinal spin operator $\sigma_j^x = (-i)^{\ell-1} \prod_{j=1}^{2\ell-1} a_j$ is the simplest and most important example of an odd operator. Its expectation value is the order parameter in the ferromagnetic phase. As we are dealing with an odd operator, its expectation value is identically zero for quenches originating in the paramagnetic phase. For quenches from the ferromagnetic phase ($h_0 < 1$) it was shown in [25, 26] that

$$\langle \Psi(t)|\sigma_j^x|\Psi(t)\rangle \simeq C^x(t)\mathrm{e}^{-t/\tau_x}, \qquad h_0 < 1, \tag{139}$$

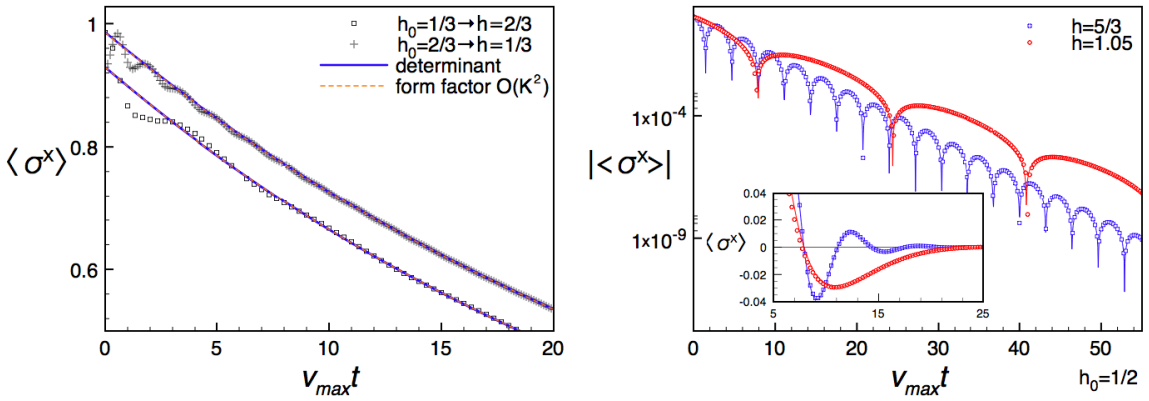

Figure 7. Expectation value of the order parameter after two quenches within the ferromagnetic phase (left) and two quenches across the critical point (right). Numerical results obtained in the thermodynamic limit are compared with the asymptotic predictions (139) (labelled as 'determinant'). In the left panel analytic results obtained by form factor methods [26] are shown as well (labelled as 'form factor'). The agreement in all cases is excellent even at the short times depicted *(Figures taken from* [26]*.)*.

where the inverse decay time is given by

$$\tau_x^{-1} = \int_0^\pi \frac{\mathrm{d}k}{\pi} \varepsilon_h'(k) \ln \left| \frac{1 - K^2(k)}{1 + K^2(k)} \right|. \tag{140}$$

Here the function $K^2(k)$ has been previously defined in (132). The prefactor $C^x(t)$ was calculated in [26]

$$C^x(t) = \begin{cases} \sqrt{\dfrac{1 - hh_0 + \sqrt{(1-h^2)(1-h_0^2)}}{2\sqrt{1-hh_0}(1-h_0^2)^{\frac{1}{4}}}} & h < 1 \\ \left[\dfrac{h\sqrt{1-h_0^2}}{h+h_0} \right]^{\frac{1}{4}} [1 + \cos(2\varepsilon_h(k_0)t + \alpha) + \ldots]^{\frac{1}{2}} & h > 1. \end{cases} \tag{141}$$

The oscillatory behaviour for $h > 1$ can be related to the presence of a gapless mode with momentum k_0 in the GGE Hamiltonian (130) ($K^2(k_0) = 1$). It was noted in [42] that the period of the oscillations in (141) coincides with cusps in the time evolution of the logarithm of the return probability per unit length $f(t) = -\lim_{L\to\infty} \frac{1}{L} \log |\langle \Psi(0)| \mathrm{e}^{-\mathrm{i}Ht} |\Psi(0)\rangle|^2$ after quenches between the phases. The result (139) has been derived in the late time limit $Jt \gg 1$. However, it gives an excellent account of the full answer except at very short times. This can be shown by comparing (139) to a numerical solution based on free fermion methods [26]. The latter works directly in the thermodynamic limit and does not suffer from finite-size effects. Figure 7 shows such comparisons for two different quenches within the ferromagnetic phase, and for two quenches from the ferromagnetic to the paramagnetic phase. The agreement is visibly excellent even at moderate times.

doi:10.1088/1742-5468/2016/06/064002

J. Stat. Mech. (2016) 064002

At first sight the exponential decay (139) of the order parameter for quenches within the ferromagnetic phase may look surprising. Even a very small quench will lead to the eventual disappearance of the order parameter. A simple way of understanding this is to note that the ferromagnetic order persists only at zero temperature $T = 0$, and melts for any $T > 0$. By means of our quantum quench we deposit a finite energy density into the system, which is very similar to imposing a finite temperature. This consideration provides an intuitive explanation for why even small quenches wipe out the long range order present in the initial state. We note that this behaviour is specific to one dimensional systems, where discrete symmetries can be spontaneously broken only at $T = 0$. In higher dimensional systems we expect order parameters to be generally stable when subjected to sufficiently small quantum quenches.

Finally we note that the expectation value $\langle\sigma_j^y(t)\rangle$ can be obtained in a simple way by considering the Heisenberg equations of motion for σ_j^x, and is given by

$$\langle\Psi(t)|\sigma_j^y|\Psi(t)\rangle = \frac{\partial}{\partial t}\frac{\langle\Psi(t)|\sigma_j^x|\Psi(t)\rangle}{2Jh}. \tag{142}$$

Transverse spin operator The spin operator $\sigma_j^z = \mathrm{i}a_{2j}a_{2j-1}$ is even and its expectation value can be straightforwardly calculated with free-fermion techniques [45, 47]. It decays like a $t^{-3/2}$ power law in time towards its stationary value $\langle\cdot\rangle_{\mathrm{GGE}}$

$$\langle\Psi(t)|\sigma_l^z|\Psi(t)\rangle|_{Jt\gg 1} = \langle\sigma_l^z\rangle_{\mathrm{GGE}} + \frac{h_0 - h}{4\sqrt{\pi}(2hJt)^{\frac{3}{2}}}\left[\frac{\sin(4J|1-h|t+\pi/4)}{\sqrt{|1-h|}\,|1-h_0|} - \frac{\sin(4J(1+h)t-\pi/4)}{\sqrt{1+h}(1+h_0)}\right] + O((Jt)^{-\frac{5}{2}}). \tag{143}$$

The relaxation to the stationary value is only algebraic, in agreement with (137).

6.4.2. Spin–spin correlators in the 'space-time scaling limit' A particularly useful way of describing the time dependence of two-point functions after a quantum quench is by considering an asymptotic expansion around the so-called *space-time scaling limit* [25, 26]. The latter refers to the behaviour along a particular ray in space-time

$$t, \ell \to \infty, \quad \frac{v_{\max}t}{\ell} = \kappa = \text{fixed}. \tag{144}$$

Here $v_{\max} = \max_k \frac{\mathrm{d}\varepsilon_h(k)}{\mathrm{d}k}$ is the maximal group velocity of elementary excitations of the post-quench Hamiltonian.

Transverse spin–spin correlator In the space-time scaling limit, the asymptotic behavior of $\rho_c^{zz}(\ell, t)$ can be evaluated by means of Wick's theorem, followed by a stationary phase approximation. The leading behaviour is a t^{-1} power-law decay, and the subleading corrections are power laws as well [26]

J. Stat. Mech. (2016) 064002

$$\rho_c^{zz}\left(\ell = \frac{v_{\max}t}{\kappa}, t\right) \sim \frac{D^z(t)}{\kappa^2 t} + o(t^{-1}). \tag{145}$$

Here $D^z(t)$ is the sum of a constant contribution and oscillatory terms with constant amplitudes.

Longitudinal spin–spin correlator In the space-time scaling limit the order parameter two-point function $\rho^{xx}(\ell, t)$ takes the form

$$\rho^{xx}(\ell, t) \simeq \mathcal{C}^x(\ell, t) \exp\left[\int_0^\pi \frac{\mathrm{d}k}{\pi} \ln\left|\frac{1 - K^2(k)}{1 + K^2(k)}\right| \min(2\varepsilon_h'(k)t, \ell)\right]. \tag{146}$$

The function $\mathcal{C}^x(\ell, t)$ has been determined in [26].

1. For quenches within the ferromagnetic phase, h_0, $h < 1$, $\mathcal{C}^x(\ell, t)$ equals the constant denoted by $\mathcal{C}^x_{\mathrm{FF}}$ in (C.3). For times smaller than the Fermi time

$$t_{\mathrm{F}} = \frac{\ell}{2v_{\max}}, \tag{147}$$

equation (146) equals the square of the one-point function (139). Thus, in the space-time scaling limit, connected correlations *vanish identically* for times $t < t_{\mathrm{F}}$ and begin to form only after the Fermi time. We stress that this does not imply that the connected correlations are exactly zero for $t < t_{\mathrm{F}}$: in any model, both on the lattice or in the continuum there are exponentially suppressed terms (in ℓ), which however vanish in the scaling limit.

2. For quenches from the ferromagnetic phase to the paramagnetic phase the prefactor is given by

$$\mathcal{C}^x(\ell, t) = \mathcal{C}^x_{\mathrm{FP}}[1 + \theta_{\mathrm{H}}(t_{\mathrm{F}} - t)(\cos(2\varepsilon_h(k_0)t + \alpha) + \ldots)], \tag{148}$$

where $\mathcal{C}^x_{\mathrm{FP}}$ is the constant defined in (C.4), while k_0 and α are the constants appearing in the one-point function (141). For $t < t_{\mathrm{F}}$, (146) is simply the square of the corresponding one-point function, which ensures that connected correlations vanish for $t < t_{\mathrm{F}}$ in the space-time scaling regime. We note that the expression for $t < t_{\mathrm{F}}$ is a conjecture [26].

3. For quenches within the paramagnetic phase one has

$$\mathcal{C}^x(\ell, t) \simeq \mathcal{C}^x_{\mathrm{PP}}(\ell) + (h^2 - 1)^{\frac{1}{4}}\sqrt{4J^2h} \int_{-\pi}^{\pi} \frac{\mathrm{d}k}{\pi} \frac{K(k)}{\varepsilon_k} \sin(2t\varepsilon_k - k\ell) + \ldots, \tag{149}$$

where $\mathcal{C}^x_{\mathrm{PP}}(\ell)$ is the function defined in (C.6). Equation (149) constitutes the leading order in a low-density expansion computed within the form-factor formalism. The exact expression for a generic (not small) quench is not known.

4. For quenches from the paramagnetic to the ferromagnetic phase, for $t > t_{\mathrm{F}}$, $\mathcal{C}^x(\ell, t)$ is independent of time and is given by $\mathcal{C}^x_{\mathrm{PF}}(\ell)$ of (C.5). For $t < t_{\mathrm{F}}$ the correlator is exponentially small and, to the best of our knowledge, there are no analytic predictions for its behaviour.

6.4.3. Long time asymptotics of connected spin–spin correlators at a fixed separation ℓ The late time asymptotics of spin–spin correlation functions at a fixed separation ℓ between the spin operators was analyzed in [26].

1. In the late time regime at fixed, large ℓ, $\rho_c^{zz}(\ell, t)$ decays in a power law fashion to its stationary value

$$\rho_c^{zz}(\ell, t) \sim \rho_c^{zz}(\ell, \infty) + \frac{E^z(t)\ell e^{-\ell/\tilde{\xi}_z}}{t^{3/2}} + o(t^{-3/2}). \tag{150}$$

Here $E^z(t) = \sum_{q=0,\pi} A_q \cos(2t\varepsilon_h(q) + \varphi_q)$ and the steady state value is exponentially small in ℓ, $\rho_c^{zz}(\ell, \infty) \propto e^{-\ell/\xi_z}$. Crucially one has (see (134))

$$\tilde{\xi}_z^{-1} = \min(|\log h_0|, |\log h|) < \xi_z^{-1}. \tag{151}$$

This implies that the time scale after which the stationary behaviour becomes apparent is in fact exponentially large in the separation ℓ. This makes the stationary behaviour difficult to observe in practice.

2. For quenches originating in the ferromagnetic phase, the stationary value of $\rho^{xx}(\ell, t)$ emerges at a time scale

$$\tau_{\mathrm{F}}^{\mathrm{x}} \sim v_{\max}^{-1} \ell^{4/3}, \tag{152}$$

where $v_{\max}$ is the maximal velocity at which information propagates. This makes the approach to the steady state straightforward to observe.

3. For quenches within the paramagnetic phase, $\rho_c^{xx}(\ell, t)$ exhibits an oscillatory power-law decay in time towards its stationary value, which is exponentially small in ℓ. Hence, in complete analogy to the case of the transverse two-point function, the time scale $\tau_{\mathrm{PP}}^{\mathrm{x}}$ after which the stationary behavior reveals itself is exponentially large

$$\tau_{\mathrm{PP}}^{\mathrm{xx}} \propto e^{2\ell/3\xi_x}, \tag{153}$$

and very difficult to observe in practice.

6.5. Reduced density matrices

As we have seen above, the quench dynamics of one and two point functions of quantum spins is rich and interesting. However, these are nonetheless very special observables. Ideally one would like to have access to the full reduced density matrix for a given subsystem size, as its matrix elements encode the evolution of all correlation functions, see (21). In practice this is only possible in very simple non-interacting examples, or for very small subsystem sizes. An example are quenches in the disordered phase of the TFIC [28, 176]. Here the reduced density matrix on the interval $[1, \ell]$ is given by

$$\rho_\ell(t) = \frac{1}{Z} \exp\left(\frac{1}{4} \sum_{\ell,n} a_l W_{lm} a_m\right), \tag{154}$$

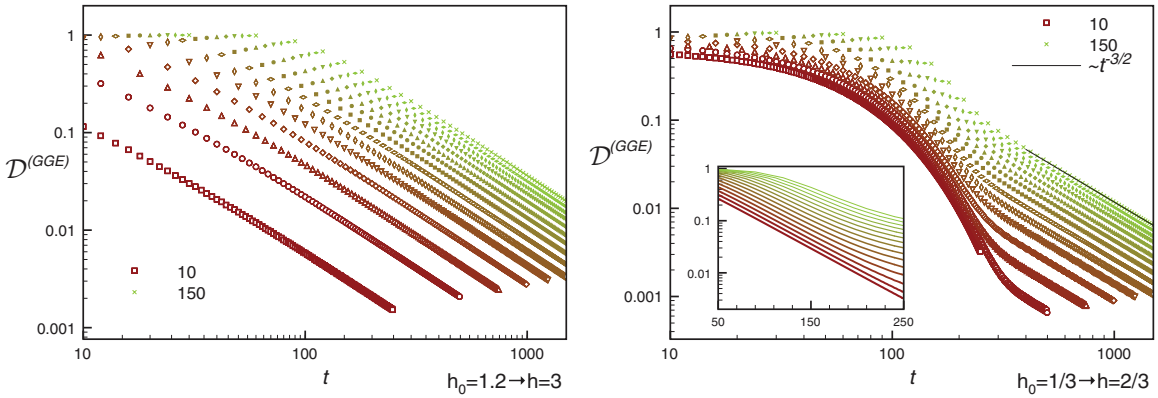

Figure 8. Normalized distance $\mathcal{D}^{(\mathrm{GGE})} = \mathcal{D}(\rho_\ell(t), \rho_\ell^{\mathrm{GGE}})$ after a quench within the paramagnetic (left) and ferromagnetic (right) phase for subsystem sizes $\ell = 10, 20, \ldots, 150$. As ℓ increases, the color changes from brown to green, the symbols become smaller and the curves narrower. At late times $D(\rho_\ell(t), \rho_\ell^{(GGE)})$ tends to zero in a universal power-law fashion $\propto (Jt)^{-3/2}$. For quenches in the ordered phase there is an intermediate time regime, in which the distance decays exponentially (inset). This stems from the non-vanishing spontaneous magnetization in the initial state for this quench *(Figures taken from* [28]*.)*.

where a_{2n} and a_{2n-1} are the Majorana fermion operators (106) and the factor Z ensures $\mathrm{Tr}(\rho_\ell(t)) = 1$. The matrix W is related to the two-point function of Majorana fermions by [123, 124, 204]

$$\tanh \frac{W}{2} = \Gamma, \qquad \Gamma_{jk} = \langle \Psi(t)| a_k a_j |\Psi(t)\rangle - \delta_{j,k} = -\Gamma_{kj}, \tag{155}$$

where the time evolved initial state $|\Psi(t)\rangle$ is given by (117). The matrix elements of the correlation matrix are simple (single) integrals and can be found in [26].

As we have argued above, at late times after global quantum quenches isolated quantum systems relax locally towards some steady states ρ^{SS}. How quickly this relaxation occurs can be efficiently measured by considering the distance of the time evolving reduced density matrix $\rho_B(t)$ from its steady state value ρ_B^{SS}, where B is a subsystem of a given size. This diagnostic can be implemented quite generally numerically as long as the subsystem size is small [205]. For models that can be mapped to non-interacting theories, it is possible to go considerably further. An example is the TFIC, which was considered in [28]. The first step is to introduce a measure of distance on the space of RDMs on a given subsystem. A convenient choice was introduced in [28]

$$\mathcal{D}(\rho_1, \rho_2) = \sqrt{\frac{\mathrm{Tr}[(\rho_1 - \rho_2)^2]}{\mathrm{Tr}[(\rho_1)^2] + \mathrm{Tr}[(\rho_1)^2]}}\,. \tag{156}$$

Figure 8 shows results for the distance between the RMDs for the time-evolving and stationary states for quantum quenches within the disordered and ordered phases in the TFIC. Subsystems consisting of ℓ neighbouring sites are considered, where ℓ ranges

from 10 to 150. In both cases the distance is seen to eventually decay as a power law in time

$$\mathcal{D}(\rho_\ell(t), \rho_\ell^{\mathrm{GGE}}) \propto \ell^2 (Jt)^{-\frac{3}{2}}. \tag{157}$$

The power-law decay of the distance in time can be interpreted by relating it to expectation values of local operators in the subsystem. Using (21) one can show that

$$\mathcal{D}(\rho_1, \rho_2) = (\overline{R(\mathcal{O})^2})^{\frac{1}{2}}, \qquad R(\mathcal{O}) = \frac{|\mathrm{Tr}[(\rho_1 - \rho_2)\mathcal{O}]|}{\sqrt{\mathrm{Tr}[\rho_1\mathcal{O}]^2 + \mathrm{Tr}[\rho_2\mathcal{O}]^2}}, \tag{158}$$

where the bar denotes an average on the space of operators acting on the spins in the subsystem, taken with respect to the probability distribution

$$P(\mathcal{O}) = \frac{\mathrm{Tr}[\rho_1\mathcal{O}]^2 + \mathrm{Tr}[\rho_2\mathcal{O}]^2}{\sum_{\mathcal{O}'} \mathrm{Tr}[\rho_1\mathcal{O}']^2 + \mathrm{Tr}[\rho_2\mathcal{O}']^2}. \tag{159}$$

Here the sum is over all operators $\sigma_1^{\alpha_1}\sigma_2^{\alpha_2}\ldots\sigma_\ell^{\alpha_\ell}$, where $\alpha_j = 0, x, y, z$ and where we have assumed for simplicity that the subsystem is the interval $[1, \ell]$. The contribution from a given operator $\mathcal{O}$ to the distance is weighted by the square of its expectation value. This shows that (158) measures a mean relative difference between the expectation values of local operators in the two states.

As $\overline{R(\mathcal{O})} \leqslant (\overline{R(\mathcal{O})^2})^{1/2} = \mathcal{D}(\rho_\ell(t), \rho_\ell^{\mathrm{GGE}})$ we may use (158) to identify a time scale t^*_{rms} associated with the relaxation of the 'typical' operator (with respect to the probability distribution (159))

$$Jt^*_{\mathrm{rms}} \sim \ell_B^{\frac{4}{3}}. \tag{160}$$

The time scale t^*_{rms} is very different from the ones governing the time evolution of the two-point functions of spin operators.

6.6. Entanglement entropy

The von Neumann entropy (also known as entanglement entropy) of a density matrix ρ is defined as

$$S_{\mathrm{vN}}[\rho] = -\mathrm{Tr}[\rho \log \rho]. \tag{161}$$

If ρ is a reduced density matrix in a system that is in a pure state, S_{vN} measures the entanglement between the subsystem and its complement. Entanglement entropies have become a standard diagnostic for detecting and identifying quantum phase transitions. In the context of quantum quenches the time evolution of the von Neumann entropy and other entanglement measures provides very useful information about the spreading of correlations [16, 31, 48, 89, 109, 127, 182, 183, 206–209]. A key result obtained in [48] is that after quenches to conformal field theories the von Neumann entropy of a subsystem of length ℓ increases linearly in time until it eventually saturates (see the review by Calabrese and Cardy [88] in this volume)

J. Stat. Mech. (2016) 064002

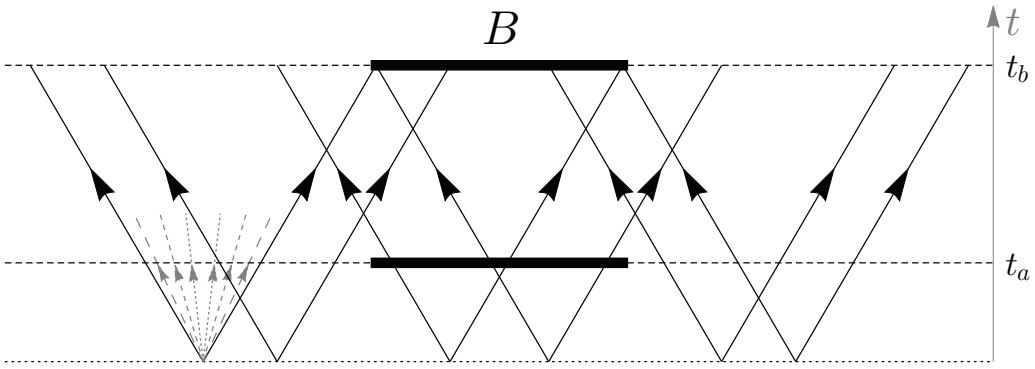

Figure 9. Space-time picture illustrating the semiclassical interpretation of entanglement entropy growth after a global quantum quench [89]. Quasi-particles moving at the maximal group velocity are indicated by thick black arrows, and are initially generated throughout the system by the quantum quench. Slower quasi-particles are shown only on the left (short dashed gray arrows). At time t_a the entanglement entropy of B is still increasing linearly in time, as there are still trajectories such that maximum velocity quasi-particle pairs are incident inside B. At times $t = t_b$ the entanglement entropy starts saturating because *any* maximum velocity quasi-particle incident in B generates entanglement with the rest of the system.

$$S_{\mathrm{vN}}[\rho] \sim \begin{cases} \dfrac{\pi c v t}{6\epsilon} & v t < \dfrac{\ell}{2} \\ \dfrac{\pi c \ell}{12\epsilon} & v t \gtrsim \dfrac{\ell}{2}. \end{cases} \tag{162}$$

Here c is the central charge of the CFT, ϵ is a constant with dimensions of length that depends on the initial state and v is the speed of light. The two behaviours in (162) connect smoothly over a region $|vt - \frac{\ell}{2}| \sim \epsilon$. A physical interpretation of the result (162) is provided by the Calabrese–Cardy quasi-particle picture [89] we already encountered in section 5. Its application to the time evolution of the entanglement entropy in integrable models initialized in squeezed states with finite correlation lengths proceeds as follows. The idea is that in a squeezed state correlations spread via the propagation of pairs of quasi-particles with equal but opposite momenta. At time $t = 0$ the quantum quench generates such quasi-particles pairs throughout the system. Correlations between quasi-particles produced at a distance larger than the correlation length in the initial state can be neglected. The entanglement between a given region B and its complement is generated by quasi-particle pairs. The entanglement entropy is interpreted as a measure of the number of correlated pairs such that, at a given time, one quasi-particle is inside B and one outside, see figure 9. Entanglement is initially generated at the boundaries of B, and the entangled region spreads outwards in the form of two light cones. This picture suggests the following semiclassical expression for the von Neumann entropy

$$S_{\mathrm{vN}}[\rho_B] \overset{\mathrm{SC}}{=} \int \mathrm{d}k \, f(k) \min(\ell_B, 2|v(k)|t). \tag{163}$$

Here $v(k)$ is the semiclassical group velocity $v(k) = \frac{\mathrm{d}\varepsilon(k)}{\mathrm{d}k}$, $\varepsilon(k)$ is the dispersion relation of the quasiparticles and $f(k)$ is an unknown function that contains information on the initial state.

This behaviour has been observed in a variety of lattice and continuum models [31, 48, 89, 109, 127, 182, 183, 206, 209], including non-integrable cases [183], in which the quasi-particle picture does not apply by virtue of the finite quasi-particle life time. The semiclassical interpretation has been generalized to prethermalized regimes in models with weak integrability breaking [127].

The linear entanglement growth after quantum quenches has important ramifications. It is a crucial limiting factor for applying matrix-product state methods such as t-DRMG [210] and i iTEBD [211] algorithms to the computation of the dynamics after global quantum quenches. We note that translational invariance is essential for the quasi-particle picture to hold, and the time evolution of the entanglement entropy in e.g. disordered models [206] is very different.

Exact results for the evolution of the entanglement entropy after quenches in the transverse field Ising chain [48] are in accordance with the structure (163) suggested by the quasi-particle picture. In the limit $1 \ll \ell, Jt$, the entanglement entropy of a block of ℓ neighbouring spins is

$$S_{\mathrm{vN}}[\rho_B] \simeq \int_{\pi}^{\pi} \frac{\mathrm{d}k}{2\pi}\, w(\langle\Psi(0)|n(k)|\Psi(0)\rangle)\ \min(\ell, 2|\varepsilon'(k)|t) + o(\ell), \tag{164}$$

where $w(x) = -x\log x - (1-x)\log(1-x)$ is the entropy per site (see appendix B), and $\langle\Psi(0)|n(k)|\Psi(0)\rangle$ is the (conserved) density of elementary excitations of the post-quench Hamiltonian H with momentum k at times $t > 0$. It is given by

$$\langle\Psi(0)|n(k)|\Psi(0)\rangle = \frac{K^2(k)}{1+K^2(k)}, \tag{165}$$

where $K^2(k)$ was defined previously in (132). It follows from (164) that the entanglement entropy increases linearly until the Fermi time (147), and then slowly approaches its stationary value set by the GGE. The latter equals the entropy per site of the GGE for the *entire* system [109]

$$\int_{\pi}^{\pi} \frac{\mathrm{d}k}{2\pi}\, w(\langle\Psi(0)|n(k)|\Psi(0)\rangle) = \lim_{L\to\infty} \frac{1}{L} S_{vN}[\rho^{\mathrm{GGE}}]. \tag{166}$$

These observations persist for quantum quenches in the TFIC starting in excited states [31].

Interestingly, the stationary value of the entropy density in the diagonal ensemble differs from that in the GGE [30, 212]. This is not a problem, because the entropy per site is a global property of the system, while the equivalence between ensembles only holds for (finite) subsystems in the thermodynamic limit. A detailed explanation of the origin of this difference for the case of the TFIC was provided in [30].

6.7. Dynamical spin–spin correlation functions

We now turn to dynamical correlation functions

$$\rho^{\alpha\alpha}(\ell, t+t_1, t+t_2) = \langle\Psi(t)|\sigma^{\alpha}_{j+\ell}(t_1)\sigma^{\alpha}_{j}(t_2)|\Psi(t)\rangle. \tag{167}$$

The transverse correlator ($\alpha = z$ in (167)) can be calculated by elementary means [45], as σ_j^z is quadratic in Jordan–Wigner fermions. The order parameter correlator ($\alpha = x$ in (167)) is much more difficult to evaluate. In [29] it was determined by means of a generalization of the form factor methods developed in [26], and by exploiting exact results in particular limits [27]. These methods are so far restricted to quenches within either the paramagnetic or the ferromagnetic phase, and lead to answers of the form [29]

$$\rho^{xx}(\ell, t+\tau, t+t_2) \simeq C^x(\ell,\tau,t)\exp\left[\int_0^\pi \frac{\mathrm{d}k}{\pi}\log\left|\frac{1-K^2(k)}{1+K^2(k)}\right|\min\{\max[\varepsilon_h'(k)\tau,\ell],\varepsilon_h'(k)(2t+\tau)\}\right]. \tag{168}$$

Here the functions $\epsilon_h(k)$ and $K^2(k)$ are given in (112) and (132) respectively, and h_0 and h are the initial and final values of the transverse field. The function $C^{(x)}(\ell,\tau,t)$ depends on the phase in which the quench is performed:

1. In the ferromagnetic phase, $h_0,\ h<1$, $C^x(\ell,\tau,t)$ equals the constant $\mathcal{C}^x_{\mathrm{FF}}$ in (C.3).

2. In the paramagnetic phase ($h_0,\ h>1$) $C^x(\ell,\tau,t)$ is given (to leading order in the form factor expansion) by [29]

$$C^x(\ell,\tau,t) = \int_{-\pi}^{\pi}\frac{\mathrm{d}k}{2\pi}\frac{J\mathrm{e}^{\mathrm{i}\ell k}}{\varepsilon_h(k)}[\mathrm{e}^{-\mathrm{i}\varepsilon_h(k)t} + 2iK(k)\cos(2\varepsilon_h(k)(2t+\tau))\mathrm{sgn}(\ell-\varepsilon_h'(k)\tau)] \times \frac{hh_0-1+\sqrt{(h^2-1)(h_0^2-1)}}{\sqrt{h_0-1/h}\sqrt[4]{h_0^2-1}}, \qquad \ell < v_{\max}(2t+\tau). \tag{169}$$

   In the complementary regime $v_{\max}(2t+\tau)<\ell$ the correlator is exponentially small and this expression no longer applies.

The form factor result gives an excellent approximation to the exact answer (which can be computed numerically using free fermion techniques) for 'small' quenches [29]. These are defined as being characterized by having low densities of excitations in the initial state.

It is possible to obtain some of these results in an alternative way by generalizing the semiclassical approach of [39] to the non-equal time case, and then elevating it using exact limiting results derived in [25, 26]. This method fails to reproduce the result for quenches in the disordered phase outside the light cone $v_{\max}\tau<\ell$, but is significantly simpler.

7. Relaxation in interacting integrable models

We now turn to *interacting* integrable models that are solvable by the Bethe Ansatz [20, 213, 214]. By 'interacting' we mean theories in which the scattering matrix is momentum dependent. Most of our discussion will focus on the example of the spin-1/2 Heisenberg chain.

J. Stat. Mech. (2016) 064002

7.1. The 'initial state problem'

Integrability allows the construction of a basis of simultaneous eigenstates of the Hamiltonian and all its conservation laws. Unlike in the non-interacting case these states have a very complicated structure described by the Bethe Ansatz [20, 213, 214]. When we consider a quench between two integrable Hamiltonians $H(h_0) \to H(h)$, we are thus faced with the problem of how to translate between the eigenbases of the two integrable theories. This is a difficult undertaking [215, 216], and no general formalism for achieving it is currently known. Progress has however been made in cases where the initial state has a simpler structure, in particular for (matrix) product states in either position [58, 63, 65, 66, 68, 69] or momentum/rapidity space [95, 97, 105, 107, 111, 113, 114]. There are two main methods for encoding the relevant information contained in the initial state.

1. Let us denote the eigenstates of the post-quench Hamiltonian $H(h)$ by $|n\rangle$. One way to implement the initial conditions is via the *overlaps* $\langle n|\Psi(0)\rangle$ [67]. If these are known, the initial state can be translated into the eigenbasis of the time evolution operator. This method is used in the quench action approach [176] (see the review by Caux [217] in this volume).

2. Let us denote the local conservation laws of $H(h)$ by $\{I^{(n)}\}$. If the set $\{I^{(n)}\}$ is in some sense complete [112, 218, 219], then the initial conditions can be encoded in the constraints

$$\lim_{L\to\infty} \frac{\langle\Psi(0)|I^{(n)}|\Psi(0)\rangle}{L} = \lim_{L\to\infty} \frac{\mathrm{Tr}(\rho^{\mathrm{SS}} I^{(n)})}{L}, \tag{170}$$

   where ρ^{SS} is one of the density matrices (GGE, GMC, diagonal ensemble) that describes the local properties of the stationary state.

In the following we will discuss implementations of the second approach.

7.2. On mode occupation operators

In free theories a convenient way for constructing the GGE is by exploiting the linear relation between the local conservation laws and the mode occupation operators, see (42). In interacting integrable models the situation is different. Like free theories they feature stable excitations. In the thermodynamic limit these can be described by creation and annihilation operators $Z_a^\dagger(\lambda)$, $Z_a(\lambda)$ (the index a labels different particle species) fulfilling the Faddeev–Zamolodchikov algebra [220, 221]

$$\begin{aligned} Z_a(\lambda_1)Z_b(\lambda_2) &= S_{ab}^{cd}(\lambda_1,\lambda_2)Z_d(\lambda_2)Z_c(\lambda_1), \\ Z_a(\lambda_1)Z_b^\dagger(\lambda_2) &= 2\pi\delta(\lambda_1-\lambda_2)\delta_{a,b} + S_{bc}^{da}(\lambda_2,\lambda_1)Z_d^\dagger(\lambda_2)Z_c(\lambda_1). \end{aligned} \tag{171}$$

Here λ parametrizes the momenta $p_a(\lambda)$ and $S_{ab}^{cd}(\lambda_1,\lambda_2)$ is the purely elastic two-particle S-matrix. The generalized mode occupation operators $N_a(\lambda) = Z_a^\dagger(\lambda)Z_a(\lambda)$ then indeed provide a set of mutually commuting conserved charges. The problem is that, due to

the interacting nature of the stable excitations, there is no simple way of defining such operators in the finite volume [95], which is the standard way of making the theory well defined (working directly in the thermodynamic limit requires the regularization of very complicated singularities [40, 95, 222], which appears impractical in general). The problem lies in the nature of the quantization conditions in the finite volume, which on a ring of length L read

$$e^{iLp_a(\lambda_j^{(a)})} = -\prod_{b,k} S_{ab}(\lambda_j^{(a)}, \lambda_k^{(b)}). \tag{172}$$

The solutions to this complicated system of coupled equations are such that the possible values of $\lambda_j^{(a)}$, and hence $p_a(\lambda_j^{(a)})$, depend in a very sensitive way on all the other particles present in a given excitation. This is fundamentally different from the non-interacting case, where the momenta are simply given by

$$p_a(\lambda_j^{(a)}) = \frac{2\pi}{L} \times \text{ integer}, \tag{173}$$

and are *independent* of the particle content of a given excitation. This makes it clear that defining finite volume analogues of $N_a(\lambda)$ is difficult.

7.3. The spin-1/2 Heisenberg model

Our paradigm for an interacting integrable model will be the spin-1/2 Heisenberg XXZ chain. Its Hamiltonian on a ring with L sites is

$$H_{\text{XXZ}} = \frac{J}{4}\sum_{j=1}^{L} \sigma_j^x\sigma_{j+1}^x + \sigma_j^y\sigma_{j+1}^y + \Delta\left[\sigma_j^z\sigma_{j+1}^z - 1\right], \tag{174}$$

where we will assume for definiteness that

$$\Delta = \cosh(\eta) \geqslant 1. \tag{175}$$

From now on we set $J = 1$.

7.3.1. Generalized microcanonical ensemble For interacting integrable models the GMC is easier to work with than the GGE. It is based on working with macro-states obtained by taking the thermodynamic limit of eigenstates constructed from the Bethe Ansatz. This procedure is an essential ingredient of the Thermodyamic Bethe Ansatz and is reviewed in several monographs [213, 225]. A very brief summary is given in appendix B.2. The upshot is that macro-states in integrable models are characterized by an (infinite) set of densities $\{\rho_{n,p}(\lambda)|n = 1, 2, \dots\}$, where n labels all distinct stable species of excitations in the model. A given macro-state corresponds to a set of micro-states $|\Phi\rangle$, called *representative states* in [176]. These are by construction simultaneous eigenstates of all local conservation laws. For the macro-state describing the stationary state after our quench, they satisfy the initial conditions

$$\lim_{L\to\infty} \frac{\langle\Phi^{\text{SS}}|I^{(n)}|\Phi^{\text{SS}}\rangle}{L} = \lim_{L\to\infty} \frac{\langle\Psi(0)|I^{(n)}|\Psi(0)\rangle}{L}. \tag{176}$$

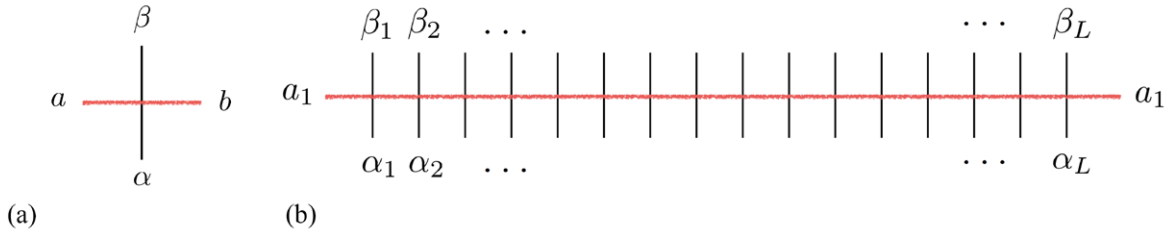

Figure 10. (a) Vertex with weight $[L_n(\lambda)]^{ab}_{\alpha\beta}$. The horizontal and vertical lines are associated with the 'auxiliary' and 'quantum' spaces respectively. (b) Transfer matrix element $\tau_{\frac{1}{2}}(\lambda)^{\beta_1\dots\beta_L}_{\alpha_1\dots\alpha_L}$.

The GMC density matrix is then defined [176] in terms of a single such 'representative' micro-state $|\Phi^{\rm SS}\rangle$

$$\rho^{\rm GMC} = |\Phi^{\rm SS}\rangle\langle\Phi^{\rm SS}|. \tag{177}$$

Here we have assumed that the stationary state is given in terms of a single macro-state constructed from the Bethe Ansatz. In principle it is possible that the steady state has a more complicated structure and requires a description in terms of a sum of several density matrices of the form (177).

7.3.2. Transfer matrix and 'ultra-local' conservation laws According to our general discussion, local observables should relax to an appropriate GGE after quenches to the XXZ chain. In order to construct this GGE, we need to know the required set of local conservation laws of (174). One family of conservation laws has been known for a long time and is most conveniently constructed by exploiting the relation of the Heisenberg Hamiltonian to the transfer matrix of the six-vertex model [20, 223, 224]. The fundamental building block of the six-vertex model is the L-operator

$$L_n(\lambda) = \frac{1}{\sinh(\eta+\mathrm{i}\lambda)}\Big[\sinh\Big(\frac{\eta}{2}+\mathrm{i}\lambda\Big)\cosh\Big(\frac{\eta}{2}\Big)+\cosh\Big(\frac{\eta}{2}+\mathrm{i}\lambda\Big)\sinh\Big(\frac{\eta}{2}\Big)\tau^z\sigma^z_n + \sinh(\eta)(\tau^-\sigma^+_n+\tau^+\sigma^-_n)\Big], \tag{178}$$

which acts on the tensor product $\mathbb{C}^2\otimes\mathbb{C}^2$ of 'auxiliary' and 'quantum' spaces through the Pauli matrices τ^α and σ^α respectively. Matrix elements in the auxiliary/quantum spaces are denotes by Roman/Greek letters respectively, e.g.

$$(\tau^-\sigma^+_n)^{ab}_{\alpha\beta} = \tau^-_{ab}(\sigma^+_n)_{\alpha\beta}. \tag{179}$$

The vertex weights of the six-vertex model are obtained by taking matrix elements $L(\lambda)^{ab}_{\alpha\beta}$ and have a graphical representation as shown in figure 10(a). The row-to-row transfer matrix is obtained as shown in figure 10(b)

$$\Big(\tau_{\frac{1}{2}}(\lambda)\Big)^{\beta_1\dots\beta_L}_{\alpha_1\dots\alpha_L} = (L_1(\lambda))^{a_1a_2}_{\alpha_1\beta_1}(L_2(\lambda))^{a_2a_3}_{\alpha_2\beta_2}\dots(L_L(\lambda))^{a_La_1}_{\alpha_L\beta_L}. \tag{180}$$

J. Stat. Mech. (2016) 064002

The partition function of the 6-vertex model on an $L \times M$ rectangular lattice with periodic boundary conditions is then

$$Z_{6-\text{vertex}} = \text{Tr}\left[\left(\tau_{\frac{1}{2}}(\lambda)\right)^M\right], \tag{181}$$

where the trace is over the quantum space. As a consequence of the Yang–Baxter relation for the L-operators [20], the transfer matrices form a commuting family

$$[\tau_{\frac{1}{2}}(\lambda), \tau_{\frac{1}{2}}(\mu)] = 0. \tag{182}$$

The Heisenberg Hamiltonian is related to the transfer matrix by taking a logarithmic derivative

$$H_{\text{XXZ}} = -\text{i}\frac{\sinh\eta}{2}\frac{\partial}{\partial\lambda}\bigg|_{\lambda=0} \ln\left[\tau_{\frac{1}{2}}(\lambda)\right]. \tag{183}$$

By virtue of the commutation relations (182) it is clear that a set of mutually commuting operators can be obtained by taking higher derivatives, i.e.

$$H^{(\frac{1}{2},k)} = \text{i}\left(-\frac{\sinh\eta}{2}\frac{\partial}{\partial\lambda}\right)^k\bigg|_{\lambda=0} \ln\left[\tau_{\frac{1}{2}}(\lambda)\right]. \tag{184}$$

Crucially, these conservation laws have the form

$$H^{(\frac{1}{2},k)} = \sum_j H^{(\frac{1}{2},k)}_{j,j+1,\ldots,j+k}, \tag{185}$$

where the densities $H^{(\frac{1}{2},k)}_{j,j+1,\ldots,j+k}$ act non-trivially only on the $k+1$ consecutive sites $j, j+1, \ldots, j+k$. These conservation laws are sometimes referred to as *ultra-local*. They have been studied extensively in the literature [20, 226–228]. We note that the above construction is not restricted to Heisenberg models, but works much more generally [20].

7.3.3. 'Ultra-local' GGE According to our general discussion, the GGE describing the steady state after a quench to the Heisenberg model should contain all of the conservation laws (184). An important question is whether these conservation laws are also sufficient. This was investigated in [58, 59, 63]. The basic idea is as follows. One considers time evolution induced by the Hamiltonian (174) starting from an initial state $|\Psi(0)\rangle$. The quantities of interest are the matrix elements of the reduced density matrix on a short interval in the steady state, see (21)

$$g_{\alpha_1,\ldots,\alpha_n} = \lim_{t\to\infty}\lim_{L\to\infty}\langle\Psi(t)|\sigma_1^{\alpha_1}\sigma_2^{\alpha_2}\ldots\sigma_n^{\alpha_n}|\Psi(t)\rangle. \tag{186}$$

The question is whether these expectation values can be obtained, to a given accuracy, from a GGE density matrix of the form

$$\rho^{(y)}_{\text{ulGGE}} = \frac{1}{Z_{\text{ulGGE}}}\exp\left(-\sum_{k=1}^{y}\lambda_k^{(y)}H^{(k,\frac{1}{2})}\right), \tag{187}$$

which takes into account the first y conservation laws in the series (184). The Lagrange multipliers $\lambda_k^{(y)}$ are in principle fixed by the requirements

$$\langle\Psi(0)|H^{\left(k,\frac{1}{2}\right)}|\Psi(0)\rangle = \mathrm{Tr}\left(\rho_{\mathrm{ulGGE}}^{(y)} H^{\left(k,\frac{1}{2}\right)}\right), \quad k = 1, \ldots, y. \tag{188}$$

In practice it is very difficult to determine the Lagrange multipliers from these conditions, even for very simple initial states $|\Psi(0)\rangle$. A method to circumvent this problem was developed in [58]. The idea is to define a generating function for the initial values (188)

$$\begin{aligned}\Omega_{\Psi(0)}^{\left(\frac{1}{2}\right)}(\lambda) &= \lim_{L\to\infty} \frac{\mathrm{i}}{L}\langle\Psi(0)|\tau'_{\frac{1}{2}}(\lambda)\tau^{-1}_{\frac{1}{2}}(\lambda)|\Psi(0)\rangle \\ &= \lim_{L\to\infty} \frac{1}{L}\sum_{k=1}\left(-\frac{2}{\sinh\eta}\right)^k \frac{\lambda^{k-1}}{(k-1)!}\frac{\langle\Psi(0)|H^{\left(k,\frac{1}{2}\right)}|\Psi(0)\rangle}{L}.\end{aligned} \tag{189}$$

For large L (and real λ) the inverse of the transfer matrix becomes

$$\tau^{-1}_{\frac{1}{2}}(\lambda) \simeq \left(\tau_{\frac{1}{2}}(\lambda)\right)^\dagger = \left[\frac{\sinh(-\mathrm{i}\lambda)}{\sinh(\eta-\mathrm{i}\lambda)}\right]^L \tau_{\frac{1}{2}}(\lambda+\mathrm{i}\eta). \tag{190}$$

Using the expression (180) of the transfer matrix as a product of L-operators, the generating function can thus be expressed in the form

$$\Omega_{\Psi(0)}^{\left(\frac{1}{2}\right)}(\lambda) = \lim_{L\to\infty} \frac{\mathrm{i}}{L}\frac{\partial}{\partial x}\bigg|_{x=\lambda} \mathrm{Sp}\langle\Psi(0)|\, V_L(x,\lambda)\ldots V_1(x,\lambda)|\Psi(0)\rangle, \tag{191}$$

where $V_n(x,\lambda)$ are 4×4 matrices with entries $(V_n(x,\lambda))^{ab}_{cd}$ that are operators acting on the 2-dimensional quantum space at site n, and Sp denotes the usual trace for 4×4 matrices. The explicit expression is

$$[(V_n(x,\lambda))^{ab}_{cd}]_{\alpha_n\beta_n} = \frac{\sinh(-\mathrm{i}\lambda)}{\sinh(\eta-\mathrm{i}\lambda)}\sum_{\gamma_n}(L_n(x))^{ab}_{\alpha_n\gamma_n}(L_n(\lambda+\mathrm{i}\eta))^{cd}_{\gamma_n\beta_n}. \tag{192}$$

The advantage of representation (191) is that it can be efficiently evaluated for initial states $|\Psi(0)\rangle$ of matrix product form [58, 63]. To understand the principle behind this let us consider a translationally invariant product state

$$|\Psi(0)\rangle = \otimes_{j=1}^L |\psi\rangle_j. \tag{193}$$

In this case the generating function is obtained from the eigenvalues of the 4×4 matrix $U(x,\lambda) = {}_1\langle\psi|\, V_1(x,\lambda)|\psi\rangle_1$ as

$$\Omega_{\Psi(0)}^{\left(\frac{1}{2}\right)}(\lambda) = \lim_{L\to\infty} \frac{\mathrm{i}}{L}\frac{\partial}{\partial x}\bigg|_{x=\lambda} \mathrm{Sp}(U(x,\lambda)^L). \tag{194}$$

J. Stat. Mech. (2016) 064002

An efficient algorithm for calculating $\Omega^{(\frac{1}{2})}_{\Psi(0)}(\lambda)$ for matrix-product states was given in [63]. Having encoded the 'initial data' of our quantum quench in the generating function $\Omega^{(\frac{1}{2})}_{\Psi(0)}(\lambda)$, we now move on to the calculation of expectation values of local operators in the state given by (187). A very useful observation is that $\rho^{(y)}_{\mathrm{ulGGE}}$ can be viewed as a Gibbs ensemble for the 'Hamiltonian'

$$H_{\mathrm{eff}} = \sum_{k=1}^{y} \lambda_k^{(y)} H^{(k,\frac{1}{2})} \tag{195}$$

at an effective inverse temperature $\beta = 1$. As all $H^{(k,\frac{1}{2})}$ commute and are obtained by taking logarithmic derivatives of the transfer matrix, finite temperature properties of (195) can be studied by standard methods [226, 229]. The *Quantum Transfer Matrix approach* (QTM) [230] is particularly useful in this regard, as it provides an efficient way to obtain explicit results for thermal averages of local operators [231, 232] (see also [233]). [58, 59, 63] employed the QTM approach to the calculation of steady state properties of the density matrix (187) for quenches from simple initial states. By employing the generating function (189), it is possible to take into account *all* ultra-local conservation laws, and arrive at explicit results for local observables without having to determine the Lagrange multipliers $\lambda_k^{(\infty)}$ [58]. In the QTM approach the stationary state is described in terms of the solution of a system of coupled, nonlinear integral equations. Remarkably, the information on the initial state enters this system only *via* the function $\Omega^{(\frac{1}{2})}_{\Psi(0)}(\lambda)$. Results for spin correlators obtained in this way were compared to t-DMRG computations for quenches from a variety of initial states in [63], and found to be compatible within the limitations of the numerical analysis.

The subsequent application of the *quench action approach* [176] (reviewed by Caux [217] in this volume) to the same problem revealed that the ultra-local GGE in fact does not correctly describe the steady state for quenches to the spin-1/2 Heisenberg chain [65, 66, 68–70], although it does provide a very good approximation for e.g. quenches from the Néel state. This suggested the existence of hitherto unknown conservation laws in the Heisenberg chain, which need to be taken into account in the construction of the GGE.

7.3.4. 'Quasi-local' GGE The 'missing' conservation laws for the spin-1/2 Heisenberg XXZ chain were discovered in [64, 234, 237] (see the review by Ilievski, Medenjak, Prosen and Zadnik [235] in this volume). Their structure is quite different from that of the ultra-local conservation laws discussed above: their densities are not local in the sense that they act non-trivially only on a finite number of neighbouring sites, but *quasi-local*. Similar conservation laws had been identified earlier in relation to transport properties of the Heisenberg chain [236]. In order to define the concept of quasi-locality one introduces an inner product on the space of operators by

$$(A, B) = \langle A^\dagger B\rangle_\infty, \qquad \langle A\rangle_\infty = \frac{1}{2^L}\mathrm{Tr}(A). \tag{196}$$

Definition 6. Quasi-local operators [234].

Let us consider an operator Q and expand it in terms of mutually orthogonal local operators $q_{j,r}$ of range r

$$Q = \sum_j \sum_r q_{j,r}. \tag{197}$$

Q is called *quasi-local* if it fulfils the following three conditions:

$$\begin{aligned} &\text{(QL1)}: && \lim_{L\to\infty} \frac{1}{L}(Q - \langle Q\rangle_\infty, Q - \langle Q\rangle_\infty) = \text{const}; \\ &\text{(QL2)}: && \lim_{L\to\infty} (Q, B_k) \ \text{exists}, \\ &\text{(QL3)}: && (q_{j,r}, q_{j,r}) < C\mathrm{e}^{-r/\xi}, \end{aligned} \tag{198}$$

where B_k is any operator that acts non-trivially only on a fixed number of k sites, and ξ and C are positive constants.

In the anisotropic Heisenberg chain quasi-local charges can be constructed as follows [64, 234]. It is well known that the six-vertex model transfer matrix (180) is part of a much larger family, built from the L-operators

$$L_n^{(S)}(\lambda) = \frac{1}{\sinh\left(\frac{\eta}{2}(1+s)+\mathrm{i}\lambda\right)}\Bigg[\sinh\left(\frac{\eta}{2}+\mathrm{i}\lambda\right)\cosh(\eta\mathcal{S}^z) + \cosh\left(\frac{\eta}{2}+\mathrm{i}\lambda\right)\sinh(\eta\mathcal{S}^z)\sigma_n^z + \sinh(\eta)(\mathcal{S}^-\sigma_n^+ + \mathcal{S}^+\sigma_n^-)\Bigg], \tag{199}$$

which again acts on the tensor product of auxiliary and quantum spaces, but now the auxiliary space is $2S+1$ dimensional. Here S is an arbitrary half integer. The operators $\mathcal{S}^\alpha$ obey a q-deformed SU(2) algebra

$$[\mathcal{S}^+, \mathcal{S}^-] = [2\mathcal{S}^z]_q, \qquad [\mathcal{S}^z, \mathcal{S}^\pm] = \pm\mathcal{S}^\pm, \tag{200}$$

where $[x]_q = \sinh(\eta x)/\sinh(\eta)$, and act on a q-deformed spin-S representation as

$$\mathcal{S}^z|k\rangle = k|k\rangle, \qquad \mathcal{S}^\pm|k\rangle = \sqrt{[S+1\pm k]_q[S\mp k]_q}\,|k\pm1\rangle, \quad k = -S, \ldots, S. \tag{201}$$

A family of row-to-row transfer matrices is then obtained as

$$(\tau_S(\lambda))^{\beta_1\ldots\beta_L}_{\alpha_1\ldots\alpha_L} = (L_1^{(S)}(\lambda))^{a_1a_2}_{\alpha_1\beta_1}(L_2^{(S)}(\lambda))^{a_2a_3}_{\alpha_2\beta_2}\ldots(L_L^{(S)}(\lambda))^{a_La_1}_{\alpha_L\beta_L}. \tag{202}$$

All $\tau_S(\lambda)$ are operators on the same quantum space (a tensor product of L spin-1/2's), and as a consequence of the Yang–Baxter relation form a commuting family

$$[\tau_S(\lambda), \tau_{S'}(\mu)] = 0. \tag{203}$$

By virtue of the commutation relations (182) it is clear that a set of mutually commuting operators can be obtained by taking higher derivatives, i.e.

$$H^{(S,k)} = \mathrm{i}\left(C_S\frac{\partial}{\partial\lambda}\right)^k\Bigg|_{\lambda=0} \ln\left[\tau_S(\lambda)\right], \tag{204}$$

where C_S are some normalization constants that can be conveniently chosen. As a consequence of (203) we have

$$[H^{(S,k)}, H^{(S',k')}] = 0. \tag{205}$$

Apart from the special case $S = 1/2$ these conservation laws are quasi-local. This means that (in the infinite volume) their general structure is

$$H^{(S>\frac{1}{2},k)} = \sum_{j=-\infty}^{\infty} \sum_{k\geqslant 1} \sum_{\alpha_1,\ldots,\alpha_k} f^{(k)}_{\alpha_1\alpha_2\ldots\alpha_k} \sigma_j^{\alpha_1}\sigma_{j+1}^{\alpha_2}\ldots\sigma_{j+k-1}^{\alpha_k}, \tag{206}$$

where $\alpha_j = 0, x, y, z$, and the coefficient functions $f^{(k)}_{\alpha_1\ldots\alpha_k}$ decay sufficiently fast with k so that the conservation laws are extensive. As shown in [64], the initial data of the quantum quench can again be encoded in suitably chosen generating functions, which are generalizations of (189)

$$\begin{aligned}\Omega^{(S)}_{\Psi(0)}(\lambda) &= \lim_{L\to\infty} \frac{\mathrm{i}}{L}\langle\Psi(0)|\tau_S'(\lambda)\tau_S^{-1}(\lambda)|\Psi(0)\rangle \\ &= \lim_{L\to\infty} \frac{\mathrm{i}}{L}\left[\frac{\sinh\left(\frac{\eta}{2}(1-2S)-\mathrm{i}\lambda\right)}{\sinh\left(\frac{\eta}{2}(1+2S)-\mathrm{i}\lambda\right)}\right]^L \langle\Psi(0)|\tau_S'(\lambda)\tau_S(\lambda-\eta)|\Psi(0)\rangle.\end{aligned} \tag{207}$$

The generating functionals $\Omega^{(S)}_{\Psi(0)}(\lambda)$ can be evaluated for matrix product states by the same method discussed above (although the computational effort increases with the value of S).

The most convenient description of the stationary state turns out to be in terms of the generalized microcanonical ensemble discussed above. The steady state is characterized by the set $\{\rho^{\mathrm{SS}}_{n.v}(\lambda)|n = 1,\ldots\}$ of particle densities or the equivalent set of hole densities $\{\rho^{\mathrm{SS}}_{n,h}(\lambda)|n = 1,\ldots\}$. Ultimately this set must be determined by the initial conditions, which are encoded in (207). We now use that $X_S(\lambda) = \tau_S'(\lambda)\tau_S^{-1}(\lambda)$ can be diagonalized by algebraic Bethe Ansatz [20, 238]. The eigenvalues of $X_S(\lambda)$ for M-particle states with $M \sim L$ are of the form

$$\nu_S(\lambda) = \sum_{k=1}^{M} \frac{2\sinh(2S\eta)}{\cos(2\lambda+2\lambda_k)-\cosh(2S\eta)} + o(L), \tag{208}$$

where the λ_k are solutions to the Bethe Ansatz equations [238]

$$\left(\frac{\sin(\lambda_j+\mathrm{i}\eta S)}{\sin(\lambda_j-\mathrm{i}\eta S)}\right)^L = \prod_{k\neq j=1}^{M} \frac{\sin(\lambda_j-\lambda_k+\mathrm{i}\eta)}{\sin(\lambda_j-\lambda_k-\mathrm{i}\eta)}, \quad j = 1,\ldots,M. \tag{209}$$

In the thermodynamic limit this can be simplified by following through the usual logic of the string hypothesis and the thermodynamic Bethe Ansatz [213, 214, 225]. Rather than with solutions to the Bethe equations (209) one then works with macro-states $|\boldsymbol{\rho}\rangle$, which are described by sets $\{\rho_{n,p}(\lambda)|n = 1,\ldots\}$ of particle densities or the equivalent set of hole densities $\{\rho_{n,h}(\lambda)|n = 1,\ldots\}$. The eigenvalue equation (208) then becomes [64]

J. Stat. Mech. (2016) 064002

$$\lim_{L\to\infty}\frac{1}{L}\langle\boldsymbol{\rho}|X_S(\mu)|\boldsymbol{\rho}\rangle=\sum_{k\in\mathbb{Z}}\frac{\mathrm{e}^{-\mathrm{i}2k\mu}}{\cosh(k\eta)}\left(\int_{-\pi/2}^{\pi/2}\mathrm{d}\lambda\,\mathrm{e}^{2\mathrm{i}k\lambda}\rho_{2S,h}(\lambda)-\mathrm{e}^{-2S|k|\eta}\right). \tag{210}$$

For $|\boldsymbol{\rho}\rangle=|\boldsymbol{\rho}^{\mathrm{SS}}\rangle$ the right hand side of (210) must agree with the initial values after the quench (207). This is achieved by setting [64]

$$\rho^{\mathrm{SS}}_{2S,h}(\lambda)=a_{2S}(\lambda)+\frac{1}{2\pi}\left[\Omega^{(S)}_{\Psi(0)}\left(\lambda+\mathrm{i}\frac{\eta}{2}\right)+\Omega^{(S)}_{\Psi(0)}\left(\lambda-\mathrm{i}\frac{\eta}{2}\right)\right], \tag{211}$$

where $a_{2S}(\lambda)$ is a function independent of the initial state that is defined in appendix B.2. This shows that the initial data (207), which involves both ultra-local and quasi-local conservation laws, completely determines the macro-state that defines the generalized microcanonical ensemble. We note that the derivation did not invoke the maximum entropy principle. For the particular case of quenches from the Néel state (211) agrees with the one obtained by the quench action approach [65, 66, 68, 69].

The generalization of the approach discussed above for quenches to particular values of Δ with $-1<\Delta<1$ in the Heisenberg model (174) was achieved in [239].

8. Outlook

We have given an introduction to quantum quenches in many-particle systems and then reviewed recent developments, focussing in particular on the role played by conservation laws. In spite of the impressive progress of the last few years, many important questions remain largely open. Let us list a few of them in no particular order.

1. In the spin-1/2 Heisenberg XXZ chain quasi-local conservation laws have been shown to play a prominent role in determining the stationary state. It is believed that this holds quite generally in interacting integrable models. The construction used in the XXZ case can in principle be generalized to the $sl(M|N)$ family of integrable graded quantum 'spin' chains, see e.g. [240], and it would be interesting to investigate the role of quasi-local charges in such models. The Hubbard model is another very interesting case, but is like to be more difficult to handle due to its non standard structure [213].

2. So far only particularly simple classes of initial states can be accommodated, see section 7.1. It would be highly desirable to have a more general method for capturing the information on the initial state.

3. In interacting theories the focus has so far been on stationary state properties. The study of the full time evolution of observables is much less developed [95, 113, 241, 242]. A promising method for analyzing the time dependence of the expectation values of local operators after a quantum quench in an interacting integrable theory is the quench action approach [176]. So far it has been implemented only in a very small number of cases [95, 113], and further studies are sorely needed.

4. As we have seen, the non-equilibrium dynamics of integrable and non-integrable models is quite different. This poses the question of what happens, when one adds a small perturbation to an integrable model. This has been investigated in a number of theoretical works [51, 127, 243–263], and is of immediate experimental relevance [264, 265] (see also the review by Langen, Gasenzer and Schmiedmayer in this volume [18]). The generic effect of adding a small integrability breaking term appears to be the generation of an intermediate 'prethermalization' time scale, below which the system retains information about being proximate in parameter space to an integrable model. At late times thermalization seems to set in [258]. So far the theoretical analyses are restricted to weak interactions and/or short times, and it is crucial to go beyond these limitations.

Acknowledgments

We owe gratitude to many colleagues for collaborations and sharing their insights on quantum quenches with us. This margin is too small to acknowledge them all, but particular thanks are due to B Bertini, P Calabrese, J Cardy, J-S Caux, M Collura, R Konik, G Mussardo, M Rigol, D Schuricht and A Silva. This work was supported by the EPSRC under grant EP/N01930X/1, the Isaac Newton Institute for Mathematical Sciences under grant EP/K032208/1, and the Agence Nationale de la Recherche under grant LabEx ENS-ICFP:ANR-10-LABX-0010/ANR- 10-IDEX-0001- 02 PSL∗.

Appendix A. Requirements on the initial state

A.1. Cluster decomposition

We have defined our quench protocol such that it results in initial states $|\Psi(0)\rangle$ that have a cluster decomposition property (12). This requirement is often relaxed in both numerical and analytical investigations, and in some cases $|\Psi(0)\rangle$ is taken to be a Schrödinger cat state, see e.g. [65, 66, 68, 69]. An example is provided by quenches where the system is initialized in a classical Néel state $|\uparrow\downarrow\uparrow\downarrow\ldots\rangle$. This breaks translational invariance and it can be calculationally convenient to work instead with a translationally invariant cat state

$$\frac{1}{\sqrt{2}}(|\uparrow\downarrow\uparrow\downarrow\uparrow\ldots\rangle + |\downarrow\uparrow\downarrow\uparrow\downarrow\ldots\rangle). \tag{A.1}$$

While for specific calculations such replacements can be useful, they significantly affect the steady state behaviour in general. This can be seen by considering a $\mathbb{Z}_2$ symmetric pre-quench Hamiltonian H_0 with a ground state that spontaneously breaks the $\mathbb{Z}_2$ symmetry. An example is provided by the transverse-field Ising chain (104) with $h < 1$. In the thermodynamic limit H_0 has two ground states $|\Psi_\pm\rangle$, both of which have a cluster decomposition property. We now consider a general linear combination

$$|\Psi(0)\rangle = \cos\theta|\Psi_+\rangle + \mathrm{e}^{\mathrm{i}\phi}\sin\theta|\Psi_-\rangle. \tag{A.2}$$

As $|\Psi_\pm\rangle$ are macroscopically distinct (as they lead to different order parameters), we conclude that expectation values of local operators $\mathcal{O}$ are given by

$$\langle\Psi(0)|\mathcal{O}|\Psi(0)\rangle = \cos^2\theta\langle\Psi_+|\mathcal{O}|\Psi_+\rangle + \sin^2\theta\langle\Psi_-|\mathcal{O}|\Psi_-\rangle. \tag{A.3}$$

As the Hamiltonian of our system is short ranged, this decomposition persists at all finite times, i.e.

$$\langle\Psi(t)|\mathcal{O}|\Psi(t)\rangle = \cos^2\theta\langle\Psi_+(t)|\mathcal{O}|\Psi_+(t)\rangle + \sin^2\theta\langle\Psi_-(t)|\mathcal{O}|\Psi_-(t)\rangle \tag{A.4}$$

To see this, we may use a result derived in [180] for the time evolution of local operators with short-ranged Hamiltonians: restricting $\mathcal{O}(t) = \mathrm{e}^{\mathrm{i}Ht}\mathcal{O}\mathrm{e}^{-\mathrm{i}Ht}$ to a subsystem S of size $|S|$ gives an error that scales as $\mathrm{e}^{(2vt-|S|)/\zeta}$, where ζ is a constant and v is the Lieb–Robinson velocity. This means that it is possible to approximate $\mathcal{O}(t)$ to a given accuracy by a local operator of a 'size' that scales as $2vt$. This in turn implies that $\langle\Psi_+|\mathcal{O}(t)|\Psi_-\rangle = 0$, because $|\Psi_\pm\rangle$ are macroscopically distinct.

On the other hand, our system relaxes locally by construction if we initialize it in $|\Psi_\pm(0)\rangle$, i.e.

$$\lim_{t\to\infty}|\Psi_\pm(t)\rangle\langle\Psi_\pm(t)| = {}_{\mathrm{loc}}\,\rho_\pm^{\mathrm{SS}}. \tag{A.5}$$

Putting everything together we conclude that

$$\lim_{t\to\infty}|\Psi(t)\rangle\langle\Psi(t)| = {}_{\mathrm{loc}}\,\rho^{\mathrm{SS}} = \cos^2\theta\rho_+^{\mathrm{SS}} + \sin^2\theta\rho_-^{\mathrm{SS}}. \tag{A.6}$$

The problem is that this form of the stationary state can be different from what one would expect on the basis of local relaxation to (generalized) Gibbs ensembles. To be specific, we consider the example of a quench to an anisotropic spin-1/2 Heisenberg chain

$$H = \frac{J}{4}\sum_\ell \sigma_\ell^y\sigma_{\ell+1}^y + \sigma_\ell^z\sigma_{\ell+1}^z + \Delta\sigma_\ell^x\sigma_{\ell+1}^x + g\sigma_\ell^x\sigma_{\ell+2}^x. \tag{A.7}$$

Imposing $\Delta, g \neq 0$ renders this model non-integrable, but is has one local conservation law

$$Q = \sum_\ell \sigma_\ell^x, \quad [H, Q] = 0. \tag{A.8}$$

Our initial state is of the form (A.2), where $|\Psi_\pm(0)\rangle$ are the two ground states of the TFIC in the thermodynamic limit at $h < 1$. We note that the energy density e of (A.7) is the same in both $|\Psi_+\rangle$ and $|\Psi_-\rangle$. As these states have a cluster decomposition property, it follows from our general discussion that the respective stationary states are locally equivalent to grand canonical ensembles

$$\lim_{t\to\infty}|\Psi_\pm(t)\rangle\langle\Psi_\pm(t)| = {}_{\mathrm{loc}}\,\rho_\pm^{\mathrm{GC}} = \frac{\mathrm{e}^{-\beta_\pm H-\mu_\pm Q}}{Z_\pm}, \tag{A.9}$$

where the values for $\beta_\pm$ and $\mu_\pm$ are obtained by fixing the energy density e and charge density $q_\pm$ to agree with their initial values at time $t = 0$. Equation (A.6) tells us that the correct stationary state in this example is then

$$\rho^{\mathrm{SS}} =_{\mathrm{loc}} \cos^2\theta\rho_+^{\mathrm{GC}} + \sin^2\theta\rho_-^{\mathrm{GC}}. \tag{A.10}$$

Crucially, while the density matrices $\rho_{\pm}^{\mathrm{GC}}$ have the cluster decomposition property, ρ^{SS} does not. This can be seen as follows. The local conservation law distinguishes between the two states $|\Psi_{\pm}\rangle$

$$q_{+} = \langle\Psi_{+}|\sigma_{\ell}^{x}|\Psi_{+}\rangle \neq \langle\Psi_{-}|\sigma_{\ell}^{x}|\Psi_{-}\rangle = q_{-}. \tag{A.11}$$

Using the cluster decomposition property of $\rho_{\pm}^{\mathrm{GC}}$ we have

$$\lim_{|n-\ell|\to\infty} \mathrm{Tr}(\rho_{\pm}^{\mathrm{GC}}\sigma_{\ell}^{x}\sigma_{n}^{x}) = q_{\pm}^{2}, \tag{A.12}$$

which in turn establishes that ρ^{SS} does not have the cluster decomposition property

$$\lim_{|n-\ell|\to\infty} [\mathrm{Tr}(\rho^{\mathrm{SS}}\sigma_{\ell}^{x}\sigma_{n}^{x}) - \mathrm{Tr}(\rho^{\mathrm{SS}}\sigma_{\ell}^{x})\mathrm{Tr}(\rho^{\mathrm{SS}}\sigma_{n}^{x})] = \frac{(q_{+}-q_{-})^{2}}{4}\sin^{2}(2\theta) \neq 0. \tag{A.13}$$

On the other hand, if we were to apply our formalism of local relaxation blindly to our Hamiltonian (A.7), we would conclude that the stationary state is locally equivalent to a grand canonical ensemble, which is expected to have a cluster decomposition property [267].

Our discussion can be summarized as follows: *If there exists at least one integral of motion that distinguishes* $|\Psi_{-}\rangle$ *from* $|\Psi_{+}\rangle$*, the stationary state associated with the time evolution of the cat state* (A.2) *does not possess the cluster decomposition property* (12) *and hence is not described by a standard generalized Gibbs ensemble.*

A.2. Probability distributions of energy and conservation laws

Let us consider a post-quench Hamiltonian H with a set of local conservation laws $I^{(n)}$, see (31) and (32). In our basic definition of a quantum quench we initialize the system in a pure state $|\Psi(0)\rangle$. Then the cluster decomposition property implies that the probability distribution of energy and all local conservation laws approach delta-functions in the thermodynamic limit, e.g.

$$P_{n}(\epsilon) = \lim_{L\to\infty}\frac{1}{L}\mathrm{Tr}\left[\rho(0)\delta(I^{(n)}-L\epsilon)\right] = \delta(\varepsilon - i^{(n)}), \quad i^{(n)} = \lim_{L\to\infty}\frac{1}{L}\mathrm{Tr}\left[\rho(0)I^{(n)}\right], \tag{A.14}$$

where $\rho(0) = |\Psi(0)\rangle\langle\Psi(0)|$. As we have pointed out, it is sometimes desirable to consider initial density matrices $\rho(0)$ that are not pure states. When doing so one must ensure that (A.14) continues to hold. In cases where it does not it is clearly impossible for the system to locally relax to a GGE, because there the probability distributions of all conservation laws approach delta functions in the thermodynamic limit. Generalizations of GGE ideas to such cases have been explored in [266].

Appendix B. 'Atypical' macro-states in integrable models

Integrable models have the unusual property of having *atypical* finite entropy eigenstates at finite energy densities. This is well known for non-interacting theories and we discuss this case first.

J. Stat. Mech. (2016) 064002

B.1. Free fermions

Let us consider a model of free fermions with Hamiltonian

$$H = \sum_k \epsilon(k) n(k), \tag{B.1}$$

where $n(k) = c^\dagger(k)c(k)$. Imposing periodic boundary conditions quantizes the allowed momenta

$$k_n = \frac{2\pi n}{L}, \quad n = -\frac{L}{2} + 1, \ldots, \frac{L}{2}. \tag{B.2}$$

We now focus on a special class of Fock states $\prod_{j=1}^N c^\dagger(k_j)|0\rangle$, for which the *particle densities*

$$\rho_p(k_j) = \frac{1}{L(k_{j+1} - k_j)} \tag{B.3}$$

approach smooth functions in the thermodynamic limit $N, L \to \infty$, $n = N/L$ fixed. For such states, the number of particles in the interval $[k_n, k_n + \Delta k]$ for large L is given by

$$\rho_p(k_n)\Delta k. \tag{B.4}$$

It is convenient to define a *hole density* by $\rho_h(k_j) = \frac{1}{2\pi} - \rho_p(k_j)$. In the thermodynamic limit many different choices of $\{k_j\}$ lead to the same *macro-state* described by a given particle density. To enumerate them we note that the number of different states in the interval $[k, k + \Delta k]$, that give rise to a given density in the thermodynamic limit, is obtained by distributing $\rho_p(k)L\Delta k$ particles among $(\rho_p(k) + \rho_h(k))L\Delta k$ vacancies. This follows a binomial distribution. For large L the latter may be approximated by Stirling's formula, and in the thermodynamic limit one obtains the well-known expression for the entropy per site

$$s[\rho_p] = \int_{-\pi}^{\pi} \mathrm{d}k \left[(\rho_p(k) + \rho_h(k)) \ln(\rho_p(k) + \rho_h(k)) - \rho_p(k) \ln(\rho_p(k)) - \rho_h(k) \ln(\rho_h(k))\right]. \tag{B.5}$$

Let us now investigate what kind of macro-states exist for a given energy density e. The most likely (maximum entropy) macro-state can be constructed using equilibrium statistical mechanics. Extremizing the free energy per site

$$f[\rho_p] = \int_{-\pi}^{\pi} \frac{\mathrm{d}k}{2\pi} \epsilon(k)\rho_p(k) - Ts[\rho_p] \tag{B.6}$$

with respect to the particle density ρ_p gives

$$\rho_p^{\mathrm{eq}}(k) = \frac{1}{2\pi} \frac{1}{1 + \mathrm{e}^{\epsilon(k)/T}}. \tag{B.7}$$

The 'temperature' T is related to the energy density e by

$$e = \int_{-\pi}^{\pi} \frac{\mathrm{d}k}{2\pi} \frac{\epsilon(k)}{1 + \mathrm{e}^{\epsilon(k)/T}}. \tag{B.8}$$

J. Stat. Mech. (2016) 064002

The entropy per site of this equilibrium state is

$$s[\rho_p^{\rm eq}] = \frac{\partial}{\partial T} T \int_{-\pi}^{\pi} \frac{{\rm d}k}{2\pi} \ln\left[1 + {\rm e}^{-\epsilon(k)/T}\right]. \tag{B.9}$$

By construction the macro-state (B.7) is the *typical* state at energy density (B.8): if we randomly pick an energy eigenstate with energy density e for a very large system size L, the probability for this state to have particle density (B.7) is exponentially close (in L) to one. On the other hand, there are *atypical* finite entropy macro-states characterized by their respective particle densities $\rho_p(k)$. As a particular example we consider our tight-binding model (40) for $\mu = 0$, which gives a dispersion $\epsilon(k) = -2J\cos(k)$. We fix the particle density to be $1/2$ and the energy density to be $e = -0.405\,838J$, which corresponds to temperature $T = J$ in (B.7), (B.8), i.e.

$$\rho_p^{\rm eq}(k) = \frac{1}{2\pi} \frac{1}{1 + {\rm e}^{-2\cos(k)}}. \tag{B.10}$$

The entropy of the equilibrium state is $s_{\rm eq} = 0.511\,571$. Let us now consider the family of macro-states described by the particle density

$$\rho_p^{(\lambda)}(k) = \frac{1}{2\pi} \frac{1}{1 + {\rm e}^{-4\cos(k) - \lambda\cos(3k)}}. \tag{B.11}$$

Fixing $\lambda = 2.430\,96...$ gives us the same particle and energy densities as for the equilibrium state, i.e. $n = 1/2$ and $e = -0.405\,838J$. The entropy density $s = 0.396\,781$ is of course lower than that of the (maximum entropy) equilibrium state. This means that if we randomly select an energy eigenstate with particle density $n = 1/2$ and energy density $e = -0.405\,838J$ for a very large system size L, we are exponentially more likely by a factor ${\rm e}^{L(s_{\rm eq} - s)}$ to end up with a state described by (B.10) than one described by (B.11). Unsurprisingly, expectation values of local operators are generally different in the two macro-states. As an example, let us consider

$$\mathcal{O}_j = c_j^\dagger c_{j+3} + c_{j+3}^\dagger c_j. \tag{B.12}$$

Setting again $\lambda = 2.430\,96...$ and taking the thermodynamic limit we have

$$\langle \rho_p^{\rm eq}(k)|\mathcal{O}_j|\rho_p^{\rm eq}(k)\rangle = -0.027\,1229 \neq \langle \rho_p^{(\lambda)}(k)|\mathcal{O}_j|\rho_p^{(\lambda)}(k)\rangle = 0.215\,148. \tag{B.13}$$

Here the expectation values may be taken with regards to any micro-state that gives rise to the appropriate macro-state in the thermodynamic limit.

B.2. Interacting theories: anisotropic spin-1/2 Heisenberg model

The situation in integrable models is analogous to what we just discussed for free fermions. The main difference arises from the more complicated structure and interacting nature of the elementary excitations in integrable models. For the sake of definiteness we consider the particular example of the spin-1/2 Heisenberg model (174) with $\Delta \geqslant 1$. Energy eigenstates $|\lambda_1, \ldots, \lambda_M\rangle$ on a ring of length L are parametrized by M rapidity variables λ_j, which fulfil the quantization conditions [225]

$$\left(\frac{\sin(\lambda_j+\mathrm{i}\frac{\eta}{2})}{\sin(\lambda_j-\mathrm{i}\frac{\eta}{2})}\right)^L=\prod_{k\neq j=1}^{M}\frac{\sin(\lambda_j-\lambda_k+\mathrm{i}\eta)}{\sin(\lambda_j-\lambda_k-\mathrm{i}\eta)},\quad j=1,\ldots,M. \tag{B.14}$$

Each λ_j is associated with an elementary 'magnon' excitation over the ferromagnetic state with all spins up, and the total energy and momentum of the eigenstate are additive $E=\sum_{j=1}^{M}e(\lambda_j)$, $P=\sum_{j=1}^{M}p(\lambda_j)$. As a result of interactions, magnons form *bound states*. These correspond to 'string solutions' of the quantization conditions (B.14)

$$\lambda_\alpha^{n,j}=\lambda_\alpha^n+\mathrm{i}\frac{\eta}{2}(n+1-2j)+\mathrm{i}\delta_\alpha^{n,j},\qquad j=1,\ldots,n, \tag{B.15}$$

where $\delta_\alpha^{n,j}$ are deviations from 'ideal' strings that become negligible when we take the thermodynamic limit at finite densities of magnons and bound states, see 6.2.A of [268]. As a consequence of integrability these bound states are *stable* excitations. The generalization of particle density description of macro-states in free theories to interacting integrable models is then clear: macro-states are characterized by an (infinite) set of densities $\{\rho_{n,p}(\lambda)|n=1,2,\ldots\}$ for magnons ($n=1$) and bound states of all lengths ($n\geqslant 2$). Just as in the case of free fermions, we can define corresponding hole densities $\rho_{n,h}(\lambda)$. The relation between particle and hole densities is fixed by the quantization conditions (B.14)

$$\rho_{n,t}(\lambda)\equiv\rho_{n,p}(\lambda)+\rho_{n,h}(\lambda)=a_n(\lambda)-\sum_{m=1}^{\infty}\int_{-\frac{\pi}{2}}^{\frac{\pi}{2}}\mathrm{d}\mu\ A_{nm}(\lambda-\mu)\rho_{m,p}(\mu), \tag{B.16}$$

where $A_{nm}(\lambda)=(1-\delta_{n,m})a_{|n-m|}(\lambda)+2a_{|n-m|+2}(\lambda)+\cdots+2a_{n+m-2}(\lambda)+a_{n+m}(\lambda)$ and $a_n(\lambda)=\frac{1}{2\pi}\frac{2\sinh(n\eta)}{\cosh(n\eta)-\cos(2\lambda)}$. Equation (B.16) allows one to express the hole densities in terms of the particle densities and vice versa, but in contrast to the non-interacting case the relationship is non-trivial. The energy and entropy per site of a macro-state are given by

$$\begin{aligned}e[\{\rho_{n,p}\}]&=-J\sinh(\eta)\sum_{n=1}^{\infty}\int_{-\frac{\pi}{2}}^{\frac{\pi}{2}}\mathrm{d}\lambda\ \rho_{n,p}(\lambda)\ a_n(\lambda),\\ s[\{\rho_{n,p},\rho_{n,h}\}]&=\sum_{n=1}^{\infty}\int_{-\frac{\pi}{2}}^{\frac{\pi}{2}}\mathrm{d}\lambda[(\rho_{n,t}(\lambda))\ln(\rho_{n,t}(\lambda))-\rho_{n,p}(\lambda)\ln(\rho_{n,p}(\lambda))-\rho_{n,h}(\lambda)\ln(\rho_{n,h}(\lambda))].\end{aligned} \tag{B.17}$$

The typical state at a given energy density is then obtained by extremizing the free energy per set $f[\{\rho_{n,p}\}]=e[\{\rho_{n,p}\}]-Ts[\{\rho_{n,p},\rho_{n,h}\}]$ with respect to particle and hole densities under the constraints (B.16). This results in the so-called Thermodynamic Bethe Ansatz equations [225]. By construction this state is *thermal*, i.e. corresponds to a standard Gibbs distribution.

Atypical finite entropy states can be constructed by specifying a set of particle densities $\{\rho_{n,p}(\lambda)\}$. The corresponding hole densities are then obtained by solving

J. Stat. Mech. (2016) 064002

equations (B.16). The entropy per site of the resulting macro-state can be calculated from (B.17), and will by construction be smaller than that of the maximum entropy state.

Appendix C. Stationary state correlators in the TFIC

In this appendix we summarize results for the amplitudes $C^{\alpha}(\ell)$ describing the subleading behaviour of stationary state spin–spin correlators in the TFIC, see equation (133).

C.1. Transverse spin correlator

Here the amplitude is of the form [26]

$$C^z(\ell) = \bar{C}^z \ell^{-\alpha^z}, \qquad \alpha^z = \begin{cases} 1 & \text{if } |\ln h| > |\ln h_0|, \\ 0 & \text{if } h_0 = 1/h, \\ 1/2 & \text{if } |\ln h| < |\ln h_0|, \end{cases} \tag{C.1}$$

where the constant is known exactly

$$C^z = \begin{cases} \dfrac{|h_0 - 1/h_0|}{4\pi} \dfrac{h_0 - h}{hh_0 - 1} & \text{if } |\ln h| > |\ln h_0|, \\ -\dfrac{(h-1/h)^2}{2\pi} & \text{if } h_0 = 1/h, \\ \dfrac{(h-1/h)\sqrt{|h_0 - 1/h_0|}\,(h_0 - h)}{8\sqrt{\pi}\,h} \sqrt{\dfrac{h_0 - h}{h_0(hh_0 - 1)}} \dfrac{\mathrm{e}^{\mathrm{sgn}(\ln h)|\ln h_0|/2}}{\sinh \frac{|\ln h| + |\ln h_0|}{2}} & \text{if } |\ln h| < |\ln h_0|. \end{cases} \tag{C.2}$$

C.2. Longitudinal spin correlator

Here the large-ℓ asymptotics of prefactor $C^x(\ell)$ are as follows.

1. Quench within the ferromagnetic phase (h_0, $h < 1$).

$$C^x(\ell) \equiv \mathcal{C}^x_{\mathrm{FF}} = \frac{1 - hh_0 + \sqrt{(1-h^2)(1-h_0^2)}}{2\sqrt{1-hh_0}\sqrt[4]{1-h_0^2}}. \tag{C.3}$$

2. Quench from the ferromagnetic to the paramagnetic phase ($h_0 < 1 < h$).

$$C^x(\ell) \equiv \mathcal{C}^x_{\mathrm{FP}} = \sqrt{\frac{h\sqrt{1-h_0^2}}{h + h_0}}. \tag{C.4}$$

3. Quench from the paramagnetic to the ferromagnetic phase ($h_0 > 1 > h$).

$$C^x(\ell) \equiv \mathcal{C}^x_{\mathrm{PF}}(\ell) = \sqrt{\frac{h_0 - h}{\sqrt{h_0^2 - 1}}} \cos\left(\ell \arctan \frac{\sqrt{(1-h^2)(h_0^2 - 1)}}{1 + h_0 h}\right). \tag{C.5}$$

4. Quench within the paramagnetic phase ($1 < h_0,\ h$).

$$C^x(\ell) \equiv \mathcal{C}^x_{\rm PP}(\ell) = \begin{cases} -\dfrac{h_0\sqrt{h}\left(hh_0 - 1 + \sqrt{(h^2-1)(h_0^2-1)}\right)^2}{4\sqrt{\pi}\,(h_0^2-1)^{3/4}(h_0h-1)^{3/2}(h-h_0)}\,\ell^{-3/2} & \text{if } 1 < h_0 < h, \\ \sqrt{\dfrac{h(h_0-h)\sqrt{h_0^2-1}}{(h+h_0)(hh_0-1)}} & \text{if } 1 < h < h_0. \end{cases} \tag{C.6}$$

References

[1] Deutsch J M 1991 Quantum statistical mechanics in a closed system *Phys. Rev.* A **43** 2046
Srednicki M 1994 Chaos and quantum thermalization *Phys. Rev.* E **50** 888

[2] Greiner M, Mandel O, Hänsch T W and Bloch I 2002 Collapse and revival of the matter wave field of a Bose–Einstein condensate *Nature* **419** 51–4

[3] Kinoshita T, Wenger T and Weiss D S 2006 A quantum Newton's cradle *Nature* **440** 900

[4] Hofferberth S, Lesanovsky I, Fischer B, Schumm T and Schmiedmayer J 2007 Non-equilibrium coherence dynamics in one-dimensional Bose gases *Nature* **449** 324–7

[5] Hackermuller L, Schneider U, Moreno-Cardoner M, Kitagawa T, Will S, Best T, Demler E, Altman E, Bloch I and Paredes B 2010 Anomalous expansion of attractively interacting fermionic atoms in an optical lattice *Science* **327** 1621

[6] Trotzky S, Flesch A, McCulloch I P, Schollwöck U, Eisert J and Bloch I 2012 Probing the relaxation towards equilibrium in an isolated strongly correlated 1D Bose gas *Nat. Phys.* **8** 325

[7] Gring M, Kuhnert M, Langen T, Kitagawa T, Rauer B, Schreitl M, Mazets I, Smith D A, Demler E and Schmiedmayer J 2012 Relaxation dynamics and pre-thermalization in an isolated quantum system *Science* **337** 1318

[8] Schneider U *et al* 2012 Fermionic transport and out-of-equilibrium dynamics in a homogeneous Hubbard model with ultracold atoms *Nat. Phys.* **8** 213

[9] Cheneau M, Barmettler P, Poletti D, Endres M, Schauss P, Fukuhara T, Gross C, Bloch I, Kollath C and Kuhr S 2012 Light-cone-like spreading of correlations in a quantum many-body system *Nature* **481** 484

[10] Langen T, Geiger R, Kuhnert M, Rauer B and Schmiedmayer J 2013 Local emergence of thermal correlations in an isolated quantum many-body system *Nat. Phys.* **9** 640

[11] Meinert F, Mark M J, Kirilov E, Lauber K, Weinmann P, Daley A J and Nägerl H-C 2013 Quantum quench in an atomic one-dimensional Ising chain *Phys. Rev. Lett.* **111** 053003

[12] Fukuhara T *et al* 2013 Quantum dynamics of a mobile spin impurity *Nat. Phys.* **9** 235

[13] Fukuhara T, Schauß P, Hild S, Cheneau M, Bloch I and Gross C 2013 Microscopic observation of magnon bound states and their dynamics *Nature* **502** 76

[14] Ronzheimer J P, Schreiber M, Braun S, Hodgman S S, Langer S, McCulloch I P, Heidrich-Meisner F, Bloch I and Schneider U 2013 Expansion dynamics of interacting bosons in homogeneous lattices in one and two dimensions *Phys. Rev. Lett.* **110** 205301

[15] Navon N, Gaunt A L, Smith R P and Hadzibabic Z 2015 Critical dynamics of spontaneous symmetry breaking in a homogeneous Bose gas *Science* **347** 167

[16] Jurcevic P, Lanyon B P, Hauke P, Hempel C, Zoller P, Blatt R and Roos C F 2014 Quasiparticle engineering and entanglement propagation in a quantum many-body system *Nature* **511** 202

[17] Richerme P, Gong Z-X, Lee A, Senko C, Smith J, Moss-Feig M, Michalakis S, Gorshkov A V and Monroe C 2014 Non-local propagation of correlations in quantum systems with long-range interactions *Nature* **511** 198

[18] Langen T, Gasenzer T and Schmiedmayer J 2016 Prethermalization and universal dynamics in near-integrable quantum systems *J. Stat. Mech.* 064009

[19] Lieb E H and Liniger W 1963 Exact analysis of an interacting Bose gas. I. The general solution and the ground state *Phys. Rev.* **130** 1605
Lieb E H 1963 Exact analysis of an interacting Bose gas. II. The excitation spectrum *Phys. Rev.* **130** 1616

[20] Korepin V E, Izergin A G and Bogoliubov N M 1993 *Quantum Inverse Scattering Method, Correlation Functions and Algebraic Bethe Ansatz* (Cambridge: Cambridge University Press)

J. Stat. Mech. (2016) 064002

[21] Davies B and Korepin V E 2011 Higher conservation laws for the quantum non-linear Schroedinger equation (arXiv:1109.6604)
[22] Cassidy A C, Clark C W and Rigol M 2011 Generalized thermalization in an integrable lattice system *Phys. Rev. Lett.* **106** 140405
[23] Gramsch C and Rigol M 2012 Quenches in a quasidisordered integrable lattice system: dynamics and statistical description of observables after relaxation *Phys. Rev.* A **86** 053615
[24] Wright T M, Rigol M, Davis M J and Kheruntsyan K V 2014 Nonequilibrium dynamics of one-dimensional hard-core anyons following a quench: complete relaxation of one-body observables *Phys. Rev. Lett.* **113** 050601
[25] Calabrese P, Essler F H L and Fagotti M 2011 Quantum quench in the transverse-field Ising chain *Phys. Rev. Lett.* **106** 227203
[26] Calabrese P, Essler F H L and Fagotti M 2012 Quantum quench in the transverse field Ising chain: I. Time evolution of order parameter correlators *J. Stat. Mech.* P07016
[27] Calabrese P, Essler F H L and Fagotti M 2012 Quantum quench in the transverse field Ising chain: II. Stationary state properties *J. Stat. Mech.* P07022
[28] Fagotti M and Essler F H L 2013 Reduced density matrix after a quantum quench *Phys. Rev.* B **87** 245107
[29] Essler F H L, Evangelisti S and Fagotti M 2012 Dynamical correlations after a quantum quench *Phys. Rev. Lett.* **109** 247206
[30] Fagotti M 2013 Finite-size corrections versus relaxation after a sudden quench *Phys. Rev.* B **87** 165106
[31] Kormos M, Bucciantini L and Calabrese P 2014 Stationary entropies after a quench from excited states in the Ising chain *Europhys. Lett.* **107** 40002
[32] Bucciantini L, Kormos M, Calabrese P 2014 Quantum quenches from excited states in the Ising chain *J. Phys. A: Math. Theor.* **47** 175002
[33] Rossini D, Silva A, Mussardo G and Santoro G E 2009 Effective thermal dynamics following a quantum quench in a spin chain *Phys. Rev. Lett.* **102** 127204
Rossini D, Suzuki S, Mussardo G, Santoro G E and Silva A 2010 Long time dynamics following a quench in an integrable quantum spin chain: local versus nonlocal operators and effective thermal behavior *Phys. Rev.* B **82** 144302
[34] Igói F and Rieger H 2000 Long-range correlations in the nonequilibrium quantum relaxation of a spin chain *Phys. Rev. Lett.* **85** 3233
[35] Sengupta K, Powell S and Sachdev S 2004 Quench dynamics across quantum critical points *Phys. Rev.* A **69** 053616
[36] Silva A 2008 Statistics of the work done on a quantum critical system by quenching a control parameter *Phys. Rev. Lett.* **101** 120603
[37] Iglói F and Rieger H 2011 Quantum relaxation after a quench in systems with boundaries *Phys. Rev. Lett.* **106** 035701
[38] Foini L, Cugliandolo L F and Gambassi A 2011 Fluctuation-dissipation relations and critical quenches in the transverse field Ising chain *Phys. Rev.* B **84** 212404
[39] Rieger H and Iglói F 2011 Semiclassical theory for quantum quenches in finite transverse Ising chains *Phys. Rev.* B **84** 165117
[40] Schuricht D and Essler F H L 2012 Dynamics in the Ising field theory after a quantum quench *J. Stat. Mech.* P04017
[41] Foini L, Cugliandolo L F and Gambassi A 2012 Dynamic correlations, fluctuation-dissipation relations, and effective temperatures after a quantum quench of the transverse field Ising chain *J. Stat. Mech.* P09011
[42] Heyl M, Polkovnikov A and Kehrein S 2013 Dynamical quantum phase transitions in the transverse-field Ising model *Phys. Rev. Lett.* **110** 135704
[43] Caneva T, Canovi E, Rossini D, Santoro G E and Silva A 2011 Applicability of the generalized Gibbs ensemble after a quench in the quantum Ising chain *J. Stat. Mech.* P07015
[44] Antal T, Racz Z, Rakos A and Schutz G M 1999 Transport in the XX chain at zero temperature: emergence of flat magnetization profiles *Phys. Rev.* E **59** 4912
[45] Barouch E, McCoy B and Dresden M 1970 Statistical mechanics of the XY model. I *Phys. Rev.* A **2** 1075
[46] Barouch E and McCoy B 1971 Statistical mechanics of the XY model. II *Phys. Rev.* A **3** 786
[47] Barouch E and McCoy B 1971 Statistical mechanics of the XY model. III *Phys. Rev.* A **3** 2137
[48] Fagotti M and Calabrese P 2008 Evolution of entanglement entropy following a quantum quench: analytic results for the XY chain in a transverse magnetic field *Phys. Rev.* A **78** 010306
[49] Cazalilla M A, Iucci A and Chung M-C 2012 Thermalization and quantum correlations in exactly solvable models *Phys. Rev.* E **85** 011133
[50] Blass B, Rieger H and Iglói F 2012 Quantum relaxation and finite-size effects in the XY chain in a transverse field after global quenches *Europhys. Lett.* **99** 30004

J. Stat. Mech. (2016) 064002

[51] Fagotti M 2014 On conservation laws, relaxation and pre-relaxation after a quantum quench *J. Stat. Mech.* P03016
[52] Fagotti M 2016 Local conservation laws in spin-1/2 XY chains with open boundary conditions *J. Stat. Mech.* 063105
[53] Collura M, Calabrese P and Essler F H L 2015 Quantum quench within the gapless phase of the spin-1/2 Heisenberg XXZ spin chain *Phys. Rev.* B **92** 125131
[54] Lancaster J and Mitra A 2010 Quantum quenches in an XXZ spin chain from a spatially inhomogeneous initial state *Phys. Rev.* E **81** 061134
[55] Sabetta T and Misguich G 2013 Nonequilibrium steady states in the quantum XXZ spin chain *Phys. Rev.* B **88** 245114
[56] Bonnes L, Essler F H L and Läuchli A 2014 'Light-Cone' dynamics after quantum quenches in spin chains *Phys. Rev. Lett.* **113** 187203
[57] Canovi E, Rossini D, Fazio R, Santoro G and Silva A 2012 Many-body localization and thermalization in the full probability distribution function of observables *New J. Phys.* **14** 095020
[58] Fagotti M and Essler F H L 2013 Stationary behaviour of observables after a quantum quench in the spin-1/2 Heisenberg XXZ chain *J. Stat. Mech.* P07012
[59] Pozsgay B 2013 The generalized Gibbs ensemble for Heisenberg spin chains *J. Stat. Mech.* P07003
[60] Fagotti M 2013 Dynamical phase transitions as properties of the stationary state: analytic results after quantum quenches in the spin-1/2 XXZ chain (arXiv:1308.0277)
Pozsgay B 2013 Dynamical free energy and the Loschmidt-echo for a class of quantum quenches in the Heisenberg spin chain *J. Stat. Mech.* P10028
[61] Liu W and Andrei N 2014 Quench dynamics of the anisotropic Heisenberg model *Phys. Rev. Lett.* **112** 257204
[62] Barmettler P, Punk M, Gritsev V, Demler E and Altman E 2009 Relaxation of antiferromagnetic order in spin-1/2 chains following a quantum quench *Phys. Rev. Lett.* **102** 130603
Barmettler P, Punk M, Gritsev V, Demler E and Altman E 2010 Quantum quenches in the anisotropic spin-1/2 Heisenberg chain: different approaches to many-body dynamics far from equilibrium *New J. Phys.* **12** 055017
[63] Fagotti M, Collura M, Essler F H L and Calabrese P 2014 Relaxation after quantum quenches in the spin-1/2 Heisenberg XXZ chain *Phys. Rev.* B **89** 125101
[64] Ilievski E, De Nardis J, Wouters B, Caux J-S, Essler F H L and Prosen T 2015 Complete generalized Gibbs ensemble in an interacting theory *Phys. Rev. Lett.* **115** 157201
[65] Brockmann M, Wouters B, Fioretto D, De Nardis J, Vlijm R and Caux J-S 2014 Quench action approach for releasing the Néel state into the spin-1/2 XXZ chain *J. Stat. Mech.* P12009
[66] Wouters B, De Nardis J, Brockmann M, Fioretto D, Rigol M and Caux J-S 2014 Quenching the anisotropic Heisenberg chain: exact solution and generalized Gibbs ensemble predictions *Phys. Rev. Lett.* **113** 117202
[67] Pozsgay B 2014 Overlaps between eigenstates of the XXZ spin-1/2 chain and a class of simple product states *J. Stat. Mech.* P06011
[68] Pozsgay B, Mestyán M, Werner M A, Kormos M, Zaránd G and Takács G 2014 Correlations after quantum quenches in the XXZ spin chain: failure of the generalized Gibbs ensemble *Phys. Rev. Lett.* **113** 117203
[69] Mestyán M, Pozsgay B, Takács G and Werner M A 2015 Quenching the XXZ spin chain: quench action approach versus generalized Gibbs ensemble *J. Stat. Mech.* P04001
[70] Rigol M 2014 Quantum quenches in the thermodynamic limit. II. Initial ground states *Phys. Rev.* E **90** 031301
[71] Mossel J and Caux J-S 2010 Relaxation dynamics in the gapped XXZ spin-1/2 chain *New J. Phys.* **12** 055028
[72] Alba V and Calabrese P 2015 The quench action approach in finite integrable spin chains (arXiv:1512.02213)
[73] Kollar M and Eckstein M 2008 Relaxation of a one-dimensional Mott insulator after an interaction quench *Phys. Rev.* A **78** 013626
[74] Enss T and Sirker J 2012 Lightcone renormalization and quantum quenches in one-dimensional Hubbard models *New J. Phys.* **14** 023008
[75] Iyer D, Mondaini R, Will S and Rigol M 2014 Coherent quench dynamics in the one-dimensional Fermi–Hubbard model *Phys. Rev.* A **90** 031602
[76] Riegger L, Orso G and Heidrich-Meisner F 2015 Interaction quantum quenches in the one-dimensional Fermi–Hubbard model with spin imbalance *Phys. Rev.* A **91** 043623
[77] Bauer A, Dorfner F and Heidrich-Meisner F 2015 Temporal decay of Néel order in the one-dimensional Fermi–Hubbard model *Phys. Rev.* A **91** 053628
[78] Sotiriadis S, Calabrese P and Cardy J 2009 Quantum quench from a thermal initial state *Europhys. Lett.* **87** 20002

J. Stat. Mech. (2016) 064002

[79] Sotiriadis S and Martelloni G 2016 Equilibration and GGE in interacting-to-free quantum quenches in dimensions $d > 1$ *J. Phys. A: Math. Theor.* **49** 095002
[80] Calabrese P and Cardy J 2007 Quantum quenches in extended systems *J. Stat. Mech.* P06008
[81] Cazalilla M A 2006 Effect of suddenly turning on interactions in the Luttinger model *Phys. Rev. Lett.* **97** 156403
[82] Iucci A and Cazalilla M A 2009 Quantum quench dynamics of the Luttinger model *Phys. Rev.* A **80** 063619
[83] Rentrop J, Schuricht D and Meden V 2012 Quench dynamics of the Tomonaga–Luttinger model with momentum-dependent interaction *New J. Phys.* **14** 075001
[84] Karrasch C, Rentrop J, Schuricht D and Meden V 2012 Luttinger-liquid universality in the time evolution after an interaction quench *Phys. Rev. Lett.* **109** 126406
[85] Dóra B, Bácsi Á and Zaránd G 2012 Generalized Gibbs ensemble and work statistics of a quenched Luttinger liquid *Phys. Rev.* B **86** 161109
[86] Nessi N and Iucci A 2013 Quantum quench dynamics of the Coulomb Luttinger model *Phys. Rev.* B **87** 085137
[87] Cazalilla M A and Chung M-C 2016 Quantum Quenches in the Luttinger model and its close relatives *J. Stat. Mech.* 064004
[88] Calabrese P and Cardy J 2016 Quantum quenches in $1 + 1$ dimensional conformal field theories *J. Stat. Mech.* 064003
[89] Calabrese P and Cardy J 2005 Evolution of entanglement entropy in one-dimensional systems *J. Stat. Mech.* P04010
[90] Calabrese P and Cardy J 2006 Time dependence of correlation functions following a quantum quench *Phys. Rev. Lett.* **96** 136801
[91] Cardy J 2014 Thermalization and revivals after a quantum quench in conformal field theory *Phys. Rev. Lett.* **112** 220401
[92] Sotiriadis S 2015 Memory-preserving equilibration after a quantum quench in a 1d critical model (arXiv:1507.07915)
[93] Cardy J 2016 Quantum quenches to a critical point in one dimension: some further results *J. Stat. Mech.* 023103
[94] Gritsev V, Demler E, Lukin M and Polkovnikov A 2007 Spectroscopy of collective excitations in interacting low-dimensional many-body systems using quench dynamics *Phys. Rev. Lett.* **99** 200404
[95] Bertini B, Schuricht D and Essler F H L 2014 Quantum quench in the sine-Gordon model *J. Stat. Mech.* P10035
[96] Kormos M and Zaránd G 2015 Quantum quenches in the sine-Gordon model: a semiclassical approach (arXiv:1507.02708)
[97] Fioretto D and Mussardo G 2010 Quantum quenches in integrable field theories *New J. Phys.* **12** 055015
[98] Bertini B, Piroli L and Calabrese P 2016 Quantum quenches in the sinh-Gordon model: steady state and one point correlation functions (arXiv:1602.08269)
[99] Pozsgay B 2011 Mean values of local operators in highly excited Bethe states *J. Stat. Mech.* P01011
[100] Mussardo G 2013 Infinite-time average of local fields in an integrable quantum field theory after a quantum quench *Phys. Rev. Lett.* **111** 100401
[101] Evangelisti S 2013 Semi-classical theory for quantum quenches in the O(3) non-linear sigma model *J. Stat. Mech.* P04003
[102] Lamacraft A 2011 Noise correlations in the expansion of an interacting one-dimensional Bose gas from a regular array *Phys. Rev.* A **84** 043632
[103] Mossel J and Caux J-S 2012 Exact time evolution of space- and time-dependent correlation functions after an interaction quench in the one-dimensional Bose gas *New J. Phys.* **14** 075006
[104] Collura M, Sotiriadis S and Calabrese P 2013 Equilibration of a Tonks–Girardeau gas following a trap release *Phys. Rev. Lett.* **110** 245301
[105] Kormos M, Shashi A, Chou Y-Z, Caux J-S and Imambekov A 2013 Interaction quenches in the one-dimensional Bose gas *Phys. Rev.* B **88** 205131
[106] Collura M, Sotiriadis S and Calabrese P 2013 Quench dynamics of a Tonks–Girardeau gas released from a harmonic trap *J. Stat. Mech.* P09025
[107] De Nardis J, Wouters B, Brockmann M and Caux J-S 2014 Solution for an interaction quench in the Lieb–Liniger Bose gas *Phys. Rev.* A **89** 033601
[108] Mazza P P, Collura M, Kormos M and Calabrese P 2014 Interaction quench in a trapped 1D Bose gas *J. Stat. Mech.* P11016
[109] Collura M, Kormos M and Calabrese P 2014 Stationary entanglement entropies following an interaction quench in 1D Bose gas *J. Stat. Mech.* P01009

J. Stat. Mech. (2016) 064002

[110] Kormos M, Collura M and Calabrese P 2014 Analytic results for a quantum quench from free to hard-core one-dimensional bosons *Phys. Rev.* A **89** 013609
[111] De Nardis J and Caux J-S 2014 Analytical expression for a post-quench time evolution of the one-body density matrix of one-dimensional hard-core bosons *J. Stat. Mech.* P12012
[112] Essler F H L, Mussardo G and Panfil M 2015 Generalized Gibbs ensembles for quantum field theories *Phys. Rev.* A **91** 051602
[113] De Nardis J, Piroli L and Caux J-S 2015 Relaxation dynamics of local observables in integrable systems *J. Phys. A: Math. Theor.* **48** 43FT01
[114] Piroli L, Calabrese P and Essler F H L 2016 Multiparticle bound-state formation following a quantum quench to the one-dimensional Bose gas with attractive interactions *Phys. Rev. Lett.* **116** 070408
[115] Collura M and Karevski D 2010 Critical quench dynamics in confined systems *Phys. Rev. Lett.* **104** 200601
[116] Dziarmaga J 2010 Dynamics of a quantum phase transition and relaxation to a steady state *Adv. Phys.* **59** 1063
De Grandi C, Gritsev V and Polkovnikov A 2010 Quench dynamics near a quantum critical point: application to the sine-Gordon model *Phys. Rev.* B **81** 224301
Dutta A, Aeppli G, Chakrabarti B K, Divakaran U, Rosenbaum T F and Sen D 2015 *Quantum Phase Transitions in Transverse Field Spin Models: from Statistical Physics to Quantum Information* (Cambridge: Cambridge University Press)
[117] Zurek W H 1996 Cosmological experiments in condensed matter systems *Phys. Rep.* **276** 177
[118] Polkovnikov A, Sengupta K, Silva A and Vengalattore M 2011 Colloquium: Nonequilibrium dynamics of closed interacting quantum systems *Rev. Mod. Phys.* **83** 863
[119] Gogolin C and Eisert J 2015 Equilibration, thermalisation, and the emergence of statistical mechanics in closed quantum systems—a review (arXiv:1503.07538)
[120] Lamacraft A and Moore J E 2011 Potential insights into non-equilibrium behavior from atomic physics *Ultracold Bosonic and Fermionic Gases* ed A Fetter *et al* (Amsterdam: Elsevier) (arXiv:1106.3567)
[121] D'Alessio L, Kafri Y, Polkovnikov A and Rigol M 2015 From quantum chaos and eigenstate thermalization to statistical mechanics and thermodynamics (arXiv:1509.06411)
[122] Barankov R A and Levitov L S 2006 Synchronization in the BCS pairing dynamics as a critical phenomenon *Phys. Rev. Lett.* **96** 230403
Yuzbashyan E A and Dzero M 2006 Dynamical vanishing of the order parameter in a fermionic condensate *Phys. Rev. Lett.* **96** 230404
[123] Vidal G, Latorre J I, Rico E and Kitaev A 2003 Entanglement in quantum critical phenomena *Phys. Rev. Lett.* **90** 227902
[124] Peschel I and Eisler V 2009 Reduced density matrices and entanglement entropy in free lattice models *J. Phys. A: Math. Theor.* **42** 504003
[125] Verstraete F, Wolf M M, Perez-Garcia D and Cirac J I 2006 Criticality, the area law, and the computational power of projected entangled pair states *Phys. Rev. Lett.* **96** 220601
Hastings M B 2007 Entropy and entanglement in quantum ground states *Phys. Rev.* B **76** 035114
de Beaudrap N, Osborne T J and Eisert J 2010 Ground states of unfrustrated spin Hamiltonians satisfy an area law *New J. Phys.* **12** 095007
[126] Barthel T and Schollwöck U 2008 Dephasing and the steady state in quantum many-particle systems *Phys. Rev. Lett.* **100** 100601
[127] Fagotti M and Collura M 2015 Universal prethermalization dynamics of entanglement entropies after a global quench (arXiv:1507.02678)
[128] Sotiriadis S and Calabrese P 2014 Validity of the GGE for quantum quenches from interacting to noninteracting models *J. Stat. Mech.* P07024
[129] Bettelheim E, Abanov A G and Wiegmann P 2006 Quantum shock waves—the case for non-linear effects in dynamics of electronic liquids *Phys. Rev. Lett.* **97** 246401
[130] Bettelheim E, Abanov A G and Wiegmann P 2006 Orthogonality catastrophe and shock waves in a non-equilibrium Fermi gas *Phys. Rev. Lett.* **97** 246402
[131] Sotiriadis S and Cardy J 2008 Inhomogeneous quantum quenches *J. Stat. Mech.* P11003
[132] Calabrese P, Hagendorf C and Le Doussal P 2008 Time evolution of 1D gapless models from a domain-wall initial state: SLE continued? *J. Stat. Mech.* P07013
[133] Bettelheim E and Wiegmann P 2011 Fermi distribution of semicalssical non-eqilibrium Fermi states *Phys. Rev.* B **84** 085102
[134] Vidmar L, Langer S, McCulloch I P, Schneider U, Schollwoeck U and Heidrich-Meisner F 2013 Sudden expansion of Mott insulators in one dimension *Phys. Rev.* B **88** 235117
[135] Eisler V and Racz Z 2013 Full counting statistics in a propagating quantum front and random matrix spectra *Phys. Rev. Lett.* **110** 060602

J. Stat. Mech. (2016) 064002

[136] Rajabpour M A and Sotiriadis S 2014 Quantum quench of the trap frequency in the harmonic Calogero model *Phys. Rev.* A **89** 033620
[137] Mei Z, Vidmar L, Heidrich-Meisner F and Bolech C J 2016 Unveiling hidden structure of many-body wavefunctions of integrable systems via sudden expansion experiments *Phys. Rev.* A **93** 021607
[138] Aschbacher W H and Pillet C-A 2003 Non-equilibrium steady states of the XY chain *J. Stat. Phys.* **112** 1153
[139] Aschbacher W H and Barbaroux J-M 2006 Out of equilibrium correlations in the XY chain *Lett. Math. Phys.* **77** 11
[140] Bernard D and Doyon B 2012 Energy flow in non-equilibrium conformal field theory *J. Phys. A: Math. Theor.* **45** 362001
[141] Caux J-S and Konik R M 2012 Constructing the generalized Gibbs ensemble after a quantum quench *Phys. Rev. Lett.* **109** 175301
[142] Bernard D and Doyon B 2015 Non-equilibrium steady states in conformal field theory *Ann. H. Poincaré* **16** 113
[143] Mintchev M and Sorba P 2013 Luttinger liquid in a non-equilibrium steady state *J. Phys. A: Math. Theor.* **49** 095006
[144] De Luca A, Viti J, Bernard D and Doyon B 2013 Nonequilibrium thermal transport in the quantum Ising chain *Phys. Rev.* B **88** 134301
[145] Doyon B, Hoogeveen M and Bernard D 2014 Energy flow and fluctuations in non-equilibrium conformal field theory on star graphs *J. Stat. Mech.* P03002
[146] Castro-Alvaredo O, Chen Y, Doyon B and Hoogeveen M 2014 Thermodynamic Bethe ansatz for non-equilibrium steady states: exact energy current and fluctuations in integrable QFT *J. Stat. Mech.* P03011
[147] De Luca A, Martelloni G and Viti J 2014 Stationary states in a free fermionic chain from the quench action method *Phys. Rev.* A **91** 021603
[148] Doyon B, Lucas A, Schalm K and Bhaseen M J 2015 Non-equilibrium steady states in the Klein–Gordon theory *J. Phys. A: Math. Theor.* **48** 095002
[149] Doyon B 2015 Lower bounds for ballistic current and noise in non-equilibrium quantum steady states *Nucl. Phys.* B **892** 190
[150] Viti J, Stéphan J M, Dubail J and Haque M 2015 Inhomogeneous quenches in a fermionic chain: exact results (arXiv:1507.08132)
[151] Platini T and Karevski D 2007 Relaxation in the XX quantum chain *J. Phys. A: Math. Theor.* **40** 1711
[152] Eisler V, Karevski D, Platini T and Peschel I 2008 Entanglement evolution after connecting finite to infinite quantum chains *J. Stat. Mech.* P01023
[153] Bernard D and Doyon B 2016 Conformal field theory out of equilibrium: a review (arXiv:1603.07765)
[154] Vasseur R and Moore J E 2016 Nonequilibrium quantum dynamics and transport: from integrability to many-body localization *J. Stat. Mech.* 064010
[155] Cramer M, Dawson C M, Eisert J and Osborne T J 2008 Exact relaxation in a class of nonequilibrium quantum lattice systems *Phys. Rev. Lett.* **100** 030602
[156] Cramer M and Eisert J 2010 A quantum central limit theorem for non-equilibrium systems: exact local relaxation of correlated states *New J. Phys.* **12** 055020
[157] Sirker J, Konstantinidis N P, Andraschko F and Sedlmayr N 2014 Locality and thermalization in closed quantum systems *Phys. Rev.* A **89** 042104
[158] Garrison J R and Grover T 2015 Does a single eigenstate encode the full Hamiltonian? (arXiv:1503.00729)
[159] Rigol M and Srednicki M 2012 Alternatives to eigenstate thermalization *Phys. Rev. Lett.* **108** 110601
[160] Rigol M, Dunjko V and Olshanii M 2008 Thermalization and its mechanism for generic isolated quantum systems *Nature* **452** 854
[161] Braun S, Ronzheimer J P, Schreiber M, Hodgman S S, Rom T, Bloch I and Schneider U 2013 Negative absolute temperature for motional degrees of freedom *Science* **339** 52
[162] Prosen T 1998 A new class of completely integrable quantum spin chains *J. Phys. A: Math. Gen.* **31** L397
Grady M 1981 Infinite set of conserved charges in the Ising model *Phys. Rev.* D **25** 1103
[163] Jaynes E T 1957 Information theory and statistical mechanics *Phys. Rev.* **106** 620
[164] Rigol M, Dunjko V, Yurovsky V and Olshanii M 2007 Relaxation in a completely integrable many-body quantum system: an *ab initio* study of the dynamics of the highly excited states of 1D lattice hard-core bosons *Phys. Rev. Lett.* **98** 50405
[165] Doyon B 2015 Thermalization and pseudolocality in extended quantum systems (arXiv:1512.03713)
[166] Rigol M 2009 Breakdown of thermalization in finite one-dimensional systems *Phys. Rev. Lett.* **103** 100403
[167] Rigol M 2009 Quantum quenches and thermalization in one-dimensional fermionic systems *Phys. Rev.* A **80** 053607

J. Stat. Mech. (2016) 064002

[168] Biroli G, Kollath C and Läuchli A M 2010 Effect of rare fluctuations on the thermalization of isolated quantum systems *Phys. Rev. Lett.* **105** 250401
[169] Santos L F and Rigol M 2010 Localization and the effects of symmetries in the thermalization properties of one-dimensional quantum systems *Phys. Rev.* E **82** 031130
[170] Rigol M and Santos L F 2010 Quantum chaos and thermalization in gapped systems *Phys. Rev.* A **82** 011604
[171] Neuenhahn C and Marquardt F 2012 Thermalization of interacting fermions and delocalization in Fock space *Phys. Rev.* E **85** 060101
[172] Steinigeweg R, Herbrych J and Prelovsek P 2013 Eigenstate thermalization within isolated spin-chain systems *Phys. Rev.* E **87** 012118
[173] Beugeling W, Moessner R and Haque M 2014 Finite-size scaling of eigenstate thermalization *Phys. Rev.* E **89** 042112
[174] Kim H, Ikeda T N and Huse D A 2014 Testing whether all eigenstates obey the eigenstate thermalization hypothesis *Phys. Rev.* E **90** 052105
[175] Beugeling W, Moessner R and Haque M 2015 Off-diagonal matrix elements of local operators in many-body quantum systems *Phys. Rev.* E **91** 012144
[176] Caux J-S and Essler F H L 2013 Time evolution of local observables after quenching to an integrable model *Phys. Rev. Lett.* **110** 257203
[177] Lieb E, Schultz T and Mattis D 1961 Two soluble models of an antiferromagnetic chain *Ann. Phys.* **16** 407
[178] Alba V 2015 Simulating the generalized Gibbs ensemble (GGE): a Hilbert space Monte Carlo approach (arXiv:1507.06994)
[179] Fröhlich B, Feld M, Vogt E, Koschorreck M, Zwerger W and Köhl M 2011 Radio-frequency spectroscopy of a strongly interacting two-dimensional Fermi gas *Phys. Rev. Lett.* **106** 105301
[180] Bravyi S, Hastings M B and Verstraete F 2006 Lieb–Robinson bounds and the generation of correlations and topological quantum order *Phys. Rev. Lett.* **97** 050401
[181] Khatami E, Pupillo G, Srednicki M and Rigol M 2013 Fluctuation-dissipation theorem in an isolated system of quantum dipolar bosons after a quench *Phys. Rev. Lett.* **111** 050403
[182] De Chiara G, Montangero S, Calabrese P and Fazio R 2006 Entanglement entropy dynamics of Heisenberg chains *J. Stat. Mech.* P03001
[183] Läuchli A and Kollath C 2008 Spreading of correlations and entanglement after a quench in the one-dimensional Bose–Hubbard model *J. Stat. Mech.* P05018
[184] Manmana S R, Wessel S, Noack R M and Muramatsu A 2009 Time evolution of correlations in strongly interacting fermions after a quantum quench *Phys. Rev.* B **79** 155104
[185] Carleo G, Becca F, Sanchez-Palencia L, Sorella S and Fabrizio M 2014 Light-cone effect and supersonic correlations in one- and two-dimensional bosonic superfluids *Phys. Rev.* A **89** 031602
[186] Hauke P and Tagliacozzo L 2013 Spread of correlations in long-range interacting quantum systems *Phys. Rev. Lett.* **111** 207202
[187] Schachenmayer J, Lanyon B P, Roos C F and Daley A J 2013 Entanglement growth in quench dynamics with variable range interactions *Phys. Rev.* X **3** 031015
[188] Eisert J, van den Worm M, Manmana S R and Kastner M 2013 Breakdown of quasilocality in long-range quantum lattice models *Phys. Rev. Lett.* **111** 260401
[189] Vodola D, Lepori L, Ercolessi E and Pupillo G 2016 Long-range Ising, Kitaev models: phases, correlations and edge modes *New J. Phys.* **18** 015001
[190] Regemortel M V, Sels D and Wouters M 2015 Information propagation and equilibration in long-range Kitaev chains (arXiv:1511.05459)
[191] Buyskikh A S, Fagotti M, Schachenmayer J, Essler F H L and Daley A J 2016 Entanglement growth and correlation spreading with variable-range interactions in spin and fermionic tunnelling models *Phys. Rev.* A **93** 053620
[192] Abraham D B, Barouch E, Gallavotti G and Martin-Löf A 1970 Thermalization of a magnetic impurity in the isotropic XY model *Phys. Rev. Lett.* **25** 1449
Abraham D B, Barouch E, Gallavotti G and Martin-Löf A 1971 Dynamics of a local perturbation in the XY model. I—approach to equilibrium *Stud. Appl. Math.* **50** 121
Kollath C, Schollwöck U and Zwerger W 2005 Spin-charge separation in cold Fermi-gases: a real time analysis *Phys. Rev. Lett.* **95** 176401
Calabrese P and Cardy J 2007 Entanglement and correlation functions following a local quench: a conformal field theory approach *J. Stat. Mech.* P10004
Stéphan J-M and Dubail J 2011 Local quantum quenches in critical one-dimensional systems: entanglement, the Loschmidt echo, and light-cone effects *J. Stat. Mech.* P08019

J. Stat. Mech. (2016) 064002

Ganahl M, Rabel E, Essler F H L and Evertz H-G 2012 Observation of complex bound states in the spin-1/2 Heisenberg XXZ chain using local quantum quenches *Phys. Rev. Lett.* **108** 077206
[193] Lieb E H and Robinson D W 1972 The finite group velocity of quantum spin systems *Commun. Math. Phys.* **28** 251
[194] Sims R and Nachtergaele B 2010 Lieb–Robinson bounds in quantum many-body physics *Entropy and the Quantum* vol 529, ed R Sims and D Ueltschi (Providence, RI: American Mathematical Society)
[195] Jünemann J, Cadarso A, Perez-Garcia D, Bermudez A and García-Ripoll J J 2013 Lieb–Robinson bounds for spin-boson lattice models and trapped ions *Phys. Rev. Lett.* **111** 230404
[196] Kliesch M, Gogolin C and Eisert J 2013 Lieb–Robinson bounds and the simulation of time evolution of local observables in lattice systems *Many-Electron Approaches in Physics, Chemistry and Mathematics: a Multidisciplinary View* ed L D Site and V Bach (Cham: Springer)
[197] Poulin D 2010 Lieb–Robinson bound and locality for general Markovian quantum dynamics *Phys. Rev. Lett.* **104** 190401
[198] Bocchieri P and Loinger A 1957 Quantum recurrence theorem *Phys. Rev.* **107** 337
[199] Sachdev S 2001 *Quantum Phase Transitions* (Cambridge: Cambridge University Press)
[200] Viehmann O, von Delft J and Marquardt F 2013 Observing the nonequilibrium dynamics of the quantum transverse-field Ising chain in circuit QED *Phys. Rev. Lett.* **110** 030601
Viehmann O, von Delft J and Marquardt F 2013 The quantum transverse-field Ising chain in circuit quantum electrodynamics: effects of disorder on the nonequilibrium dynamics *New J. Phys.* **15** 035013
[201] Lieb E, Schultz T and Mattis D 1961 Two soluble models of an antiferromagnetic chain *Annal. Phys.* **16** 407
[202] McCoy B M, Barouch E and Abraham D B 1971 Statistical mechanics of the XY model. IV. time-dependent spin-correlation functions *Phys. Rev.* A **4** 2331
Derzhko O and Krokhmalskii T 1997 Dynamic structure factor of the spin-1/2 transverse Ising chain *Phys. Rev.* **56** 11659
Derzhko O and Krokhmalskii T 1998 Numerical approach for the study of the spin-1/2 xy chains dynamic properties *Phys. Stat. Sol.* **208** 221
[203] Bugrij A 2001 Correlation function of the two-dimensional Ising model on the finite lattice. I *Theor. Math. Phys.* **127** 528
Bugrij A and Lisovyy O 2003 Spin matrix elements in 2D Ising model on the finite lattice *Phys. Lett.* A **319** 390
von Gehlen G, Iorgov N, Pakuliak S, Shadura V and Tykhyy Y 2008 Form-factors in the Baxter–Bazhanov–Stroganov model II: Ising model on the finite lattice *J. Phys. A: Math. Theor.* **41** 095003
Iorgov N, Shadura V and Tykhyy Yu 2011 Spin operator matrix elements in the quantum Ising chain: fermion approach *J. Stat. Mech.* P02028
[204] Peschel I 2003 Calculation of reduced density matrices from correlation functions *J. Phys. A: Math. Gen.* **36** L205
[205] Bañuls M C, Cirac J I and Hastings M B 2011 Strong and weak thermalization of infinite nonintegrable quantum systems *Phys. Rev. Lett.* **106** 050405
[206] Iglói F, Szatmári Z and Lin Y-C 2012 Entanglement entropy dynamics of disordered quantum spin chains *Phys. Rev.* B **85** 094417
[207] Torlai G, Tagliacozzo L and De Chiara G 2014 Dynamics of the entanglement spectrum in spin chains *J. Stat. Mech.* P06001
[208] Coser A, Tonni E and Calabrese P 2014 Entanglement negativity after a global quantum quench *J. Stat. Mech.* P12017
[209] Nezhadhaghighi M G and Rajabpour M A 2014 Entanglement dynamics in short- and long-range harmonic oscillators *Phys. Rev.* B **90** 205438
[210] White S R and Feiguin A E 2004 Real-time evolution using the density matrix renormalization group *Phys. Rev. Lett.* **93** 076401
Daley A J, Kollath C, Schollwöck U and Vidal G 2004 Time-dependent density-matrix renormalization-group using adaptive effective Hilbert spaces *J. Stat. Mech.* P04005
[211] Vidal G 2007 Classical simulation of infinite-size quantum lattice systems in one spatial dimension *Phys. Rev. Lett.* **98** 070201
[212] Gurarie V 2013 Global large time dynamics and the generalized Gibbs ensemble *J. Stat. Mech.* P02014
[213] Essler F H L, Frahm H, Göhmann F, Klümper A and Korepin V E 2005 *The One-Dimensional Hubbard Model* (Cambridge: Cambridge University Press)
[214] Gaudin M 1983 *La Fonction d'onde de Bethe* (Paris: Masson)
Caux J-S 2014 (Cambridge: Cambridge University Press) (Engl. transl.)
[215] Sotiriadis S, Fioretto D and Mussardo G 2012 Zamolodchikov–Faddeev algebra and quantum quenches in integrable field theories *J. Stat. Mech.* P02017

J. Stat. Mech. (2016) 064002

[216] Horváth D X, Sotiriadis S and Takács G 2016 Initial states in integrable quantum field theory quenches from an integral equation hierarchy *Nucl. Phys.* B **902** 508
[217] Caux J-S 2016 The quench action *J. Stat. Mech.* 064006
[218] Pozsgay B 2014 Quantum quenches and generalized Gibbs ensemble in a Bethe Ansatz solvable lattice model of interacting bosons *J. Stat. Mech.* P10045
[219] Goldstein G and Andrei N 2014 Failure of the GGE hypothesis for integrable models with bound states (arXiv:1405.4224)
[220] Zamolodchikov A B and Zamolodchikov Al B 1979 Factorized S-matrices in two dimensions as the exact solutions of certain relativistic quantum field theory models *Ann. Phys.* **120** 253
[221] Faddeev L D 1980 Quantum completely integral models of field theory *Sov. Sci. Rev. Math. Phys.* C **1** 107
[222] Essler F H L and Konik R M 2009 Finite temperature dynamical correlations in massive integrable quantum field theories *J. Stat. Mech.* P09018
[223] Lieb E H 1967 Exact solution of the problem of the entropy of two-dimensional ice *Phys. Rev. Lett.* **18** 692
Lieb E H 1967 Exact solution of the two-dimensional slater KDP model of a ferroelectric *Phys. Rev. Lett.* **19** 108
Sutherland B 1967 Exact solution of a two-dimensional model for hydrogen-bonded crystals *Phys. Rev. Lett.* **19** 103
[224] Faddeev L D and Takhtadzhyan L 1984 Spectrum and scattering of excitations in the one-dimensional isotropic Heisenberg model *J. Sov. Math.* **24** 241
[225] Takahashi M and Suzuki M 1972 One-dimensional anisotropic Heisenberg model at finite temperatures *Prog. Theor. Phys.* **48** 2187
Takahashi M 1999 *Thermodynamics of One Dimensional Solvable Models* (Cambridge: Cambridge University Press)
[226] Tsvelik A M 1990 Incommensurate phases of quantum one-dimensional magnetics *Phys. Rev.* B **42** 779
Frahm H 1992 Integrable spin-1/2 XXZ Heisenberg chain with competing interactions *J. Phys. A: Math. Gen.* **25** 1417
Zvyagin A A and Klümper A 2003 Quantum phase transitions and thermodynamics of quantum antiferromagnets with next-nearest-neighbor couplings *Phys. Rev.* B **68** 144426
[227] Muramoto N and Takahashi M 1999 Integrable magnetic model of two chains coupled by four-body interactions *J. Phys. Soc. Japan* **68** 2098
[228] Grabowski M P and Mathieu P 1995 Structure of the conservation laws in quantum integrable spin chains with short range interactions *Ann. Phys.* **243** 299
[229] Klümper A and Sakai K 2002 The thermal conductivity of the spin-1/2 XXZ chain at arbitrary temperature *J. Phys. A: Math. Gen.* **35** 2173
Sakai K and Klümper A 2003 Non-dissipative thermal transport in the massive regimes of the XXZ chain *J. Phys. A: Math. Gen.* **36** 11617
[230] Klümper A 1993 Thermodynamics of the anisotropic spin-1/2 Heisenberg chain and related quantum chains *Z. Phys.* B **91** 507
Destri C and de Vega H J 1995 Unified approach to thermodynamic Bethe Ansatz and finite size corrections for lattice models and field theories *Nucl. Phys.* B **438** 314
[231] Bortz M and Göhmann F 2005 Exact thermodynamic limit of short-range correlation functions of the antiferromagnetic XXZ-chain at finite temperatures *Eur. Phys. J.* B **46** 399
Boos H E, Göhmann F, Klümper A and Suzuki J 2007 Factorization of the finite temperature correlation functions of the XXZ chain in a magnetic field *J. Phys. A: Math. Theor.* **40** 10699
Boos H E, Damerau J, Göhmann F, Klümper A, Suzuki J and Weiße A 2008 Short-distance thermal correlations in the XXZ chain *J. Stat. Mech.* P08010
Trippe C, Göhmann F and Klümper A 2010 Short-distance thermal correlations in the massive XXZ chain *Eur. Phys. J.* B **73** 253
[232] Göhmann F, Klümper A and Seel A 2004 Integral representation of the density matrix of the XXZ chain at finite temperatures *J. Phys. A: Math Gen.* **37** 7625
[233] Boos H E, Jimbo M, Miwa T, Smirnov F and Takeyama Y 2006 Algebraic representation of correlation functions in integrable spin chains *Ann. Henri Poincare* **7** 1395
Boos H E, Jimbo M, Miwa T, Smirnov F and Takeyama Y 2007 Hidden Grassmann structure in the XXZ model *Commun. Math. Phys.* **272** 263
Boos H E, Jimbo M, Miwa T, Smirnov F and Takeyama Y 2009 Hidden Grassmann structure in the XXZ model II: creation operators *Commun. Math. Phys.* **286** 875
Jimbo M, Miwa T and Smirnov F 2009 Hidden Grassmann structure in the XXZ model III: introducing the Matsubara direction *J. Phys. A: Math. Theor.* **42** 304018

J. Stat. Mech. (2016) 064002

[234] Ilievski E, Medenjak M and Prosen T 2015 Quasilocal conserved operators in the isotropic Heisenberg spin-1/2 chain *Phys. Rev. Lett.* **115** 120601
[235] Ilievski E, Medenjak M, Prosen T and Zadnik L 2016 *J. Stat. Mech.* 064008
[236] Prosen T 2011 Open XXZ spin chain: nonequilibrium steady state and a strict bound on ballistic transport *Phys. Rev. Lett.* **106** 217206
Prosen T and Ilievski E 2013 Families of quasilocal conservation laws and quantum spin transport *Phys. Rev. Lett.* **111** 057203
Prosen T 2014 Quasilocal conservation laws in XXZ spin-1/2 chains: open, periodic and twisted boundary conditions *Nucl. Phys.* B **886** 1177
Pereira R G, Pasquier V, Sirker J and Affleck I 2014 Exactly conserved quasilocal operators for the XXZ spin chain *J. Stat. Mech.* P09037
Piroli L and Vernier E 2016 Quasi-local conserved charges and spin transport in spin-1 integrable chains (arXiv:1601.07289)
[237] Sirker J, Pereira R G and Affleck I 2011 Conservation laws, integrability and transport in one-dimensional quantum systems *Phys. Rev.* B **83** 035115
[238] Takhtajan L A 1982 The picture of low-lying excitations in the isotropic Heisenberg chain of arbitrary spins *Phys. Lett.* A **87** 479
Babujian H M 1983 Exact solution of the isotropic Heisenberg chain with arbitrary spins: thermodynamics of the model *Nucl. Phys.* B **215** 317
Kirillov A N and Reshetikhin N Yu 1987 Exact solution of the integrable XXZ Heisenberg models with arbitrary spin. I. The ground state and the excitation spectrum *J. Phys. A: Math. Gen.* **20** 1565
Kirillov A N and Reshetikhin N Yu 1987 Exact solution of the integrable XXZ Heisenberg model with arbitrary spin. II. Thermodynamics of the system *J. Phys. A: Math. Gen.* **20** 1587
[239] Ilievski E, Quinn E, De Nardis J and Brockmann M 2015 String-charge duality in integrable lattice models (arXiv:1512.04454)
[240] Sutherland B 1975 Model for a multicomponent quantum system *Phys. Rev.* B **12** 3795
Kulish P P and Sklyanin E K 1982 Solutions of the Yang–Baxter equation *J. Sov. Math.* **19** 1596
Andrei N and Johannesson H 1984 Higher dimensional representations of the SU(N) Heisenberg model *Phys. Lett.* A **104** 370
Kulish P P 1985 Integrable graded magnets *J. Sov. Math.* **35** 2648
Essler F H L and Korepin V E 1992 Algebraic Bethe Ansatz and higher conservation laws for the supersymmetric t-J model *Phys. Rev.* B **46** 9147
Foerster A and Karowski M 1993 Algebraic properties of the Bethe ansatz for an *spl*(2, 1) supersymmetric t-J model *Nucl. Phys.* B **396** 611
Essler F H L, Korepin V E and Schoutens K 1994 Exact solution of an electronic model of superconductivity I *Int. J. Mod. Phys.* B **8** 3205
Göhmann F 2001 Algebraic Bethe ansatz for the gl(1 | 2) generalized model and Lieb–Wu equations *Nucl. Phys.* B **620** 501
Belliard S and Ragoucy E 2008 Nested Bethe ansatz for 'all' closed spin chains *J. Phys. A: Math. Theor.* **41** 295202
[241] Pozsgay B and Eisler V 2016 Real-time dynamics in a strongly interacting bosonic hopping model: global quenches and mapping to the XX chain (arXiv:1602.03065)
[242] Mazza P P, Stéphan J-M, Canovi E, Alba V, Brockmann M and Haque M 2016 Overlap distributions for quantum quenches in the anisotropic Heisenberg chain *J. Stat. Mech.* 013104
[243] Kollath C, Läuchli A M and Altman E 2007 Quench dynamics and nonequilibrium phase diagram of the Bose–Hubbard model *Phys. Rev. Lett.* **98** 180601
[244] Moeckel M and Kehrein S 2008 Interaction quench in the Hubbard model *Phys. Rev. Lett.* **100** 175702
[245] Moeckel M and Kehrein S 2009 Real-time evolution for weak interaction quenches in quantum systems *Ann. Phys.* **324** 2146
[246] Sotiriadis S and Cardy J 2010 Quantum quench in interacting field theory: a self-consistent approximation *Phys. Rev.* B **81** 134305
[247] Kollar M, Wolf F A and Eckstein M 2011 Generalized Gibbs ensemble prediction of prethermalization plateaus and their relation to nonthermal steady states in integrable systems *Phys. Rev.* B **84** 054304
[248] Mitra A and Giamarchi T 2011 Mode-coupling-induced dissipative and thermal effects at long times after a quantum quench *Phys. Rev. Lett.* **107** 150602
[249] Carleo G, Becca F, Schiró M and Fabrizio M 2012 Localization and glassy dynamics Of many-body quantum systems *Sci. Rep.* **2** 243
[250] Marino J and Silva A 2012 Relaxation, prethermalization, and diffusion in a noisy quantum Ising chain *Phys. Rev.* B **86** 060408

J. Stat. Mech. (2016) 064002

[251] Stark M and Kollar M 2013 Kinetic description of thermalization dynamics in weakly interacting quantum systems (arXiv:1308.1610)
[252] Marcuzzi M, Marino J, Gambassi A and Silva A 2013 Prethermalization in a nonintegrable quantum spin chain after a quench *Phys. Rev. Lett.* **111** 197203
[253] Mitra A 2013 Correlation functions in the prethermalized regime after a quantum quench of a spin-chain *Phys. Rev.* B **87** 205109
[254] Essler F H L, Kehrein S, Manmana S R and Robinson N J 2014 Quench dynamics in a model with tuneable integrability breaking *Phys. Rev.* B **89** 165104
[255] Nowak B, Schole J and Gasenzer T 2014 Universal dynamics on the way to thermalisation *New J. Phys.* **16** 093052
[256] Delfino G 2014 Quantum quenches with integrable pre-quench dynamics *J. Phys. A: Math. Theor.* **47** 402001
[257] Bertini B and Fagotti M 2015 Pre-relaxation in weakly interacting models *J. Stat. Mech.* P07012
[258] Bertini B, Essler F H L, Groha S and Robinson N J 2015 Prethermalization and thermalization in models with weak integrability breaking *Phys. Rev. Lett.* **115** 180601
[259] Brandino G P, Caux J-S and Konik R M 2015 Glimmers of a quantum KAM theorem: insights from quantum quenches in one-dimensional Bose gases *Phys. Rev.* X **5** 041043
[260] Babadi M, Demler E and Knap M 2015 Far-from-equilibrium field theory of many-body quantum spin systems: prethermalization and relaxation of spin spiral states in three dimensions *Phys. Rev.* X **5** 041043
[261] Olshanii M 2015 Geometry of quantum observables and thermodynamics of small systems *Phys. Rev. Lett.* **114** 060401
[262] Fagotti M 2015 Control of global properties in a closed many-body quantum system by means of a local switch (arXiv:1508.04401)
[263] Nessi N and Iucci A 2015 Glass-like behavior in a system of one dimensional fermions after a quantum quench (arXiv:1503.02507)
[264] Kitagawa T, Imambekov A, Schmiedmayer J and Demler E 2011 The dynamics and prethermalization of one-dimensional quantum systems probed through the full distributions of quantum noise *New J. Phys.* **13** 073018
[265] Langen T, Erne S, Geiger R, Rauer B, Schweigler T, Kuhnert M, Rohringer W, Mazets I E, Gasenzer T and Schmiedmayer J 2015 Experimental observation of a generalized Gibbs ensemble *Science* **348** 207
[266] Goldstein G and Andrei N 2013 Equilibration and generalized GGE in the Lieb Liniger gas (arXiv:1309.3471)
[267] Kliesch M, Gogolin C, Kastoryano M J, Riera A and Eisert J 2014 Locality of temperature *Phys. Rev.* X **4** 031019
[268] Tsvelick A M and Wiegmann P B 1983 Exact results in the theory of magnetic alloys *Adv. Phys.* **32** 453

J. Stat. Mech. (2016) 064002